T.J Wipf, F.W. Klaiber, B.M. Phares

Investigation of Two Bridge Alternates for Low Volume Roads

Volume 1 of 2

Concept 1: Precast Steel Beam Units

Sponsored by the
Iowa Department of Transportation
Project Development Division and the
Iowa Highway Research Board

April 1997

Iowa DOT Project HR-382
ISU-ERI-Ames-97405

Iowa Department of Transportation

report

College of Engineering
Iowa State University

The opinions, findings, and conclusions expressed in this publication are those of the authors and not necessarily those of the Iowa Department of Transportation

T.J Wipf, F.W. Klaiber, B.M. Phares

Investigation of Two Bridge Alternates for Low Volume Roads

Volume 1 of 2

Concept 1: Precast Steel Beam Units

Sponsored by the
Iowa Department of Transportation
Project Development Division and the
Iowa Highway Research Board

Iowa DOT Project HR-382
ISU-ERI-Ames-97405

engineering research institute
iowa state university

ABSTRACT

Recent reports have indicated that 23.5 percent of the nation's highway bridges are structurally deficient and 17.7 percent are functionally obsolete. A significant number of these bridges are on the Iowa secondary road system where over 86 percent of the rural bridge management responsibilities are assigned to the counties. Some of the bridges can be strengthened or otherwise rehabilitated, but many more are in need of immediate replacement.

In a recent investigation, HR-365 "Evaluation of Bridge Replacement Alternatives for the County Bridge System" several types of replacement bridges that are currently being used on low volume roads were identified. It was also determined that a large number of counties (69 percent) have the ability and are interested in utilizing their own forces to design and construct short span bridges. In reviewing the results from HR-365, the research team developed one "new" bridge replacement concept and a modification of a replacement system currently being used.

Both of these bridge replacement alternatives were investigated in this study the results of which are presented in two volumes. This volume (Volume 1) presents the results of Concept 1 - Precast Steel Beam Units while Concept 2 - Modification of the Beam-in-Slab Bridge is presented in Volume 2. Concept 1, involves the fabrication of precast units (two steel beams connected by a concrete slab) by county work forces. Deck thickness is limited so that the units can be fabricated at one site and then transported to the bridge site where they are connected and the remaining portion of the deck placed. Since the Concept 1 bridge is primarily intended for use on low-volume roads, the precast units can be constructed with new or used beams.

In the experimental part of the investigation, there were three types of static load tests: small scale connector tests, "handling strength" tests, and service and overload tests of a model bridge. Three finite element models for analyzing the bridge in various states of construction were also developed.

Small scale connector tests were completed to determine the best method of connecting the precast double-T (PCDT) units. "Handling strength" tests on an individual PCDT unit were performed to determine the strength and behavior of the precast unit in this configuration.

The majority of the testing was completed on the model bridge (L = 9,750 mm (32 ft), W = 6,400 mm (21 ft)) which was fabricated using the precast units developed. Some of the variables investigated in the model bridge tests were number of connectors required to connect adjacent precast units, contribution of diaphragms to load distribution, influence of position of diaphragms on bridge strength and load distribution, and effect of cast-in-place portion of deck on load distribution. In addition to the service load tests, the bridge was also subjected to overload conditions. Using the finite element models developed, one can predict the behavior and strength of bridges similar to the laboratory model as well as design them.

Concept 1 has successfully passed all laboratory testing; the next (and final step prior to implementation of this type of bridge in the field) is to field test it in a demonstration project.

TABLE OF CONTENTS

Page

Page

LIST OF FIGURES

Page

Page

Page

Page

1. INTRODUCTION

1.1 Background

Recent reports have indicated that 23.5 percent of the nation's highway bridge are structurally deficient and 17.7 percent are functionally obsolete (1). Unfortunately, a significant number of these bridges are on the Iowa county roads system. According to a 1989 report (2), 86.4 percent of rural bridge maintenance responsibilities are assigned to the county. Some of the bridges can be strengthened and rehabilitated, but many are in need of replacement. A recent questionnaire sent to all of the county engineers in Iowa asked the need and interest in a study to review and evaluate replacement bridges. Over 76 percent of the respondents replied such a study would be beneficial or very beneficial.

Such a study was recently completed in project, HR-365 "Evaluation of Bridge Replacement Alternatives for the County Bridge System" (3). In this investigation, several replacement bridges currently being used on the county road system in Iowa and surrounding states were identified and evaluated. This investigation (HR-365) documented several unique replacement bridge types that are currently being used on low volume roads. It also determined that a large number of counties (69 percent) have the ability and are interested in using their own forces to design and construct short span bridges provided the construction procedures are relatively simple. To minimize the initial cost of replacement and subsequent maintenance costs, it is important to select the right replacement bridge type for a particular site. Cost can obviously be minimized by selecting bridges that can be designed and constructed by local work forces.

From the evaluation of the questionnaire responses from the Iowa counties and investigation of the various bridge replacement concepts currently in use, the research team developed one "new" bridge replacement concept and a modification of a replacement system currently being used. To determine if there is interest in these two concepts, the researchers recently contacted several county and city engineers to obtain their input on the two bridge concepts. Each county engineer contacted thought both concepts had merit and would be interested in participating in a demonstration project involving the replacement systems if the research went that far.

For discussion purposes the "new" idea, precast steel beam units, will be identified as Concept 1. The portion of the project that involves the modification of a current replacement system, beam-in-slab bridge, will be referenced as Concept 2. The extensive results from this investigation have been published in two volumes. Concept 1 is presented in this volume (Volume 1) while Concept 2 is presented in Volume 2.

Concept 1, precast steel beam units, involves the fabrication of the precast units (two steel beams connected by a concrete deck) by county work forces. Deck thickness is limited so that the units can be fabricated at one site and then transported to the bridge site. The number of units required is obviously a function of the width of bridge desired. After connecting the precast units together, the remaining portion of the deck is placed. The surface of the precast units is scarified so that the two layers of concrete are bonded together thus providing the required deck thickness. Since the Concept 1 bridge is primarily intended for use on low-volume roads, the precast units could be constructed with new or used steel beams.

1.2 Objectives and Scope

The overall objective of this investigation was to obtain structural behavior and strength data on the two concepts though laboratory testings. The work completed on Concept 1 is presented in the following paragraphs.

Basically, the investigation involved a literature review, laboratory testing, and an analytical modeling of the bridge. Since Concept 1 is "new", no literature was found on it or similar systems. Several references on precast construction, bonding layers of concrete, etc. were found that are related to the concept.

Laboratory testing involved several different tests: small scale connector tests, "handling strength" tests, service and overload tests of a model bridge constructed using the precast units developed.

Small scale connector tests were completed to determine the best method of connecting the precast units. Tests were completed with and without cast-in-place concrete (i.e., only the precast concrete). All small scale specimens were instrumented for strain and deflection measurements.

Since the precast steel beam units have a relatively thin slab of composite concrete connecting the two steel beams, there was concern that these units had sufficient strength for transporting them from a fabrication site to the bridge site. "Handling strength" tests on an individual unit were performed to determine the strength and behavior of the precast units in this configuration.

The majority of the testing was completed on a model bridge which was fabricated using the precast units developed. The model bridge was tested with and without the cast-in-place concrete. Some of the variable investigated were

- number of connectors required to connect adjacent precast units
- contribution of diaphragms to load distribution
- influence of position of diaphragms on bridge strength and load distribution
- effect of cast-in-place portion of deck on load distribution

In addition to some of the service load tests just described, the bridge was also subjected to overload conditions.

In the analytical portion of the investigation, three finite element models were developed to predict the behavior of the bridge in various states of construction. These analytical models were validated using the data from the tests completed. Using the analytical models developed, one can predict the behavior and strength of not only the laboratory model bridge but also other similar bridges (i.e., different widths, lengths, deck thicknesses, etc.) The finite element models may also be used to design this type of bridge.

The results of this portion of the investigation (Concept 1) are summarized in this report. The literature review in presented in Chp. 2. Descriptions of the various test specimens are presented in Chp. 3, while instrumentation used as well as a description of the numerous tests performed are presented in Chp. 4. The three finite element models developed are presented in Chp. 5. Results from the numerous laboratory tests are summarized in Chp. 6. The summary and conclusions of the investigation are presented in Chp. 7.

2. LITERATURE REVIEW

A literature search was conducted to collect available information on similar types of bridge systems to determine the suitability of precast connection details currently being used. Several methods of searching were used. Initially, the Transportation Research Information Service through the Iowa Department of Transportation (Iowa DOT) was searched. A search of the Geodex System-Structural Information Service in the ISU Bridge Engineering Center Library as well as several computerized search through the university library were also made.

The literature reviewed in this report, is not intended to be all inclusive but focus on issues that are pertinent to this phase of the investigation.

In the following sections, a number of pertinent bridge articles that were reviewed are summarized. These are presented in two sections: structural concrete overlays in bridge deck rehabilitation and precast concrete connection details.

2.1 Structural Concrete Overlays In Bridge Deck Rehabilitation

A popular rehabilitation technique to repair deteriorated bridge decks is to overlay the existing concrete bridge deck with additional structural concrete. The main concern with this type of rehabilitation is obtaining effective horizontal shear transfer between the existing concrete and the overlay. Surface preparation and how much, if any, shear reinforcement is needed at the interlayer have been two of the main concerns. Differential shrinkage of the two concrete lifts and the long term performance under cyclic loading complicates the problem. The placement of dowels in the existing concrete deck is time consuming and labor intensive; the effectiveness of the dowel reinforcement in this method

of deck rehabilitation is also questionable. In 1988, Seible (4) investigated the shear transfer between existing concrete decks and structural concrete overlays.

Current AASHTO (5) specifications require a minimum amount of reinforcement across interlayer joints which may be determined using the following equations:

$$A_d = \frac{50 b_v s}{f_{dy}} \qquad (1)$$

where

A_d = reinforcement area crossing the interlayer, in^2.
b_v = width of contact section investigated for horizontal shear, in.
f_{dy} = yield strength of the shear reinforcement, psi.
s = spacing of the shear reinforcement, in.

With Grade 60 reinforcing steel, this translates to approximately a #3 reinforcing bar per square foot of deck.

The objective of the study performed by Seible focused on three areas: (1) to determine performance differences for different surface preparations typically used in overlay rehabilitation work, (2) to develop an experimental database and constitutive information on the interlayer slip for calibrating nonlinear analytical models, and (3) to verify proposed design recommendations derived from the analytical studies and the experimental testing.

The first two criteria were established from block shear tests and full scale transverse deck slab panels. Various surface preparations typically found in bridge deck overlay work were investigated.

From the block tests shown schematically in Fig 2.1, two major conclusions were developed. In specimens without dowels, the surface preparation had a distinct influence

on the load capacity at the beginning of interlayer delamination. After delamination, the load capacity decreased dramatically and there was minimal strength remaining in the joint. In specimens with dowel reinforcement, the strength was completely controlled by the amount of reinforcement; the type of surface preparation had little effect on the strength.

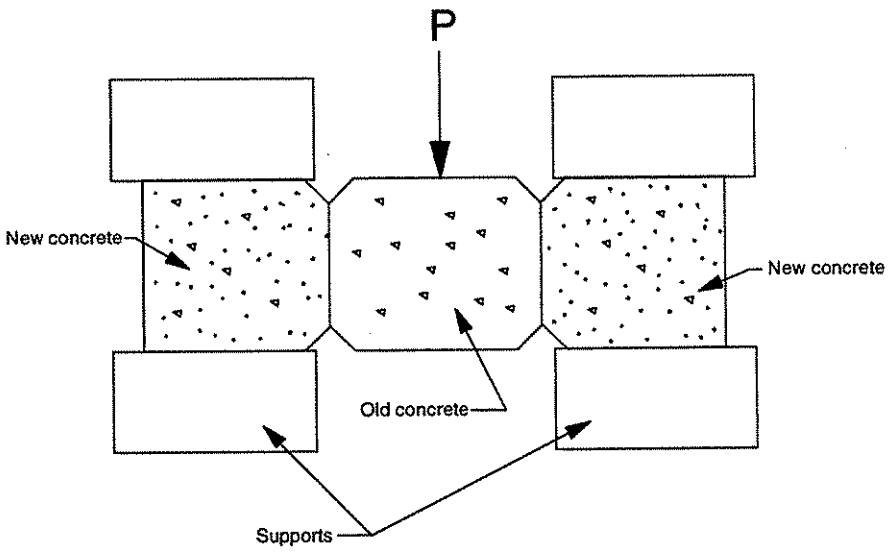

Figure 2.1. Schematic of Seible's block shear test.

From the slab panel tests shown in Fig. 2.2, the following conclusions were reached:

1. The use of dowels helped to control interlayer cracking resulting from differential shrinkage.
2. The behavior of specimens with wood troweled surfaces that were sand blasting was almost identical to the monolithic condition with the exception of interlayer cracking from differential shrinkage.

3. The behavior of specimens with the surface scarified (3 mm (1/8 in.) to 6 mm (1/4 in.) deep grooves on 25 mm (1 in.) centers) was virtually identical to the monolithic condition.
4. The use of minimal amounts of dowel reinforcement proved to be ineffective in increasing load capacity for all surface types tested, however even minimal amounts of dowel reinforcement did reduce the amount of differential shrinkage cracks.

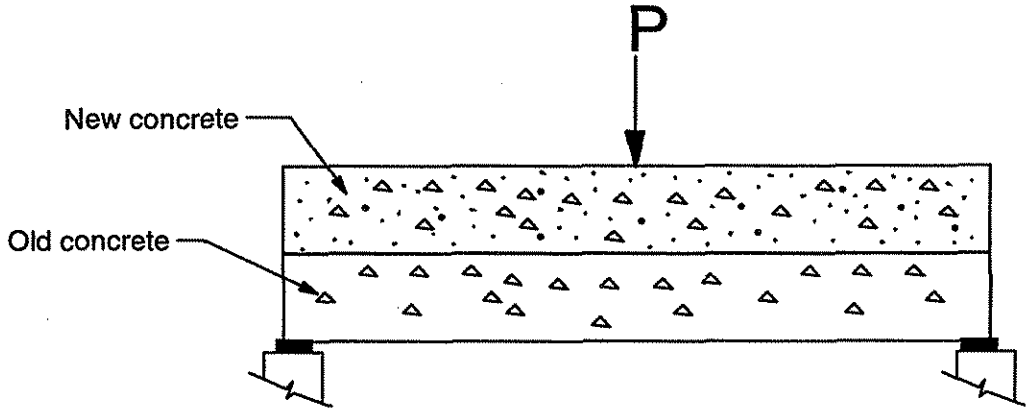

Figure 2.2. Schematic of Seible's slab panel test.

From these two series of tests, two conclusions were reached. First, dowel reinforcement is ineffective from a strength point of view unless actual relative displacement takes place at the interface. Second, the use of dowels provided additional restraint that was effective in reducing cracking due to interlayer shrinkage.

In addition to the laboratory tests, a full scale test was completed in-situ. In this test, linear elastic behavior was observed and no interlayer delamination occurred with the presence of minimal dowel reinforcement.

Based on the analytical and experimental results of this study, a set of design recommendations, to ensure proper interlayer shear transfer with the reduction or elimination of interlayer delamination due to differential shrinkage, was developed. The design recommendations are summarized below as given by Seible (4).

To ensure horizontal shear strength at the overlay interface the following relationship must be satisfied.

$$V_{uh} \leq \phi V_{nh} \tag{2}$$

where

V_{uh} = Ultimate shear to be resisted, kips.
V_{nh} = Nominal shear strength, kips.
ϕ = Strength reduction factor.

Due to the in-plane stiffness of the structural concrete overlays, the horizontal interface shear shall be determined as the average shear force acting over a segment interface length L_h, defined as

$$L_h = L/2 \quad L \leq 8h$$

$$L_h = 4h \quad L > 8h \tag{3}$$

where

h = Structural depth of section, in.
L = Span length, in.

If $L < 4h$, no horizontal interface shear design is required. The nominal shear strength, V_{nh}, is defined as

$$V_{nh} = b_v L_h v_{nh} \tag{4}$$

with

$$v_{nh} = v_c = 2.0\sqrt{f_c'} \tag{5}$$

where

b_v = Effective width of the overlay interface, in.
L_h = Segment interface length, in.
f_c' = Nominal concrete compressive strength, psi.
V_{nh} = Nominal horizontal interface shear, kips.

for intentionally roughened surfaces, and

$$v_{nh} = v_d = A_d f_{dy} \tag{6}$$

where

A_d = Area of interface dowel reinforcement, in^2.
f_{dy} = nominal yield of dowel reinforcement, ksi.

for non-intentionally roughened surfaces with dowel reinforcement.

The factored horizontal shear stress, v_{uh}, shall be determined for arbitrary cross sections in the longitudinal bridge direction as

$$v_{uh} = \frac{V_u S_0}{I\, b_v} \tag{7}$$

where

V_u = Factored shear force, kips.
S_o = First moment of overlay with respect to neutral axis, in^3.
I = Moment of inertia, in^4.
b_v = Effective width of overlay interface, in.

and in the transverse bridge direction as

$$v_{uh} = \frac{V_u}{b_v h} \tag{8}$$

where

V_u = Factored shear force, kips.
b_v = Effective width of overlay interface, in.
h = Structural height of section, in.

For concentrated wheel loads, an effective width, b_v, can be determined based on a shear force distribution angle of $2x30^o$ at a distance 2h from the loaded area.

The factored horizontal segment shear is then defined as

$$V_{uh} = v_{uh} b_v L_h \tag{9}$$

where

v_{uh} = Factored ultimate interface shear stress, ksi.
b_v = Effective width of overlay interface, in.
L_h = Segment interface length, in.

If interface dowel reinforcement is required, the dowel area over the segment length can be determined as

$$A_d = \frac{V_{uh}}{\phi f_{dy}} \tag{10}$$

where

V_{uh} = Factored horizontal segment shear, kips.
ϕ = Strength reduction factor.
f_{dy} = Nominal yield strength of dowel reinforcement, ksi.

A minimum interface dowel reinforcement ratio of

$$\rho = \frac{\phi 2\sqrt{f_c'}}{f_{dy}} \tag{11}$$

where

f_c' = Nominal concrete design strength, psi.
ϕ = Strength reduction factor.
f_{dy} = Nominal yield strength of dowel reinforcement, ksi.

is implied by the above design approach for intentionally roughened contact surfaces which require interface dowels. All dowels must be adequately anchored into interconnected elements.

Perimeter dowel reinforcement is recommended along free edges of the bridge deck where there is potential for overlay curl up due to environmental effects. The nominal curl up length, L_c shall be computed with h_o as

$$L_c \cong 45\sqrt{h_o} \tag{12}$$

where

h_o = Overlay thickness, in.
L_c = curl up length, in.

and the perimeter force per unit length as

$$P_p = 4800\frac{h_o^2}{L_c} - \frac{2}{5}h_o L_c \tag{13}$$

where

h_o = Overlay thickness, in.
L_c = Curl up length, in.

Perimeter dowel reinforcement shall be designed based on an allowable dowel stress of

$$f_{da} = 0.4 f_{dy} \tag{14}$$

where

f_{da} = Nominal yield of dowel reinforcement, ksi.

and the area of dowels as

$$A_{dp} = \frac{P_p}{f_{da}} \tag{15}$$

where

P_p= Perimeter force, lbs/ft.
f_{da} = Allowable dowel service level stress, psi.

The required perimeter force to prevent overlay curl up can be reduced in cases where additional edge dead loads (curbs, parapets, etc.) are present.

2.2 Precast Concrete Connection Details

The idea of transverse shear transfer in multi-beam bridges was discussed in a paper by Bakht, et. al (6). Multi-beam bridges are defined as bridges that consist of precast beams that are placed side by side and are connected by longitudinal shear keys. The majority of bridges of this type are constructed of prestressed concrete elements. The effective transfer of shear across the common edges of beams placed side-by-side is essential to ensure that load is effieiently distributed to all beams. Traditionally, the void between the beams (i.e., the shear key) has been filled with in-situ concrete. The design of these shear keys has previously been based on empirical methods. Presented in this paper is a simplified method for determining the magnitude of transverse shear between adjacent

beams. The multi-beam bridges have been successfully analyzed by idealizing them as articulated plates. An articulated plate is a special case of an orthotropic plate, in which the transverse flexural rigidity is taken to be zero. In an articulated plate, it is assumed that the distribution of loads takes place through transverse shear.

The issue of load distribution and connection design for precast stemmed mutibeam bridge superstructures has also been addressed by Stanton and Mattock (7). The objective of their research was to develop information on the behavior of stemmed mutlibeam structures with an emphasis on the load distribution characteristics and the methodology for designing the connection details. With their design methodology, one can design the steel portion of the steel connectors that are embedded in the flanges of the members. According to Stanton and Mattock, the primary function of connections is to transfer shear forces between adjacent precast members for lateral distribution of concentrated wheel loads. The connections also serve to carry any in-plane tension forces that may occur due to the torsional stiffness of the members. During construction, individual welded connectors are sometimes used to hold adjacent members in alignment while the keyway between the members is grouted. Currently, the AASHTO Standard Specifications for Highway Bridges (5) gives no design recommendations for the transfer of forces across precast panel joints. In practice, it appears that the grout key requirements as far as geometry and connector details, are based on "rule-of-thumb" methods and past experience rather than on any rational methodologies. Stanton and Mattock reported that it appears that "for fully precast bridges of the type under consideration, the most widely used connection between adjacent precast concrete members is a combination of a continuous grouted shear key and welded connectors at

intervals from 4 ft to 8 ft." Examples of these typical types of connection details are shown in Figs. 2.3 and 2.4 where four different keyway details are shown (Figs. 2.3a and b, Figs. 2.4a and b) and four different welded connections are illustrated (Figs. 2.3c and d, Figs. 2.4c and d). It is noted that a less frequently used connection detail consists of continuously grouted post-tension tendons which are tensioned to approximately 517 kpa (75 psi) to produce compression along the joint.. An alternate form of construction of the full depth precast concrete stemmed beams is the combination of a thin flanged tee or double tee with a cast-in-place slab to form a composite system. This system is quite similar to the one being investigated in this study. In the precast concrete stemmed beam system, the precast flange is typically on the order of 50 mm (2 in.) thick and the cast-in-place depth is typically 127 mm (5 in.) to 152 mm (6 in.) and is designed to carry the transverse moments.

To obtain information on details used in practice, Staton and Mattock developed a survey which was sent to state DOTs as well as to several county engineers in the state of Washington. Of particular interest are the responses to questions concerning the design of the connection between fully precast members. Typical responses include: 'not designed', 'details used many years with reasonable success', 'standard details', 'industry suggested connection', 'design by fabricator', and so on. Thus, the connection details currently in use today seem to be based on the "trial and error" method of design. Because of this, a wide variety of joint geometries exists. In addition, the suggested shape, configuration, and location of the shear key is highly debatable and has developed into a variety of "standard" keyways.

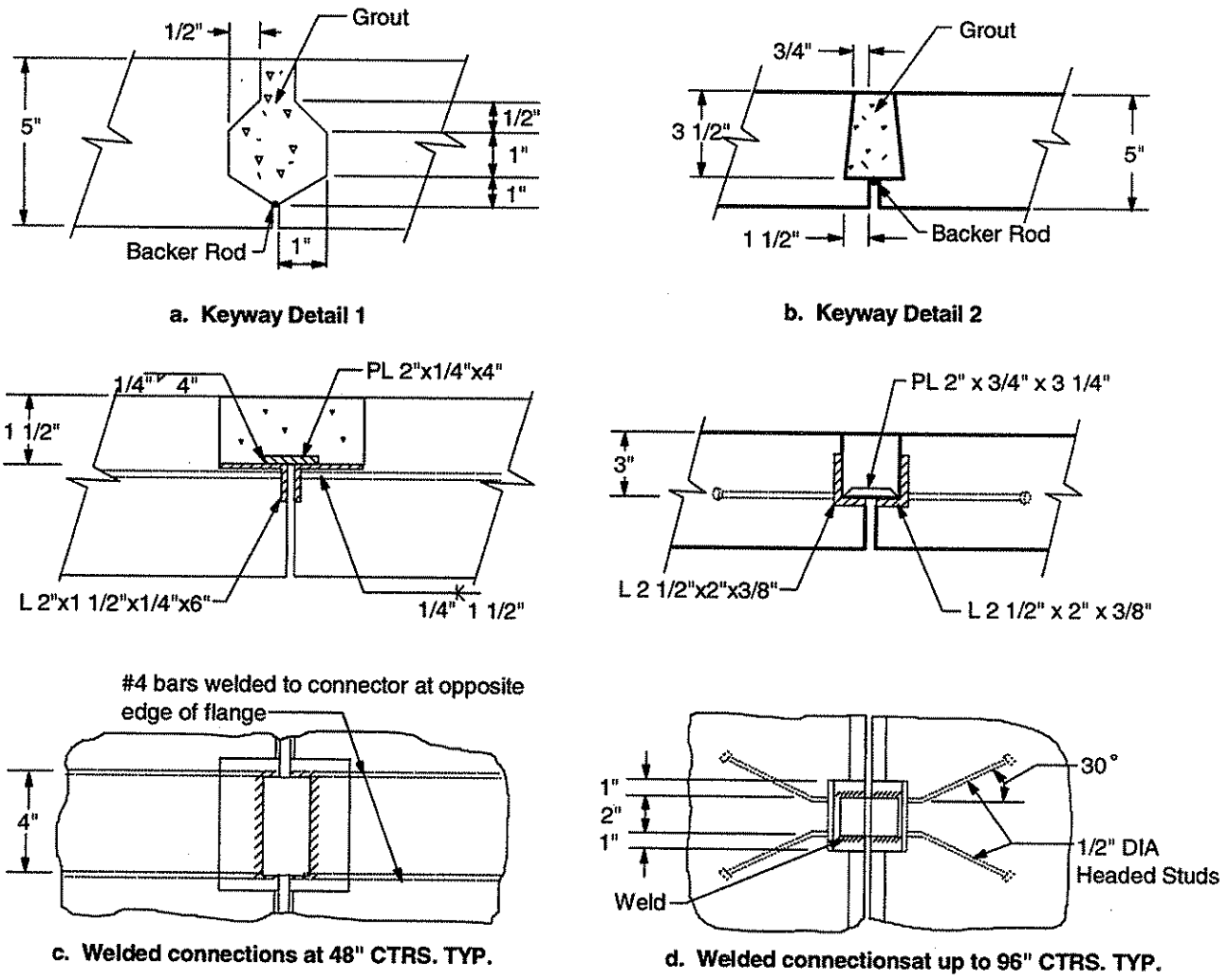

Figure 2.3. Typical flange connection detail used by Concrete Technology Corporation and by Central Premix Concrete Company.

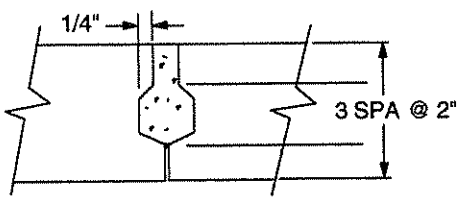

a. Keyway Detail 3

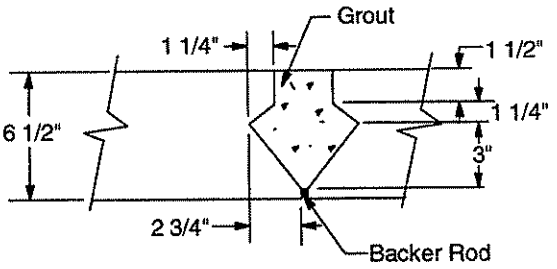

b. Keyway Detail 4

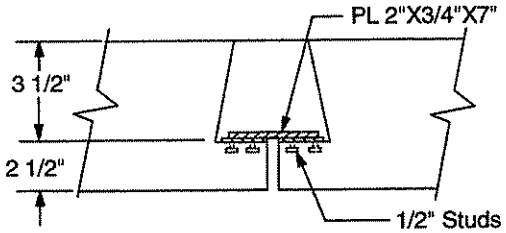

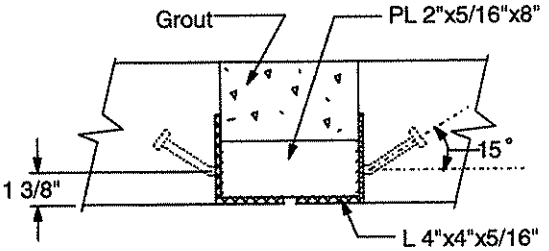

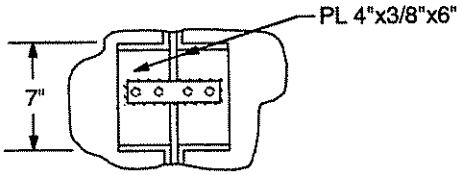

c. Welded connection at 60" CTRS. TYP.

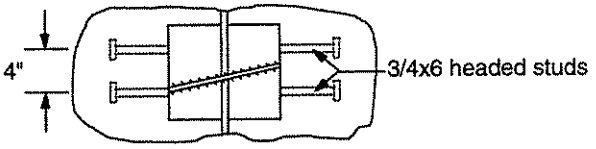

d. Welded connections at 55" CTRS. TYP.

Figure 2.4. Typical connection detail used by Stanley Structures and by Genstar Structures and the Alberta DOT, Canada.

Stanton and Mattock state that their search of currently available literature did not yield any specifics for the design of the steel portion of the connection details. The only quantitative recommendation that could be found was that the plate in the welded connectors be 19 mm (3/4 in.) thick and located typically on 1829 mm (6 ft) to 2438 mm (8 ft) centers. Dimensions are not usually sprecified but are similar to those shown in Figs. 2.3 and 2.4. One referenced article suggested that the connection between adjacent precast members be designed to resist half of the total weight of the bridge deck. This recommendation is derived from the realization that temperature and shrinkage would cause the precast members to shrink and therefore induce tensile forces. It is suggested that the welded connection be adequate to take these tensile forces.

There exist a few variations to the previously presented connection details with the primary difference being that the some of the hardware is replaced by lighter weight elements. Generally, these connection details have been used in prestressed concrete to equalize deflections due to camber in addition to transferring the shear across the joint.

Stanton and Mattock also discuss the behavior of such connections in service. It is noted that "In those very few cases where problems have occurred, they have mostly been associated with the grout key usually cracking at the grout/concrete interface; however in two cases, failure of the grout key was reported. In one case, this was attributed to the low quality of the grout; and in the other case, to rocking of the beam due to a problem with the beam bearing details." There were only three instances of problems with the welded connection detail. In the first case, the problem was attributed to improper welding, in the second case, to improper anchorage fabrication, and in the third case, to failure of the welds which caused concrete spalling in the region.

Stanton and Mattock report only three investigations of connection details between adjoining edges of precast concrete slabs. The first researchers drew the conclusion that "...a properly grouted keyway in combination with either transverse tie rods or welded connectors between adjacent member edges is a very effective way to transfer shear between adjacent members." Stanton and Mattock discounted the work by another researcher due to the fact that the laboratory testing was completed without realistic connection details. In the third investigation, failure modes similar to those observed in the field were indicated. However, the test apparatus did not correctly model field bridge conditions.

From their literature review, experimental investigation, and analytical work, Stanton and Mattock have arrived at the following conclusions:

1. Where a grout key and steel connectors are used to join members, forces from wheel loads are transferred through the grout key. The steel connectors carry shear forces induced before grouting, tension forces due to shrinkage, and tension forces due to twisting under truck loading. They must also provide the clamping forces to mobilize the full shear resistance of the connection, while simultaneously undergoing any imposed rotations.
2. The spacing and strength of steel flange connectors should be based on the shear forces induced before grouting and tension and moments afterwards. Twisting of the girders under live loads is shown to induce tension in the connectors along the joint between the two outer members of a bridge. However, this tension arises largely from compatibility, and not equilibrium

requirements, and its value is significantly reduced by small deformations of the connectors.

3. The edge thickness of precast members should be $6\{(5000)(f_c')\}^{0.5}$ but not less than 152 mm (6in.).
4. The spacing of welded connectors should be not more than the lesser of 1,520 mm (5 ft) and the width of the flange of the precast member.
5. Welded connector anchors should be located within the middle third of the slab thickness.
6. The tensile strength of each connector and of its anchor, T_n should be not less than

$$T_n = T_1 + T_2 \tag{16}$$

with:

$$T_1 = \frac{16(\sin\alpha - \mu_1 \cos\alpha)}{\cos\alpha + \mu_1 \sin\alpha} \geq 6 \tag{17}$$

and

$$T_2 = 0.5 s W_m N_m \mu_2 \tag{18}$$

where

α = Maximum inclination of sloping faces of grout keys, deg.
μ_1 = Coefficient of friction between key and concrete (0.5).
μ_2 = Coefficient of friction between beams and bearings.
s = Longitudinal spacing of welded connector, ft.
W_m= Weight per foot of beams and topping, lbs/ft.
N_m = Number of members in width of bridge.

A variety of precast concrete connection details are outlined by Biswas (8) in a special report on Precast Bridge Deck Design Systems. These are summarized in Figs. 2.5 through 2.9. Generally, these details are quite complicated and the wide variation in parameters leads to the conclusion that their behavior is not well understood.

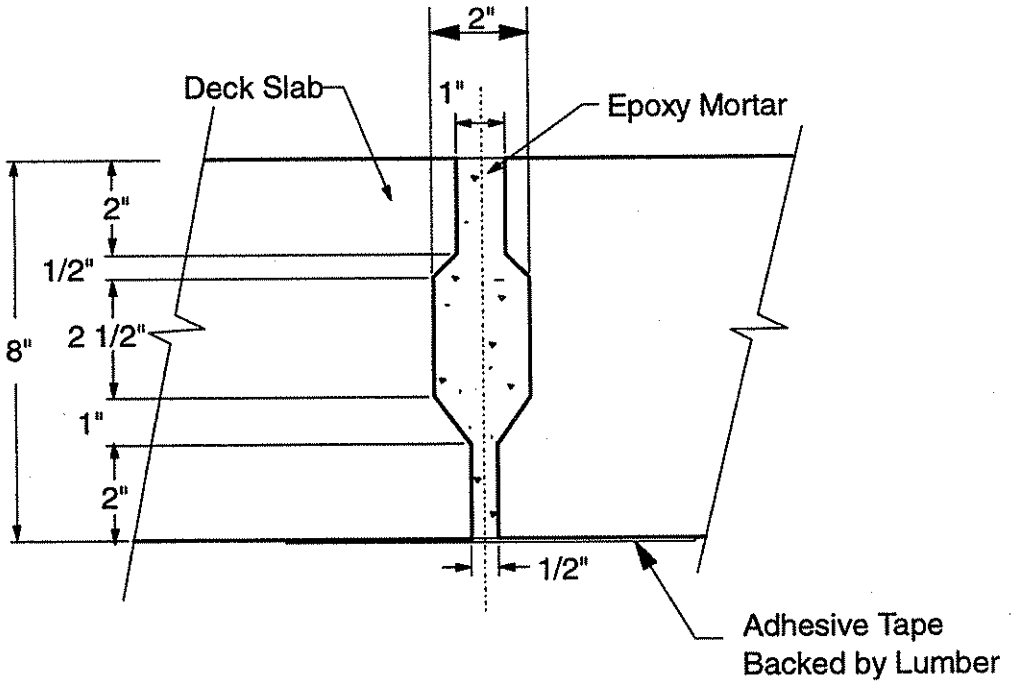

Figure 2.5. Joint between precast slabs, New York Thruway Authority.

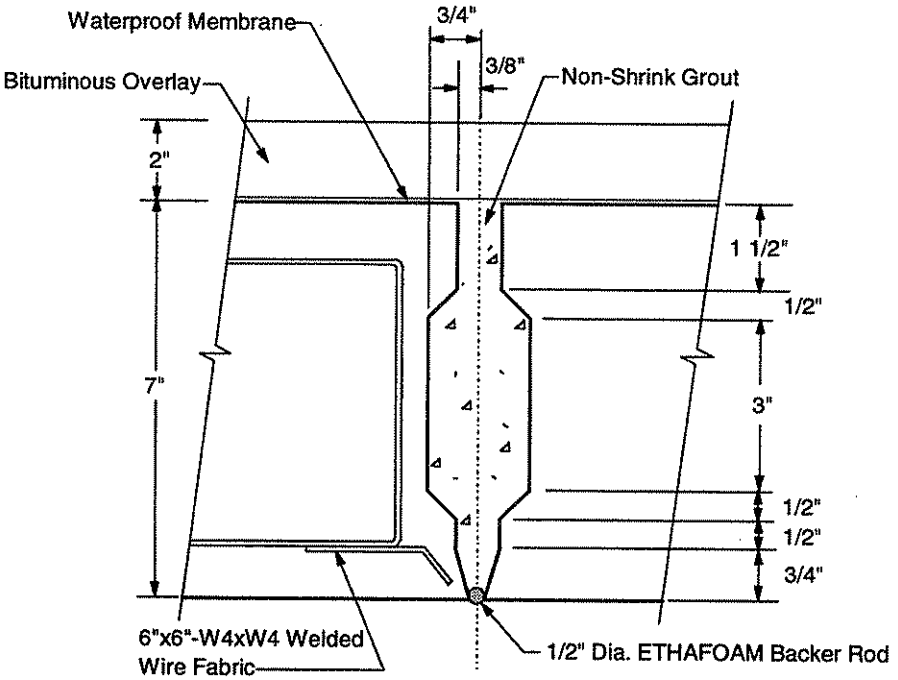

Figure 2.6. Joint detail, Connecticut River Bridge.

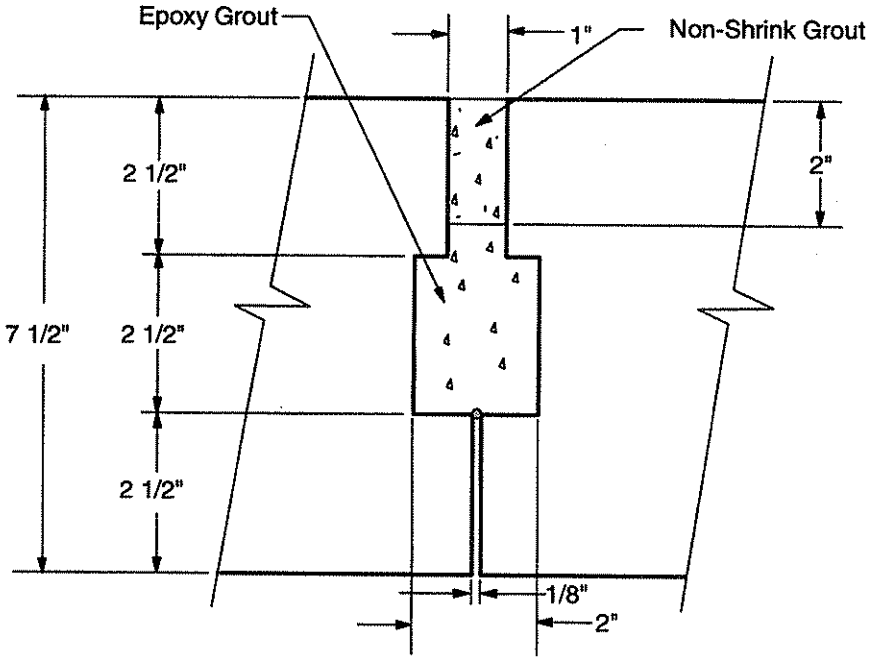

Figure 2.7. Connection details, Bridge No. 6, NYSDOT.

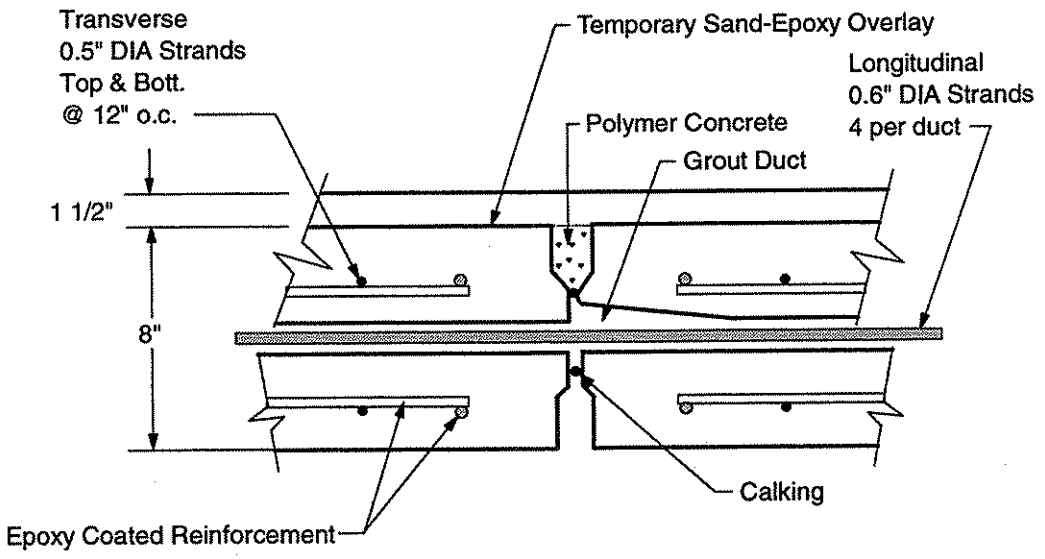

Figure 2.8. Joint section details, Woodrow Wilson Memorial Bridge.

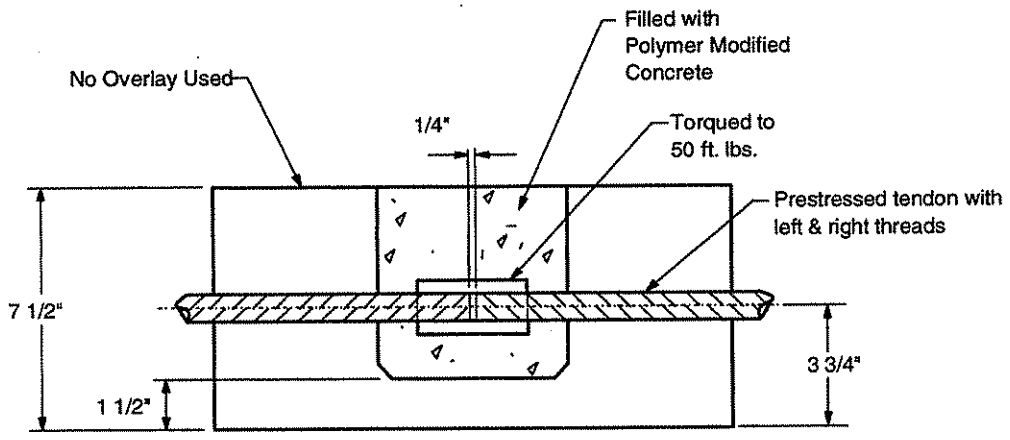

Figure 2.9. Transverse joint details, Milford, Montague Toll Bridge.

Berger (9) discusses the advantages and disadvantages of butted, keyed, and grouted joints, as well as giving examples of typical joint details. As for butt joints Berger states, "The butt joint is simple to cast and erect but has the disadvantage of providing no inherent shear transfer capacity. This can be developed through frictional resistance from longitudinal postensioning."

Keyed joints, although much more difficult to construct due to the tight tolerances required to ensure proper behavior, offer the advantage of a positive shear transfer mechanism. Typical keyed joints are shown in Fig. 2.10. Typically, these have been hard to construct in a precise manner and, unless great care has been exercised, the final result is less than desireable.

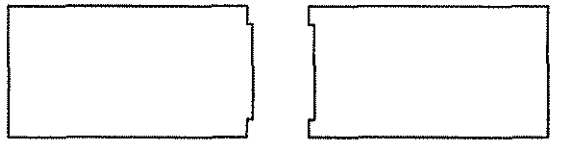

a. Detail 1

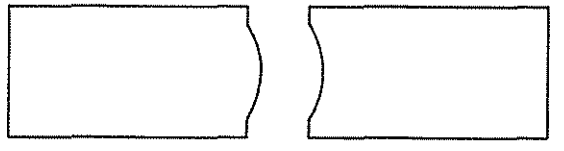

b. Detail 2

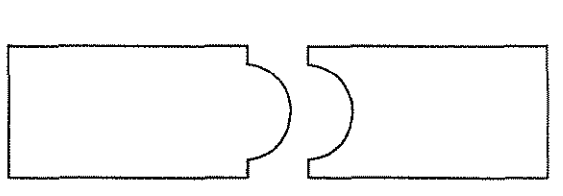

c. Detail 3

Figure 2.10. Typical keyed joint details.

Grouted joints have been effectively used by a number of different agencies. The advantage of the grouted joint over the keyed joint is the fact that the construction tolerances are much wider while at the same time offering the positive shear transfer mechanism.

Hucklebridge, El-Esnawi, and Moses (10), based on their investigation of shear keys, have formulated some conclusions on their performance in-situ. Every structure that was investigated had some magnitude of relative displacement across precast panel joints. These relative displacements are thus assumed to occur due to the fracture of the grouted joint. A finite element investigation along with the field observations lead to the conclusion that "an intact shear key should not permit more than 0.0254 mm (.001 in.) relative displacement between adjacent girders...".

Additionally, they noted that joints that were obviously distressed (evidence of water leakage or reflective cracking in the cast-in-place deck) consistently gave the highest magnitudes of relative displacements except when the load was applied far away from the damaged joint. However, most of the structures (even those with obvious distress) still exhibited reasonably good load distribution across the precast girders.

From their observations, it was concluded that tie bars basically had no effect on the shear transfer or the performance of the joint in-situ. Generally, joints that showed distress (i.e., leakage and/or reflective cracking) with or without tie bars basically had the same effectiveness in transferring shear forces across the precast joints. They also noted that shear key failure is the rule and not the exception. Failed shear keys results in degradation of the concrete deck and reinforcing steel due to the introduction of water and deicing salts in the failed joint.

3. SPECIMEN DETAILS

3.1 Overview

The various specimens that were tested in this investigation are described in this chapter. Where possible, full scale specimens were used. In some instances, as described in the following sections, small scale specimens were used. These small scale specimens were appropriately modeled to satisfy the principles of similitude and were fabricated using the same materials as used in the prototype (i.e., concrete and steel).

3.2 Small Scale Connector Specimens

One of the major concerns in the proposed bridge system was the connection of adjacent Precast double-T units, henceforth, referred to as PCDT units. Connections used between PC concrete units by others were reviewed in Chp. 2. Since none of these connections has been effective in eliminating reflective cracking in the cast-in-place (CIP) portion of the deck, alternate connection details were investigated in this study. Although the connections need to resist a number of different types of loads at various times during construction, simplicity of construction was also of concern. Many of the connections presented in Chp. 2 required the use of multiple components and were therefore deemed inappropriate for the proposed system.

When constructing a bridge using precast units, the transfer of forces from unit to unit is critical to the bridge's structural performance. Load transfer is accomplished by two mechanisms. First, the CIP portion of the deck (reinforcement plus concrete) provides a continuous shear transfer mechanism. Any degradation of the concrete or reinforcing steel will obviously reduce the effectiveness of this transfer mechanism. Propagation of reflective

cracking over the interface between PCDT units due to relative displacements between the units can result in degradation of the CIP portion of the deck. To reduce the possibility of this reflective cracking, two connections were developed to reduce relative deflections between adjacent PCDT units.

After the PCDT units are placed, connections between the units have to resist various types of construction loads. To ensure that construction loads can be distributed between the PCDT units during construction, the connections have to resist shear forces, axial forces, as well as moments. Of primary concern at this stage of construction is the transfer of moment. With this in mind, the research team decided that a connection that was symmetric about the mid-depth of the PC slab would be most efficient. On the other hand, the internal force transferred through a connection after the CIP concrete deck is in place is primarily a shear force; thus, the connection needs sufficient strength to resist these forces as well. Details of the first connection investigated are shown in Figs 3.1 and 3.2. Shown in Fig. 3.1 are the dimensions of the connection; note the reinforcement is on 102 mm (4 in.) centers so that there is adequate clear distance to develop the full strength of the reinforcement. The connection illustrated consists of a C4x7¼ channel with three Grade 60 #4 reinforcing bars shop welded to the face of the channel. The reinforcing steel is embedded in the PC concrete (see Fig. 3.2) thereby developing the connection's moment resistance. The length of the reinforcing steel was set at 640 mm (24 in.) to ensure that the full capacity of the reinforcing steel could be developed, assuming the PC concrete has a 28 day compressive strength of 24,130 kPa (3500 psi). Additionally, when the connection is used in bridges this length of reinforcement extends into the transverse negative moment region of the deck so that the steel

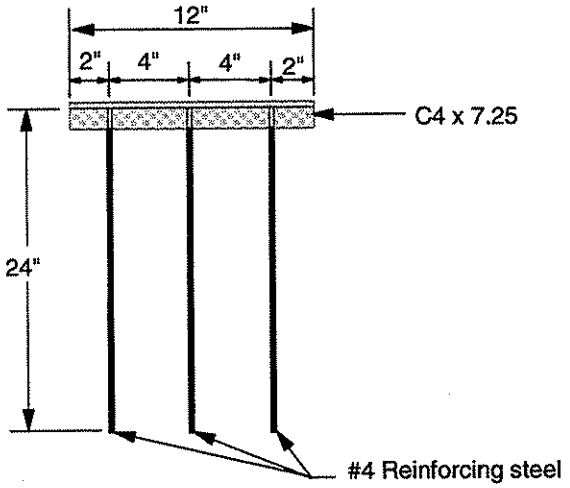

a. Top View

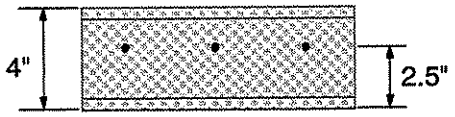

b. Front View

Figure 3.1. Individual PC concrete connection details.

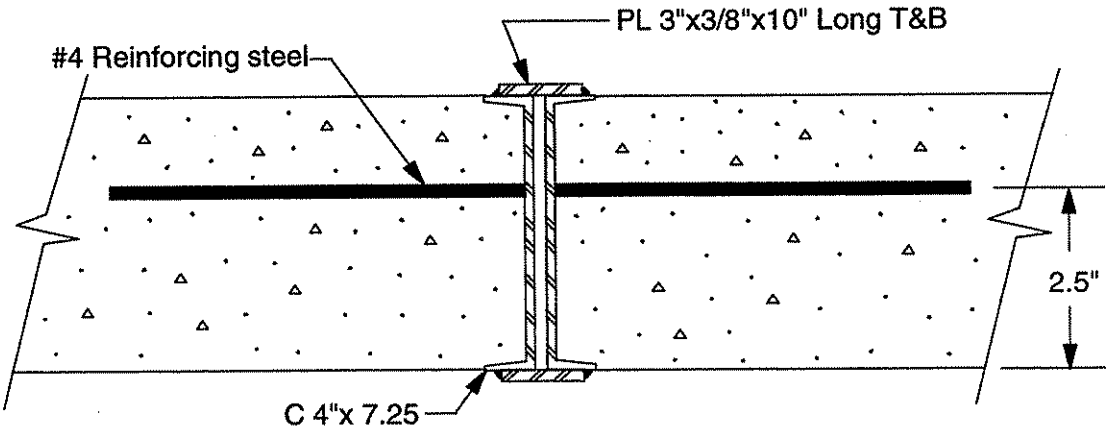

Figure 3.2. Side view of connection after welding two units together.

is not terminated in a tension zone. The welds in all the PC connectors were performed by an uncertified welder with minimal experience to simulate conditions one might find in the field. All welds were performed with a stick welder and consist of two passes of a 5 mm (3/16 in.) EE70 weld metal.

Shown in Fig. 3.2 is the connection detail when two adjacent units are connected. Plates, 76 mm x 10 mm x 254 mm (3 in. x 3/8 in. x 10 in. long), are welded to the top and bottom flanges of the channels as shown. Under normal construction conditions, the channels most likely will be slightly misaligned. Thus, filler plates may be needed to fill any "gaps" between the channels in two adjacent units. Welding of the plates was also completed by an uncertified welder with minimal experience.

As previously noted, the channels in adjacent units were not always "flush" when the units were placed next to each other. Generally, the gap was less than 25 mm (1 in.) but was as much as 51 mm (2 in.) in a couple of instances. The misalignment was due to a number of things. First, during pouring of the PC concrete, the channels had a tendency to move due to the impact forces that occurred during pouring and screeding of the concrete. Secondly, the formwork used to cast the small scale speciemns and PCDT units was not "perfectly" straight.

The second detail developed was a bolted connection similar to the first one. The connection consisted of casting voids (i.e., bolt holes) in the PC concrete to accommodate through bolts. Adjacent PCDT units were then connected by top and bottom steel plates which were bolted (using the bolt holes) to the PCDT units. Reinforcement bar hooks, that wrapped around the bolt holes, were provided to transfer connection forces into the PC

concrete. Even though the bolted connection was being employed on small-scale specimens in the laboratory, there were misalignment problems. Under field conditions with full scale PCDT bridge elements, it was envisioned that there would be even greater misalignment problems. Thus, it was concluded that the bolted connection was not feasible.

Shown in Fig. 3.3 is a sketch of the PC slab elements used in the testing of the connections; two of these units were connected (see Fig. 3.2) in the connection tests. As shown, the length of the elements was 533 mm (21 in.) and the width was 457 mm (18 in.). The depth of the concrete varied from 102 mm (4 in.) when there was only PC concrete (as shown in Fig. 3.3) to 204 mm (8 in.) when there was 102 mm (4 in.) of PC concrete plus 102 mm (4 in.) of CIP concrete. Note the PC concrete was scarified to obtain bond with the CIP concrete.

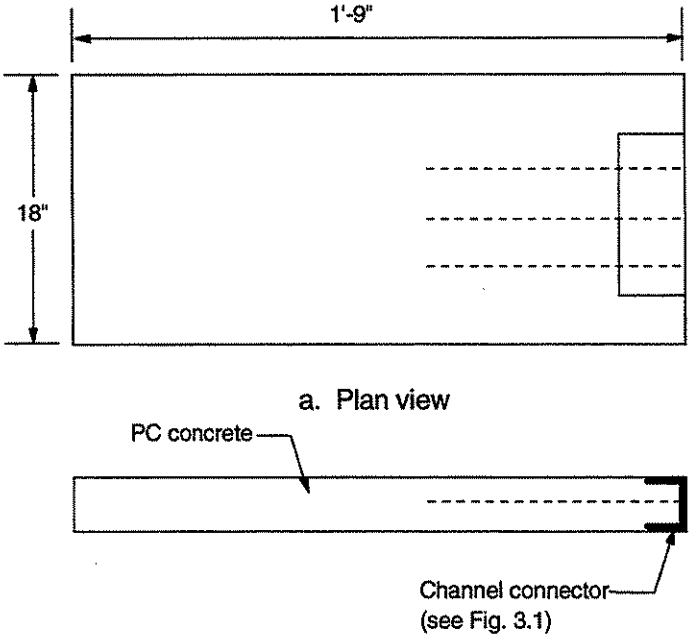

Figure 3.3. PC slab elements used in small scale connector tests.

3.3 PCDT Specimens

The bridge replacement alternative (Concept 1) presented in this report utilizes pre-fabricated PCDT units composed of two steel beams and a composite concrete deck. The units may be constructed off site and then transported to the field where multiple units can be connected together to give the desired width of bridge. A CIP concrete deck is then constructed over the connected PCDT units to obtain the required depth of bridge deck. It is envisioned in certain situations that this type of bridge could be constructed using salvage steel bridge beams thus reducing construction costs. The model bridge presented in the subsequent sections of this report was constructed using salvage steel beams.

As shown in Fig. 3.4, the PCDT unit specimens that were constructed for the model bridge were 2137 mm (7 ft) wide. Three units were used to provide and overall bridge width of 6401 mm (21 ft). Although a 8534 mm (28 ft) wide model bridge (4 PCDT units) was desired, there was inadequate space in the Iowa State University (ISU) Structural Engineering Laboratory (SEL).

The PCDT units used in the model bridge have a 102 mm (4 in.) thick deck and two W21x62 steel beams with a center-to-center spacing of 1077 mm (3.5 ft). This deck thickness was selected to minimize the weight of the individual units yet provide sufficient structural strength so that the units could be moved without damaging them. The span length of the PCDT units was limited to 9754 mm (32 ft) for two reasons - space limitation in the SEL and the length of beams available for use in the project.

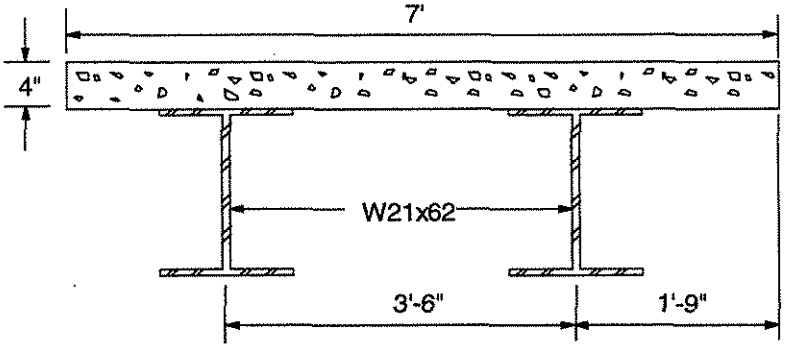

Figure 3.4. Nominal cross sectional dimensions of PCDT units used in model bridge.

3.3.1 Reinforcing Steel in the PC Deck

Steel reinforcement used in the PC deck is shown in Fig. 3.5 As can be seen, the PC deck has #3 reinforcement spaced transversely on 305 mm (12 in.) centers and #4 reinforcement spaced longitudinally on 165 mm (6.5 in.). The reinforcement is Grade 60 deformed bars. The reinforcement was designed according to AASHTO (5) LFD requirements for bridge decks and serves as the bottom slab steel for the complete bridge deck (PC concrete plus CIP concrete). Reinforcement used in the CIP portion of the deck (which serves as the top steel reinforcing) is described in Sec. 3.5. In Fig 3.5b, one may observe the 38 mm (1.5 in.) bar supports used and the welded shear studs (which are discussed in Sec. 3.3.2). The Dywidag bars that are attached to the top flanges of the two steel beams are for connecting the lift brackets shown in Fig. 3.6. There are four of these brackets per unit. To control the differential shrinkage between the PC and CIP concrete due to the age difference, # 4 reinforcement spaced at 1676 mm (5.5 ft) was extended from the PC concrete into the CIP concrete. The placement of #4's at 1676 mm (5.5 ft) along the edges follows the recommendations of Seible (4) for concrete overlays in bridge rehabilitation (see Chp. 2).

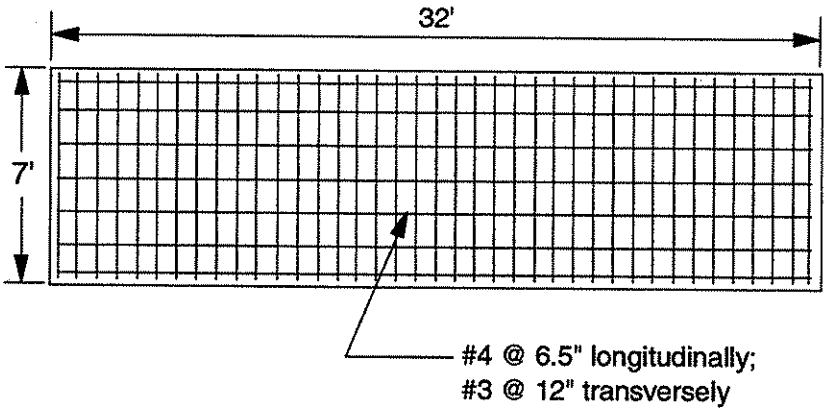

a. Plan view

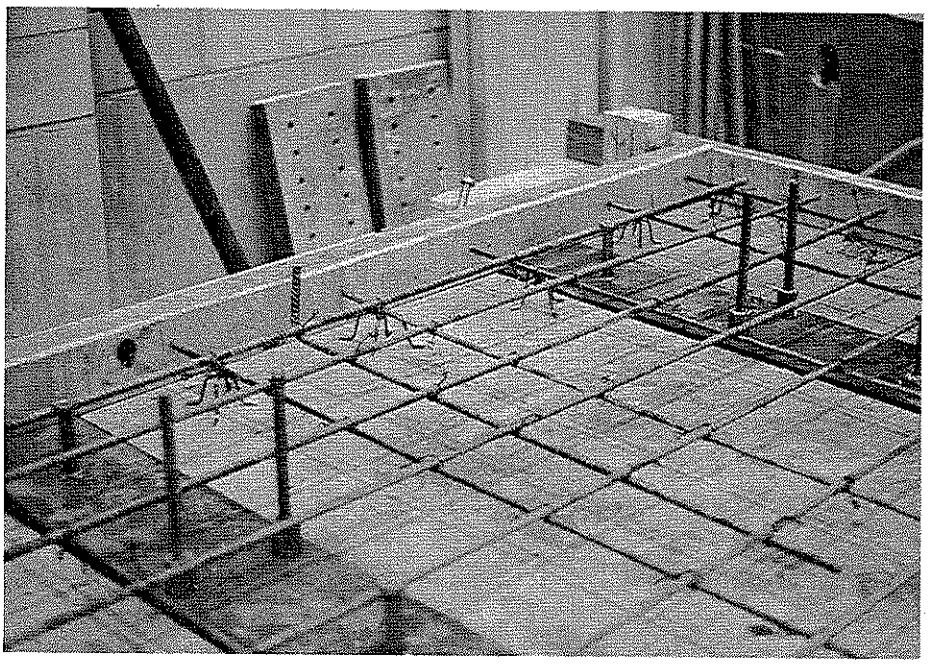

b. Photograph of reinforcement used in PC deck

Figure 3.5. Reinforcement details in the deck of the PCDT units.

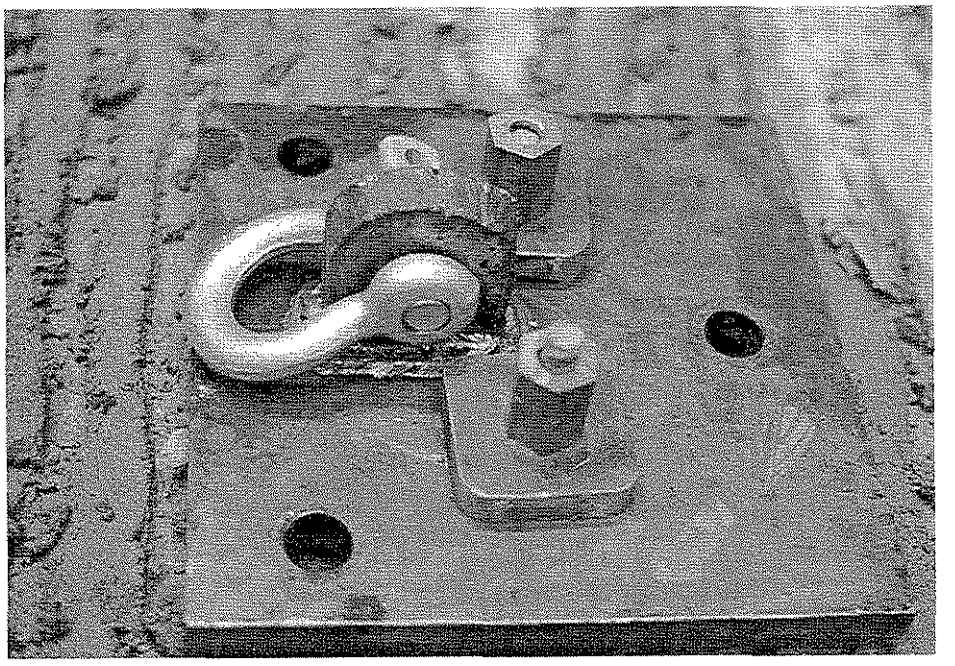

Figure 3.6. Photograph of lifting bracket.

3.3.2 Welded Shear Studs

Composite action between the PC concrete deck and steel beams was obtained by using S3L ¾"x4" welded shear studs (16 per beam, 32 per unit). The location of the studs is shown in Fig. 3.7. The number of shear connectors was determined using the design strengths of the studs provided by the manufacturer for strength alone (i.e., fatigue requirements were neglected as the laboratory bridge would be tested under static loads only). As the length of the shear studs and the deck thickness are both 102 mm (4 in.), the top of the shear stud is at the top surface of the deck (i.e., no cover). This will not be a problem, as 102 mm (4 in.) of

CIP concrete will be added in the field, which will provide adequate cover. Prior to installing the shear studs, the top surface of the top beam flange was prepared by removing the rust from the steel beams by grinding to a smooth surface. The shear stud locations were then marked and the studs "shot" into place. To ensure that the stud welds have achieved full penetration, the normal test of bending the stud at the beam level to a 45° angle was employed. All welded studs tested in this manner passed this strength test.

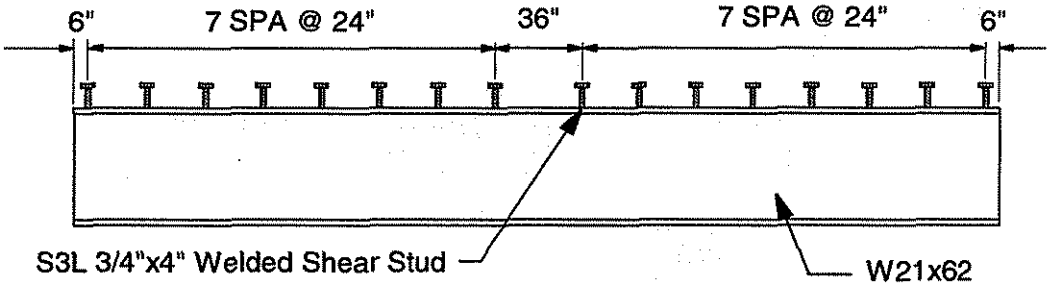

Figure 3.7. Location of shear studs.

3.4 Construction of PCDT Units

The individual PCDT units that comprise the model bridge were constructed over a two month period. The units were fabricated and cast using normal construction procedures; individual units were cast in a shored condition. Since they were available, surplus beams of the same size were used to support the formwork. In situations where extra beams are not available, one would use a system of deck hangers to support the formwork. As previously noted, each PCDT unit consists of two steel beams. However during casting, an additional seven beams were used to support the formwork as shown in Fig. 3.8.

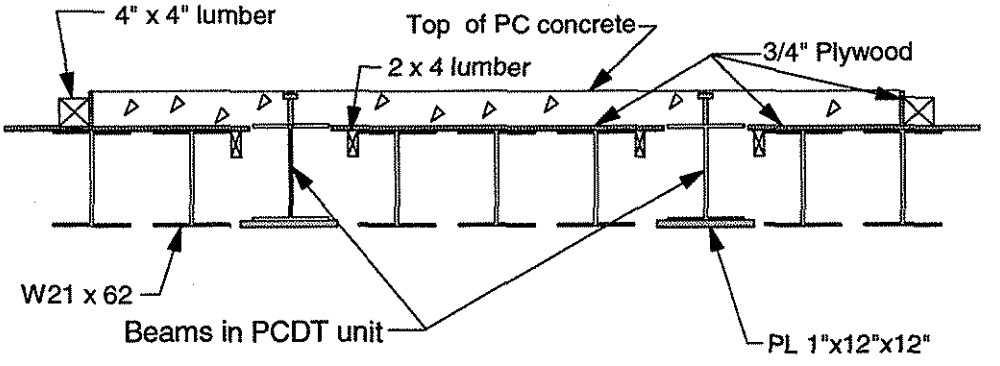

Figure 3.8. Formwork used to cast individual PCDT units.

The beams that were part of the PC units were placed on 25 mm (1 in.) thick plates placed continuously along the length of the beams so that the elevation of the top flange of the two beams in the PC units was 25 mm (1 in.) higher than the top flange of the support beams. The formwork consisted of 19 mm (¾ in.) plywood which gave a nominal 6 mm (1/4 in.) overlap between the steel flanges and the concrete. This 6 mm (1/4 in.) overlap will provide sufficient lateral support to the top flange of the steel beams in the laboratory specimens, however it is not recommended for use in actual practice. In the field, formwork should be placed so that the entire top flange is supported (i.e., bottom surface of concrete and bottom surface of top flange are at the same elevation). The 102 mm x 102 mm (4 in. x 4 in.) lumber and vertical 19 mm (¾ in.) plywood provided the lateral containment for the concrete and provided a guide for screeding the concrete to the desired depth. The cross-section in Fig. 3.8 is near mid-span of the beams; the same formwork scheme was used to form the ends of the specimens. A photograph of the formwork is shown in Fig. 3.9; the shear studs previously described are also seen in this figure.

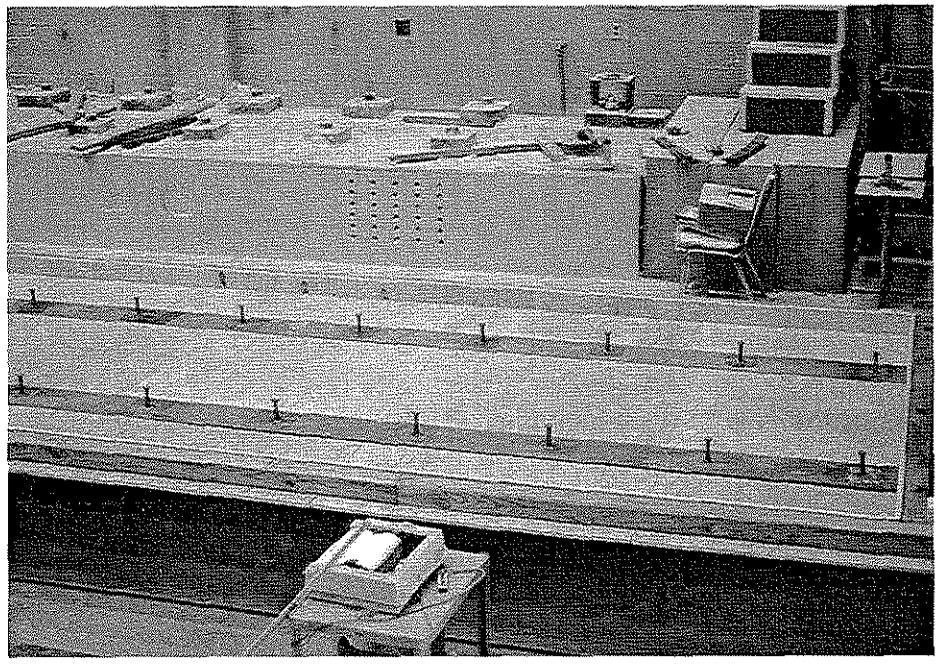

Figure 3.9. Photograph of formwork for PC concrete deck.

To accommodate the forming of the 102 mm (4 in.) CIP deck, anchors for supporting the formwork for the CIP deck were positioned in the PC portion of the deck. The anchors were for 13 mm (½ in.) spiral bolts with a maximum depth of embedment of 38 mm (1.5 in.); an example of these anchors is shown in Fig. 3.10. The anchors were tied to the reinforcing steel to ensure that they would remain in the desired position during casting. Although some of the anchors did move during placement of the concrete, they were easily located since the formwork had been premarked with their approximate location. In some cases, the concrete had to be chipped away as the anchor had moved into the concrete. These anchors were placed on approximately 1219 mm (4 ft) centers. Rather than anchoring the spiral anchors to

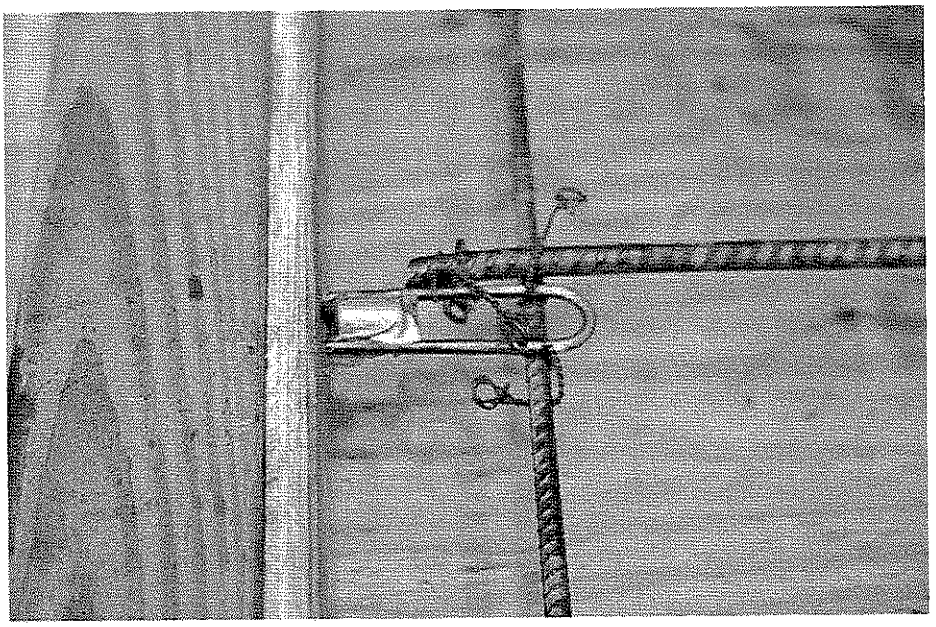

Figure 3.10. Photograph of anchors for attaching the CIP concrete formwork.

the reinforcement, it is recommended that holes be drilled in the formwork and the spiral anchors be "bolted" to the formwork. One of the channel connectors previously described is shown in Fig. 3.11.

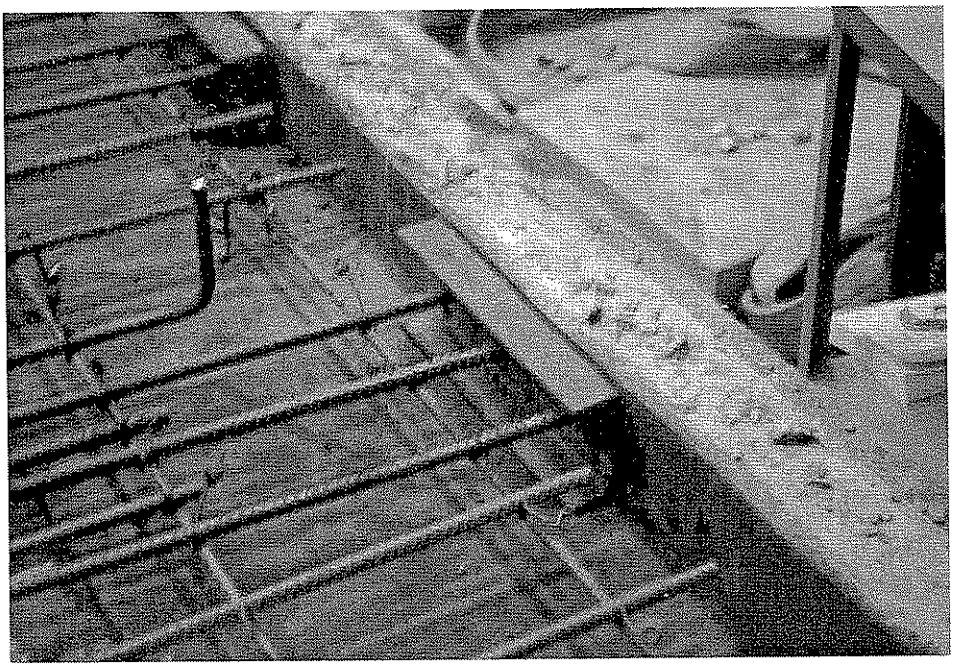

Figure 3.11. Photograph of PC portion of connection.

Casting of the concrete in the individual PCDT units was completed in one continuous pour. Before any concrete was placed, the ready-mixed concrete was tested for air and slump requirements and cylinders were cast. Concrete was transported from the ready-mix truck to the formwork using a concrete bucket and the SEL overhead crane. Using this combination, the concrete was "dumped" into the formwork and spread accordingly. After adequate spreading, the concrete was vibrated with an internal vibrator. The top surface was then screeded to obtain the desired deck thickness. A light trowling was then completed to ensure that no voids had been missed in screeding. Since composite action between the two portions of the concrete deck was required, the top surface of the PC portion of the deck was intentionally scarified in the transverse direction to provide a mechanism for shear transfer across the interface between the PC concrete and the CIP concrete. "Grooves" were scarified in the wet concrete to a depth of approximately 6 mm (¼ in.) spaced at 25 mm (1 in.) intervals as shown in Fig. 3.12. The process of scarifying the deck is shown in Fig. 3.12a while the final product is shown in Fig. 3.12b. As previously described, the two Dywidag bars projecting from the concrete are for attaching lifting brackets .

To remove the units from the formwork, the end formwork was removed and the units were lifted using the overhead crane in the SEL. Chains were connected to the units with the lifting devices shown in Fig. 3.6. These devices were fabricated using 305 mm x 305 mm x 25 mm (12 in. x 12 in. x 1 in.) steel plates with an 25 mm (1 in.) thick "eye" welded normal to the plate. A clevice of adequate strength was placed in the eye to accommodate the lifting chains. The lifting brackets (4 per unit) were attached to the PCDT units using 10 mm (3/8 in.) Dywidag bars (2 per bracket) that had been bolted to the upper flanges of the steel beams

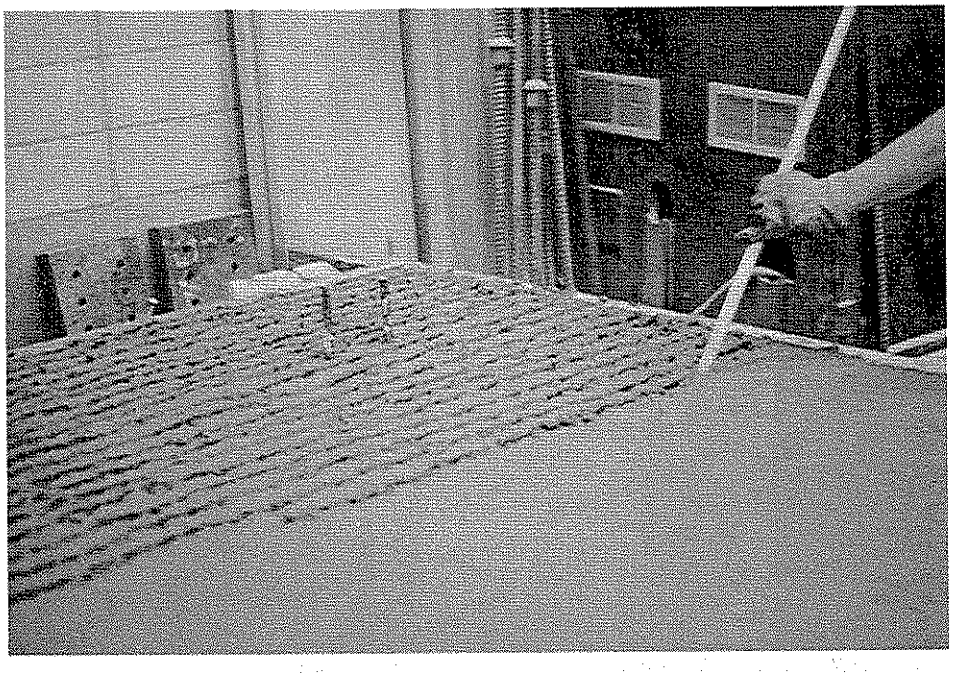

a. Scarification of PC concrete.

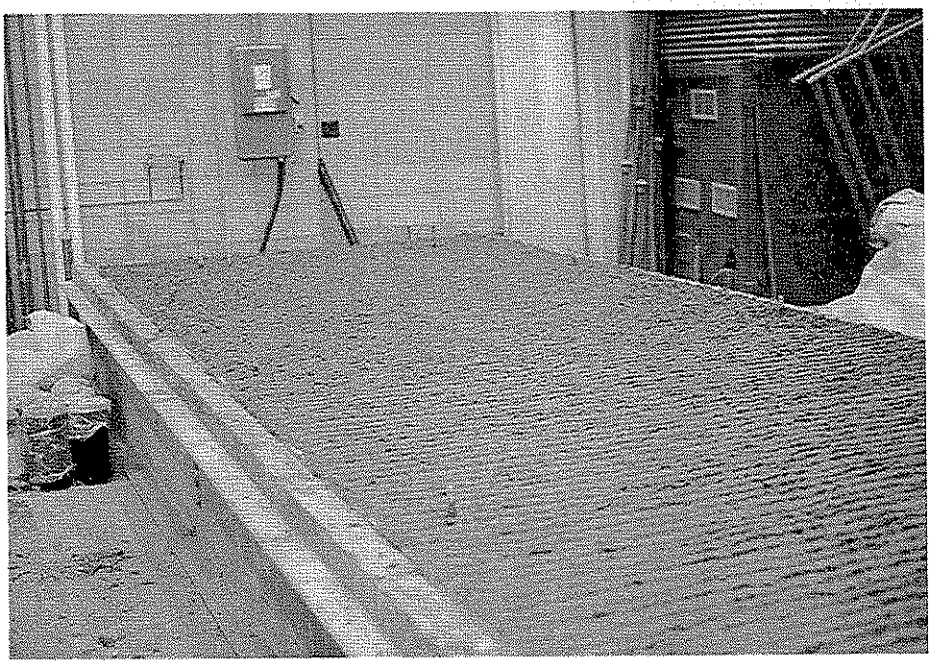

b. Scarified PC deck

Figure 3.12. Photographs of scarified PC deck.

prior to casting (see Fig. 3.5). This arrangement transmits the majority of the load (i.e., approximately one-fourth the specimen weight to each bracket) to the steel beams rather than to the "new" concrete. Figure 3.13 shows one of the PCDT units as it is being lifted from its formwork.

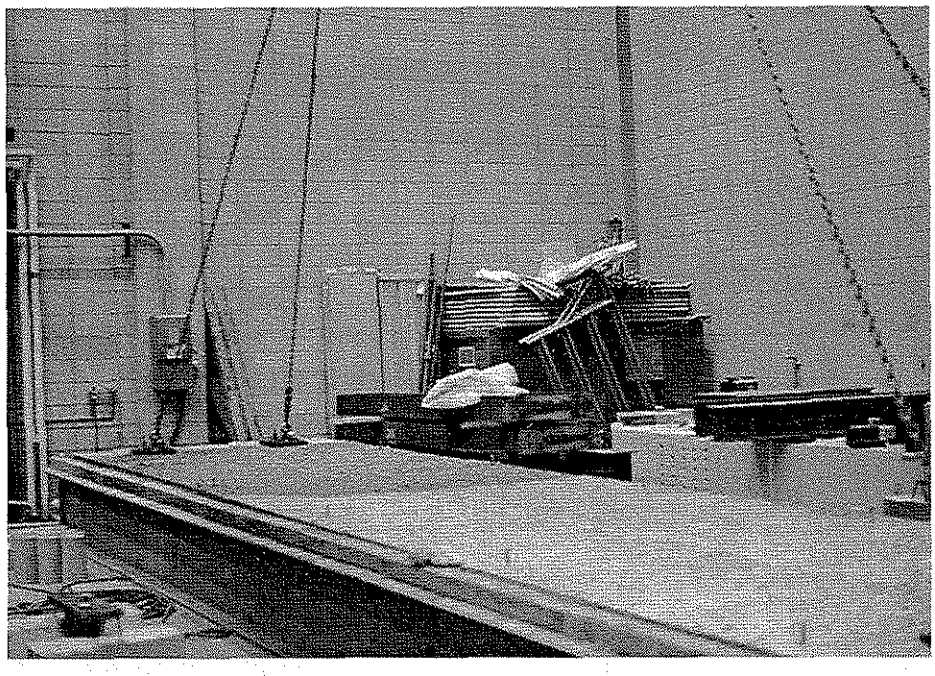

Figure 3.13. Photograph of lifting PCDT unit from formwork.

3.5 Model Bridge Specimen

As previously discussed, the model bridge specimen was comprised of three 2134 mm (7 ft) wide PC units. Overall dimensions of the model bridge are shown in Fig. 3.14 as well as the location of the diaphragms.

3.5.1 Reinforcing Steel

Steel reinforcement used in the CIP concrete is shown in Fig. 3.15. As can be seen, the CIP deck has #3 reinforcement spaced transversely on 241 mm (9.5 in.) centers and #4

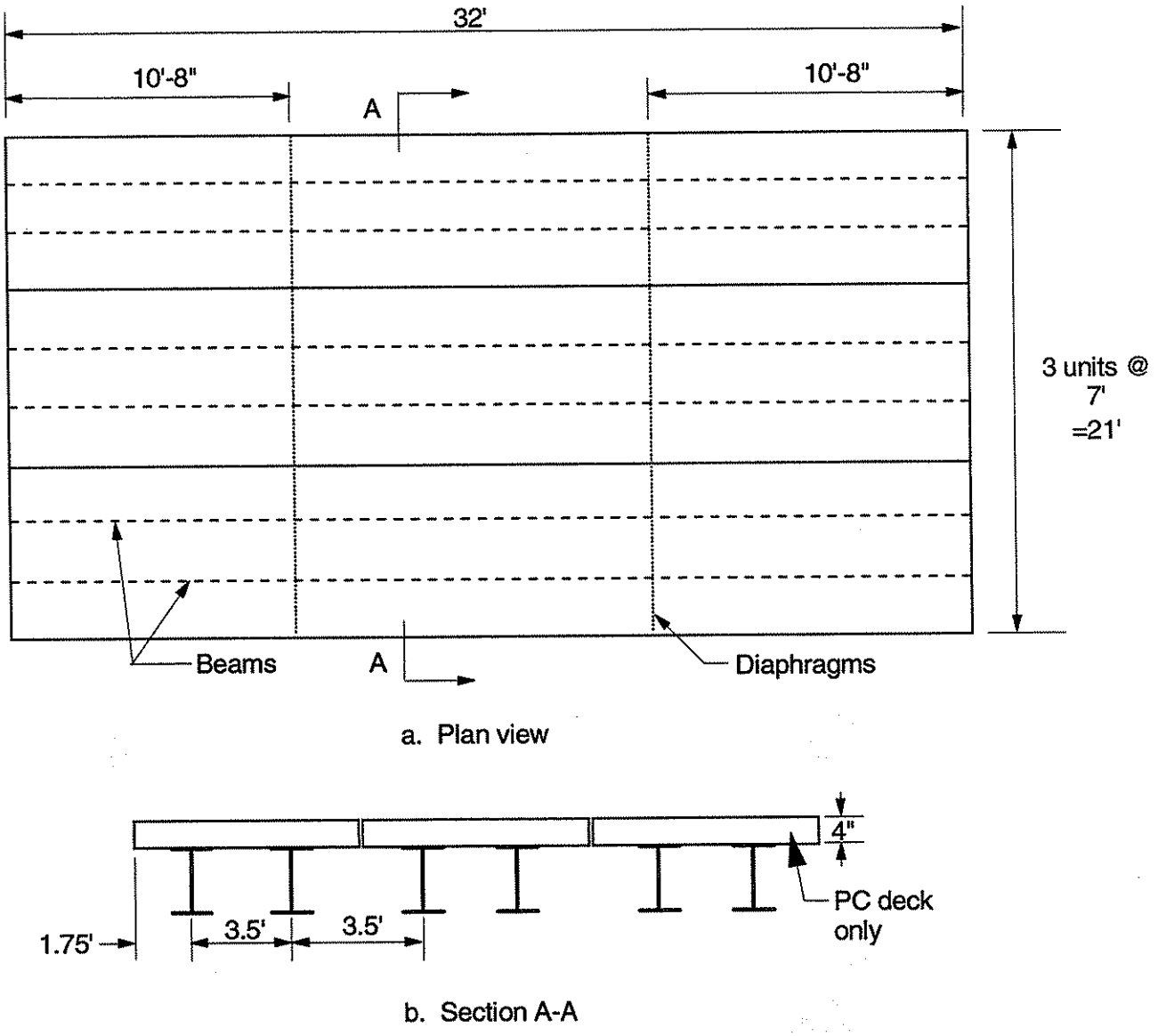

Figure 3.14. Overall dimensions of model bridge.

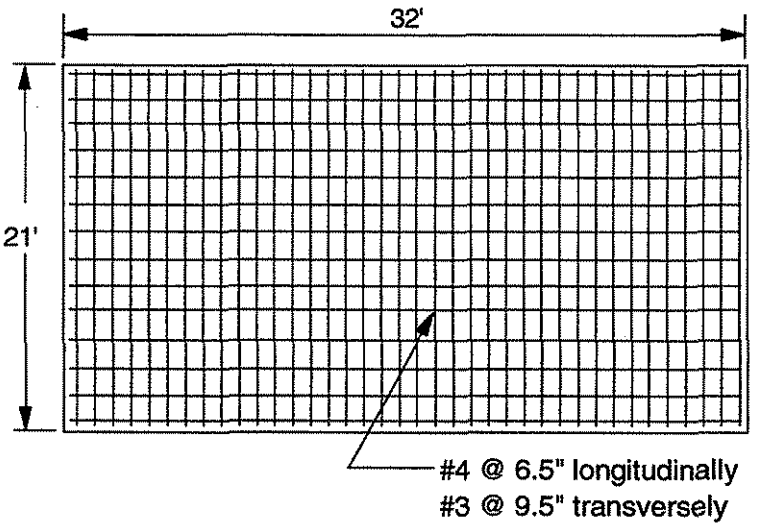

a. Plan view

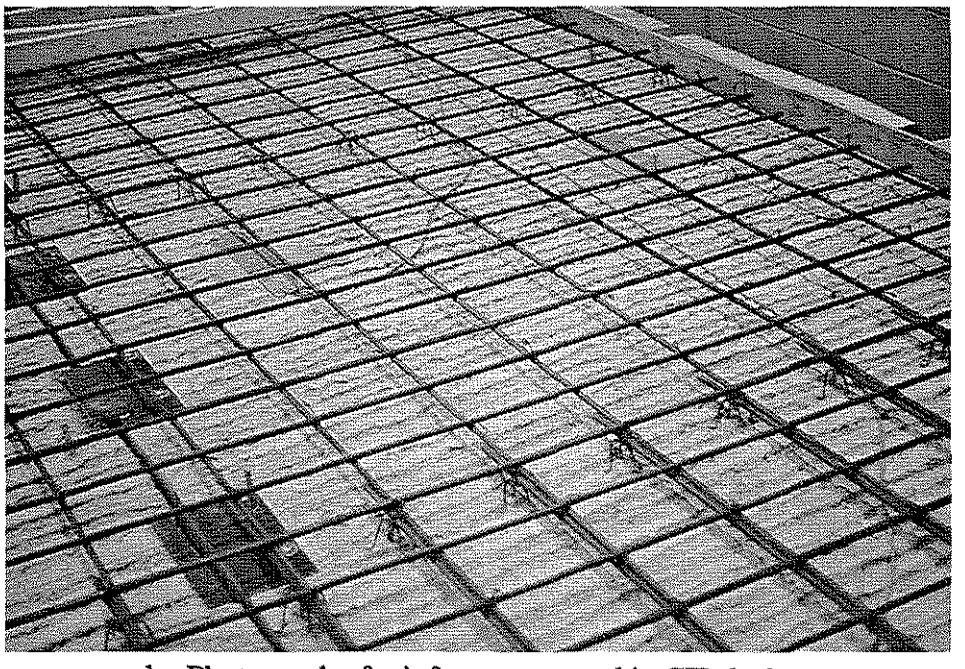

b. Photograph of reinforcement used in CIP deck

Figure 3.15. Reinforcement details in the CIP portion of the deck.

reinforcement spaced longitudinally on 165 mm (6.5 in.) centers. The reinforcement is Grade 60 deformed bars. The reinforcement was designed according to AASHTO (4) LFD specifications for bridge decks and serves as the top layer of steel in the complete bridge deck.

The first PCDT unit was constructed for use in the "handling strength" tests which are described in Chp. 4. Since the specifics of the connection detail had not been finalized, no PC connections were included in this unit. However, since this unit was not damaged in the handling strength tests it was concluded that this unit could be used in the model bridge with some type of retrofit connection. Although there was some concern with the strength and stiffness of this connection, there were no problems with its performance in any of the tests. A bolted connection was designed that could be retrofitted to the first cast unit. Details of this retrofitted connection are illustrated in Fig. 3.16.. Shown in Fig. 3.17 is a photograph of the retrofitted connection detail in the left PCDT unit aligning with the channel connection in the right PCDT unit. The first cast PCDT unit needed to be modified to accept the retrofitted connection. At the locations where it was desired to install the retrofit connections, the PC concrete was ground on the top and bottom surfaces to the depth of the connection plates (see Fig. 3.16). Holes were then drilled through the PC concrete and top and bottom plates. Through bolts were installed and tightened thus connecting the steel plates to the deck.

3.5.2 Diaphragms

Determining the influence of interior diaphragms on load distribution was another objective of this investigation. As shown in Fig. 3.14, diaphragms were installed at the 1/3 points of the span (3251 mm (128 in.) from each end). The diaphragms consisted of MC8x20

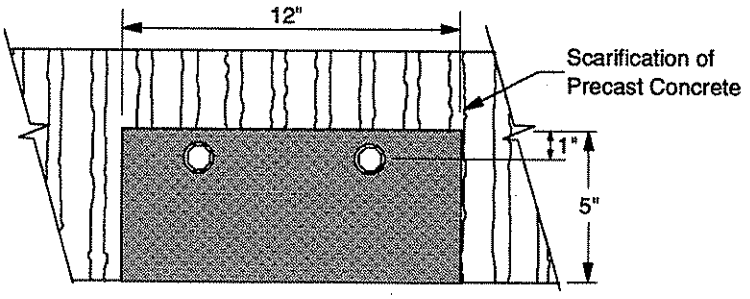

a. Plan view

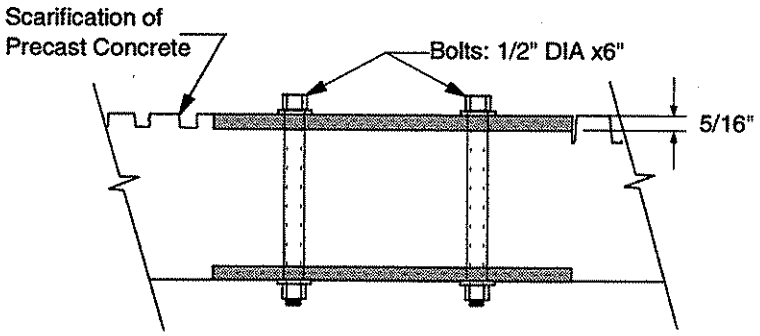

b. Side view

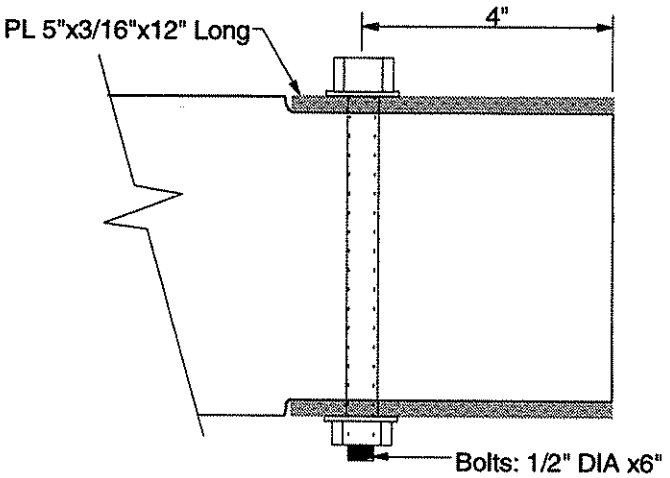

c. End view

Figure 3.16. Retrofitted PC connection.

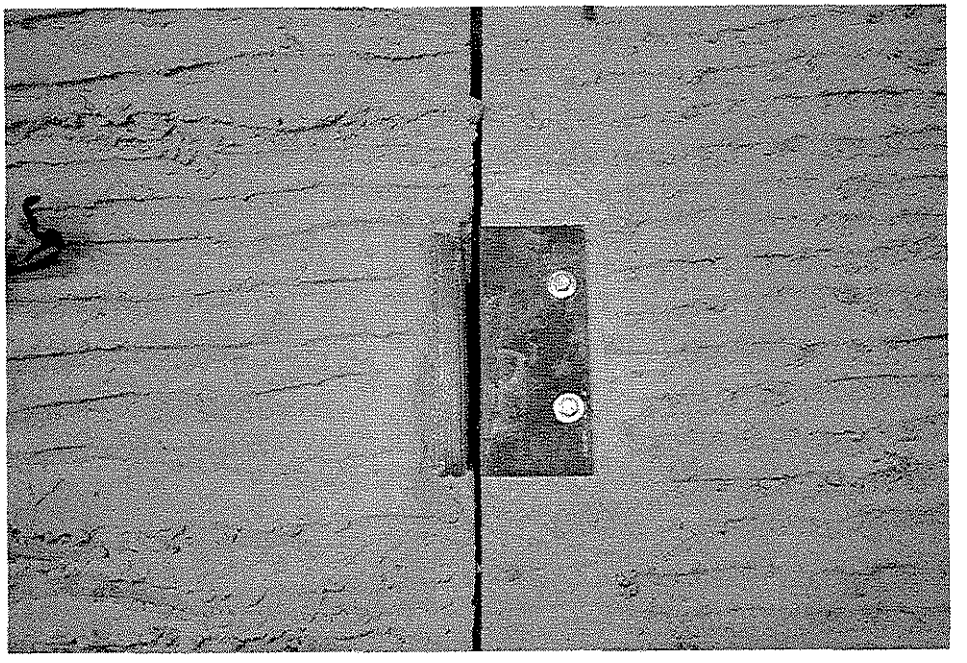

Figure 3.17. Photograph of retrofitted and channel connections.

channels bolted to 127 mm x 76 mm x 10 mm (5 in. x 3 in. x 3/8 in.) angles that were in turn bolted to the webs of the beams as shown in Fig. 3.18. The diaphragm detail consists of bolted connections that were tightened to slip critical conditions by the turn of the nut method; all bolts are 19 mm (3/4 in.) in diameter and are high strength A325 with washers appropriately placed.

The details for the angles and the channels are shown in Figs. 3.19 and 3.20, respectively. All holes were drilled to 3 mm (1/8 in.) in diameter larger than the bolt diameter. As shown in Fig. 3.21, the diaphragms were installed at two different positions on the web to determine the influence of position on the behavior of the bridge. The channels were

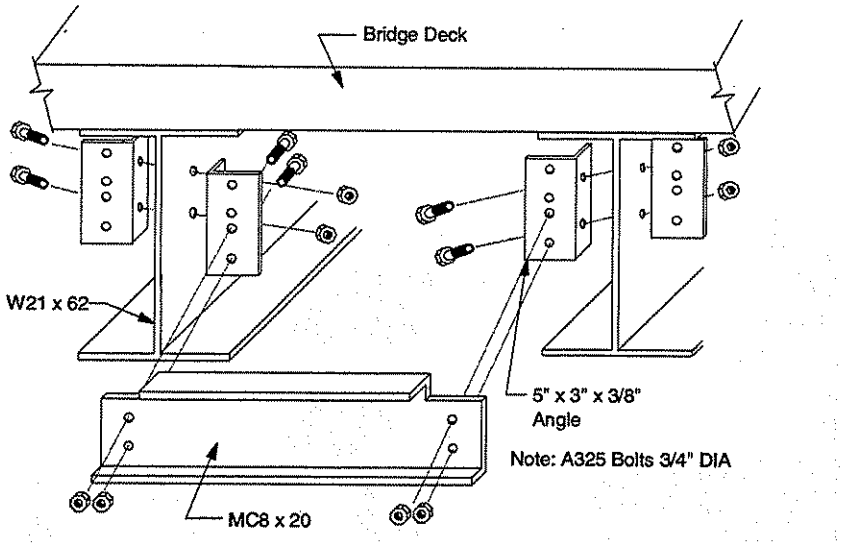

Figure 3.18. Overview of diaphragm details.

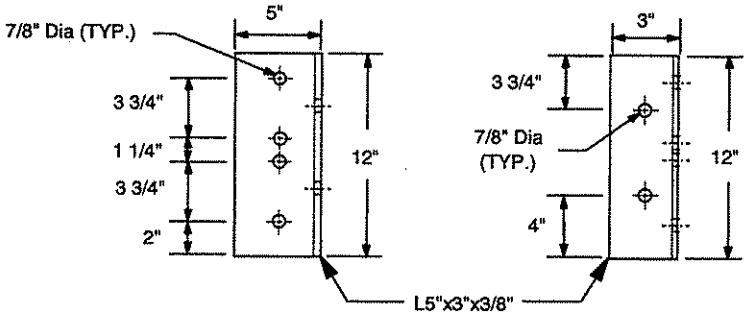

Figure 3.19. Details of diaphragm angles.

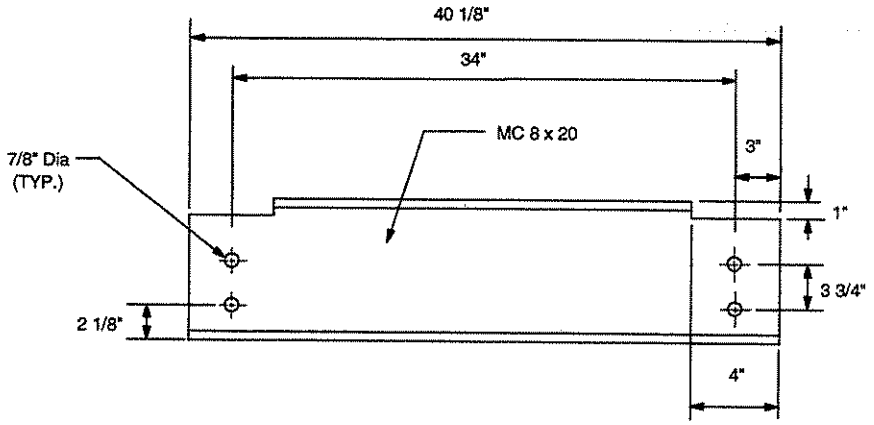

Figure 3.20. Details of diaphragm channels.

first placed at mid-height of the web (Fig. 3.21a) and then directly under the bottom surface of the concrete deck (Fig. 3.21b). In each case, the diaphragms were positioned and leveled in both directions prior to tightening the nuts.

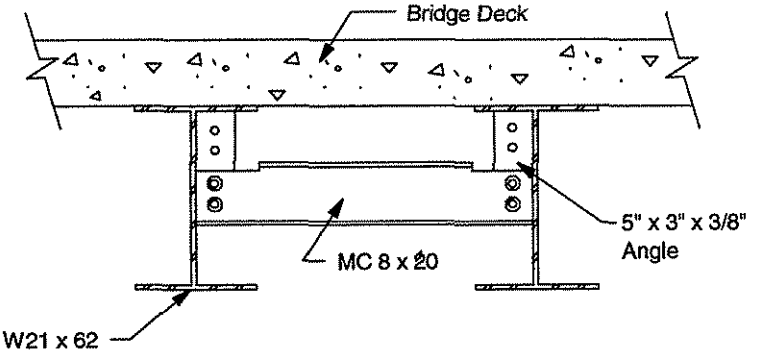

a. Diaphragm at mid-height of web

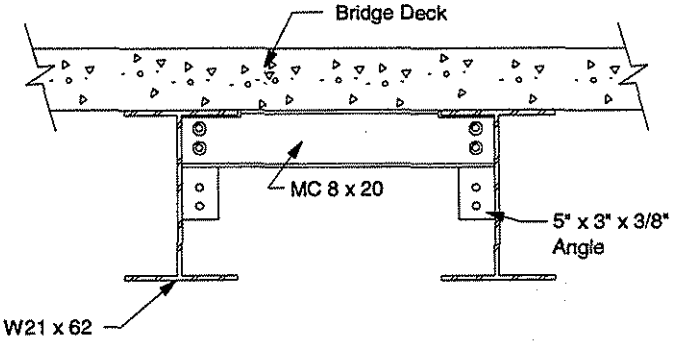

b. Diaphragm directly under concrete deck

Figure 3.21. Positions of diaphragms tested.

3.6 Construction of Model Bridge

The construction of the model bridge was completed in three phases which are described in the following sections. Note that although the phases are described separately, many of the construction operations were undertaken simultaneously.

3.6.1 Phase I Construction

After fabricating and curing the three PCDT units required for constructing the 6401 mm (21 ft) wide bridge, the three units were positioned side by side on abutments. Figure 3.22 shows the bridge model after placement of the three PCDT units. The scarification of the PC concrete is obvious and the connection details can be seen along the two joint lines. The model was placed on ideal pin and roller supports consisting of steel bars 25 mm (1 in.) in diameter and top and bottom 305 mm x 305 mm x 25 mm (12 in. x 12 in. x 1 in.) steel plates. For the pin supports, the steel bars were welded to the bottom plates; for the roller supports, the steel bars were not connected to either plate, thus permitting rotation and longitudinal movement. The pin and roller supports for the six steel beams in the bridge were positioned so that the span length for each of the PCDT units was the same. Note, in Fig. 3.22 the "patches" on the PC deck surface are for installation of strain gage instrumentation.

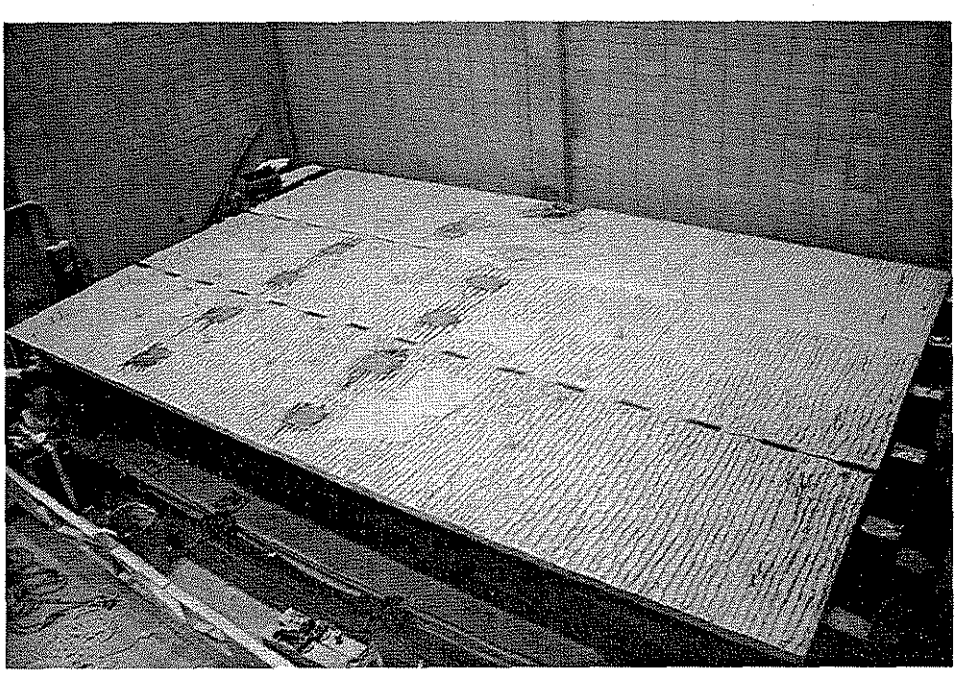

Figure 3.22. Photograph of model bridge with PCDT units in place.

3.6.2 Phase II Construction

With the three units of the bridge model in place, the next step was to weld the top and bottom plates of the PC deck connectors. The plates that make the connection were welded as indicated previously in Fig. 3.2. As will be explained in Chp. 4, the model was tested varying the number of connections. Once the number of connections required for obtaining the desired load distribution was determined, all unneeded connections were removed.

3.6.3 Phase III Construction

At this time, the bridge model was ready for the CIP concrete portion of the deck. Formwork was attached to the PCDT units using the inserts in the PC deck previously described. The formwork which consists of four components is schematically shown in Fig. 3.23. First, 19 mm (¾ in.) thick plywood was cut to a nominal 203 mm (8 in.) depth in 2438 mm (8 ft) lengths. The plywood and connecting angles were then bolted to the PC concrete using the inserts which had been positioned around the perimeter of the deck. To ensure that the formwork was strong enough to resist the forces from screeding, 2x4 lumber was attached to the plywood between the angles to provide additional strength. This combination (angles, plywood, plus 2x4's) gave a formwork system that was effective in retaining the plastic concrete and resisting the screeding forces.

Once the formwork had been constructed, the next step was to place the reinforcing steel. The steel was tied into a mat and positioned on high chairs to give the desired top cover of 51 mm (2 in.) (see Fig. 3.15). With the reinforcement in place, the final step in constructing

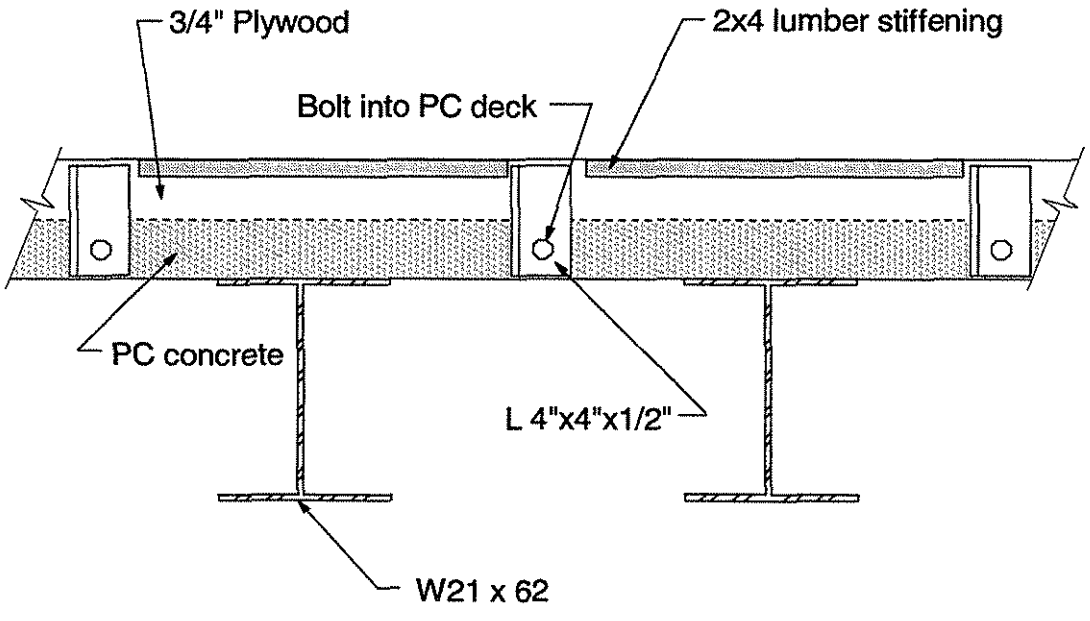

Figure 3.23. Details of CIP concrete formwork.

the CIP deck was to pour the concrete. As with the PC concrete, the deck was poured using standard Iowa DOT C-4 ready-mixed concrete. The concrete was placed and vibrated similarly to the process used in placing the PC concrete. Initially, it was thought that the CIP deck could be placed in the same manner as the PC deck using a very stiff screed and then finish the top surface with a bullfloat. Attempts to use the 7010 mm (23 ft) long screed were unsuccessful for several reasons. First, the model was positioned very close to an exterior wall in the SEL which limited work space on one side of the deck and secondly, the concrete was very stiff (a slump of 89 mm (3.5 in.)) and was not easily "pushed" (see Fig. 3.24). Because of the lack of success with the screed, the next option was to finish the surface with hand trowels. Five people finished the surface with hand trowels while kneeling on platforms

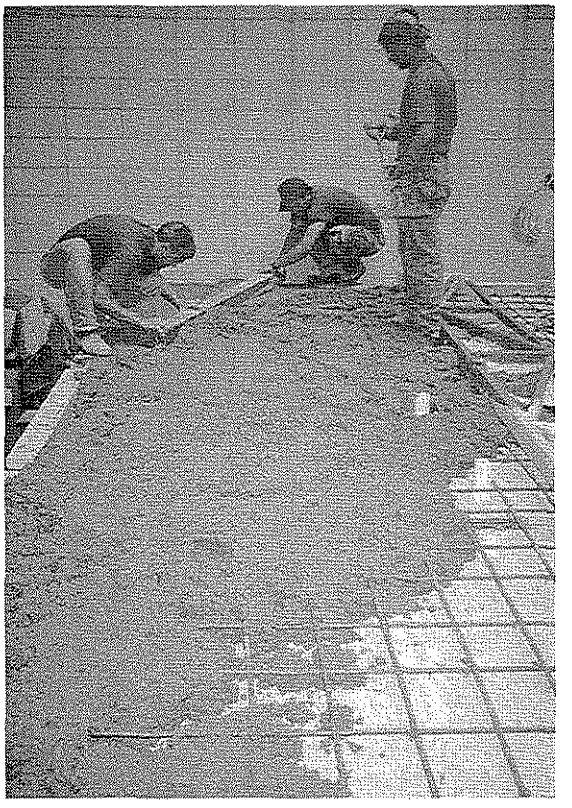

Figure 3.24. Initial attempt to screed the CIP concrete.

that had been laid across the bridge. This platform was on top of the formwork and therefore provided a reference surface that resulted in a reasonably level surface (i.e., constant deck thickness). It should be noted at this time that this is definitely not a recommended procedure to finish the CIP portion of the deck in this bridge system. The final step in pouring the CIP deck was to finish the surface of the concrete with a bullfloat as shown in Fig. 3.25. The bullfloat was used to remove voids and to reduce uneveness left by using the hand trowels. Shown in Fig. 3.26 is a photograph of the PC and CIP portions of the deck after the CIP formwork had been removed. Although there was some variation in the total deck thickness, in general the deck was 204 mm (8 in.) thick - 102 mm (4 in.) PC and 102 mm (4 in.) CIP.

Figure 3.25. Bullfloating the CIP concrete.

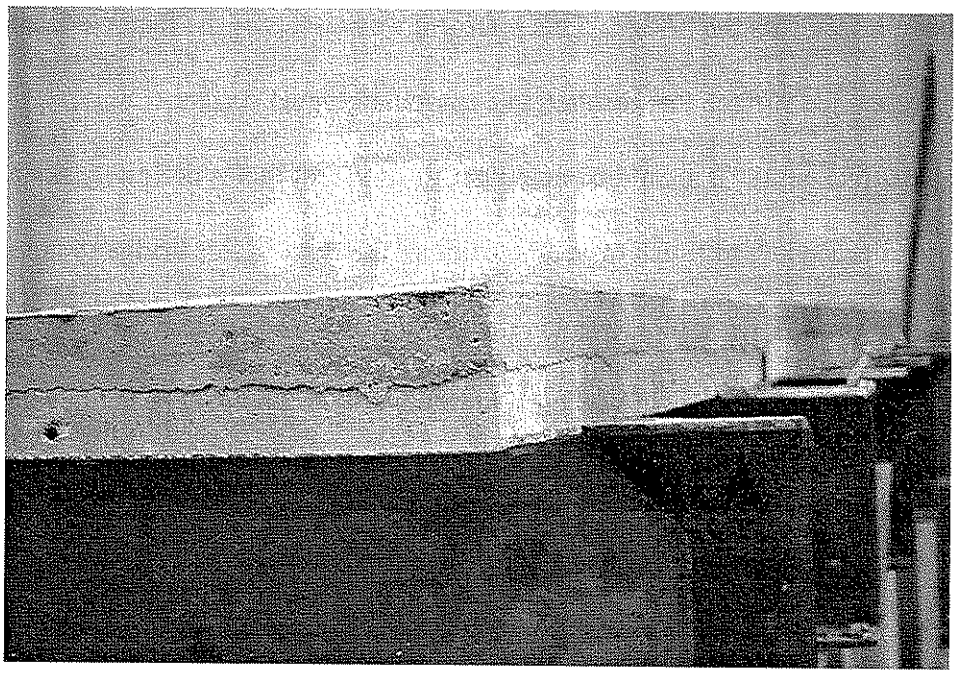

Figure 3.26. Photograph showing PC and CIP portions of reinforced concrete deck.

4. TESTING PROGRAM

4.1 Overview

A laboratory testing program was initiated to gain an understanding of the global as well as local vertical loading response of the precast bridge system (Concept 1). The testing program consisted of a series of small scale tests on different types of PC deck connections, "handling strength" tests of a PCDT unit, four series of 16 tests each on the model bridge with only the PC portion of the deck in place to determine load distribution, and four series of 16 tests each on the fully constructed model under various configurations of loading to determine load distribution as well as overload strength.

As previously noted, the full scale specimens were constructed of ready mix concrete (Iowa DOT C-4 mix) and W21x62 used steel beams. The concrete was controlled during placement to assure proper amounts of entrained air and slump. Cylinders cast during pouring were tested to monitor the concrete compressive strength and split cylinder strength. The modulus of rupture strength was determined by testing standard modulus beams which were also cast during pouring. Concrete testing was completed following all applicable American Society of Testing and Materials specifications.

4.2 Small Scale Connector Tests

The small scale connector tests consisted of testing bridge deck specimens with the different connection assemblies, described in Chp 3. These tests were undertaken to: (1) determine the type of connection that could be practically implemented, (2) investigate the structural response and strength of the different connections, and (3) obtain behavior data of the connection details for validation of a finite element model (FEM) of the connection.

Three different connections were investigated. As was described in Chp. 3, two of the connections consisted of plates welded to channels that had been cast in the PC portion of the specimen; one of the connections had plates welded to both the top and bottom flanges of the channel while the other only had a plate welded to the bottom flange. The third detail investigated was a bolted connection which was described in Sec. 3.2. As previously noted, due to alignment problems with bolt holes, this connection was eliminated from future consideration. The specimens (shown in Fig. 3.3) were 533 mm (21 in.) in length and 457 mm (18 in.) wide. The length of each panel specimen was half of the beam spacing used in the model bridge while the 457 mm (18 in.) width provided adequate room for the full scale connections.

As shown in Fig. 4.1, two different types of tests were completed: (1) nominal 102 mm (4 in.) thick PC panels were subjected to flexural loading and (2) panels consisting of the PC portion of the deck plus the CIP portion of the deck were also subjected to flexural loading. These latter specimens would therefore had a nominal total thickness of 204 mm (8 in.) - 102 mm (4 in.) PC and 102 mm (4 in.) CIP. The PC portion of all specimens tested were from one batch of ready-mixed concrete and therefore had the same nominal concrete strength. Concrete used in fabricating the CIP portion of the full depth specimens also came from a single ready-mixed batch of concrete.

Each specimen was subjected to flexural loading as previously noted. In the following discussion, failure load is taken to mean load that cause the behavior of the specimen to change significantly (i.e., when the specimen continued to deflect without an increase in

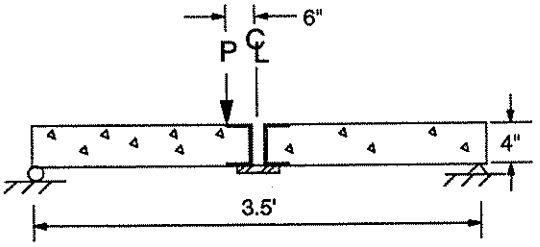

a. No CIP; only welded bottom plate-Specimen 1

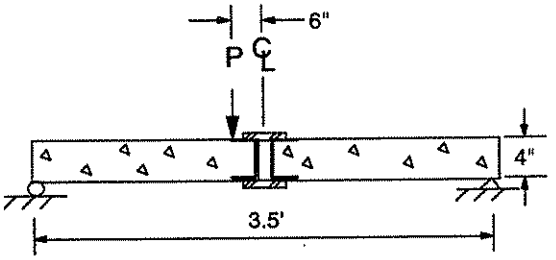

b. No CIP; top and bottom welded plate-Specimen 2

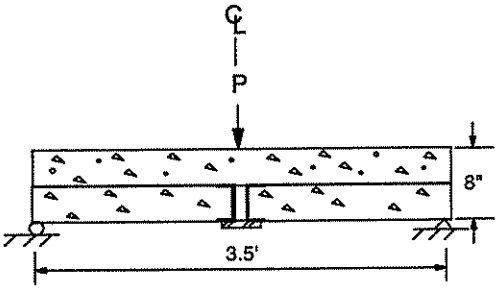

c. With CIP; only welded bottom plate-Specimen 3

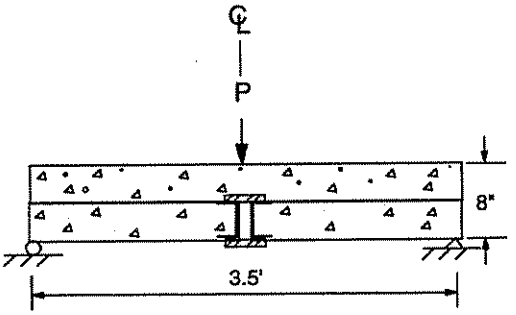

d. With CIP; top and bottom welded plate-Specimen 4

Figure 4.1. Small scale connector specimens.

applied load). Tests were terminated when such a change in behavior was noted. Photographs of the test setup are presented in Fig 4.2. The load on the specimens (Specimens 1 and 2) with only the PC deck were tested with the load offset from midspan by 152 mm (6 in.) so that the load was not applied directly to the connection detail (see Fig. 4.2a). However, for tests with the CIP in place (Specimens 3 and 4), the load was applied directly at midspan. The load was applied as a "line load" using structural tubing, and 25 mm (1 in.) thick neoprene pads for distribution; load was applied in increments of 445 N (100 lbs). The specimens were simply supported with a pin and roller arrangement.

All instrumentation was monitored and recorded using a computer controlled data acquisition system (DAS). Loads applied to the specimen were measured using load cells. As illustrated in Fig. 4.3, longitudinal concrete strains were monitored along the bottom surface of the specimens at the quarter points - (267 mm (10.5 in.)) from each support. Longitudinal steel strains were measured on the bottom surface of the bottom connection plate at midspan. Celescos (deflection transducers) were used to measure vertical deflection at these same locations.

4.3 "Handling Strength" Tests of PCDT Unit

This type of testing was completed to determine: (1) the "handling strength" of the PCDT units during erection, (2) the amount of composite action obtained between the PC concrete and the steel beams, and (3) the response of the PCDT units to load for verification of the FEM. In this task, the first PCDT unit constructed was subjected to a two point load configuration illustrated in Fig. 4.4. Loads were applied at the third points of the specimens

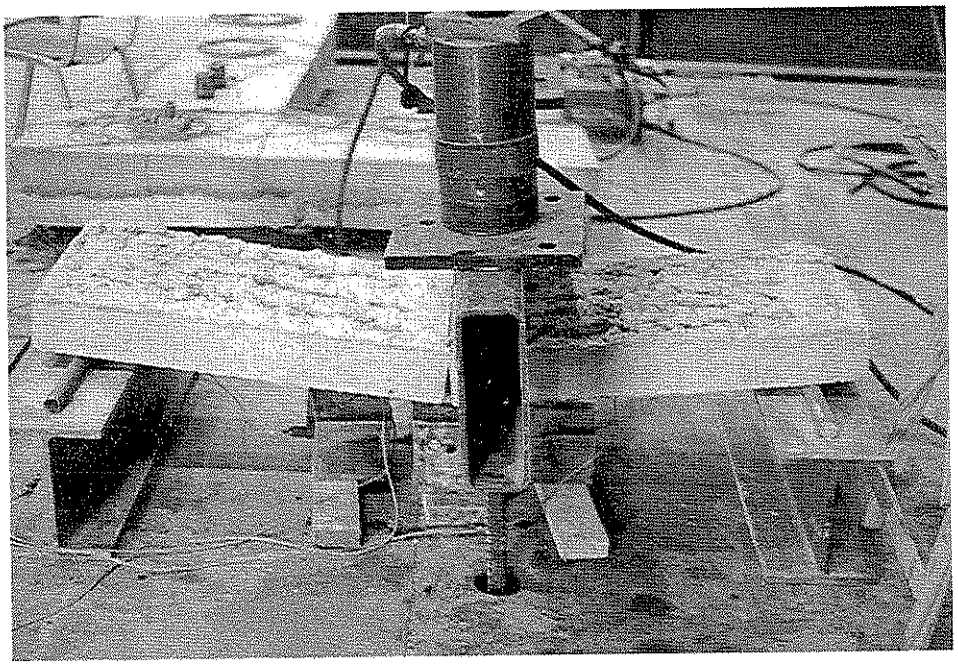

a. Connector test with only PC concrete deck

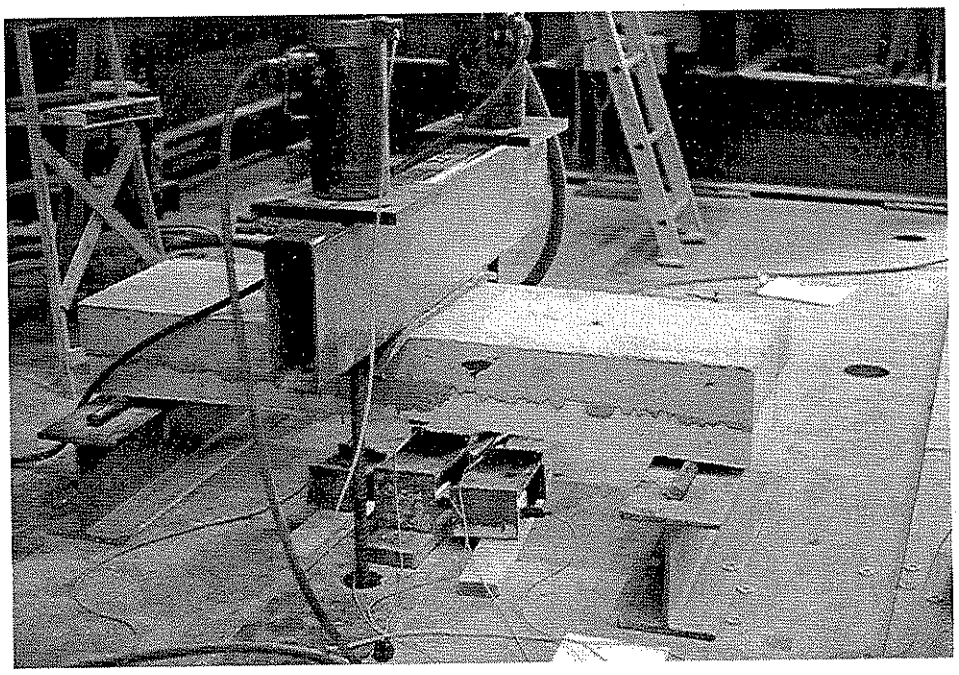

b. Connector test with CIP concrete deck in place

Figure 4.2. Photographs of small scale connector tests.

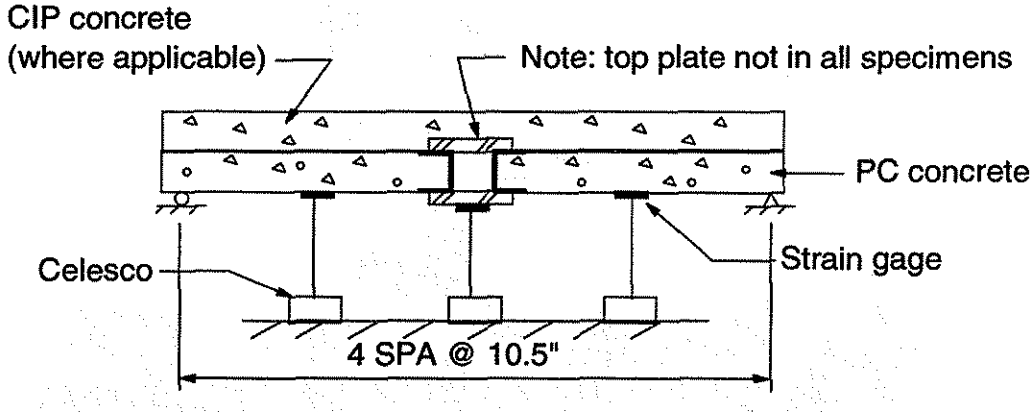

Figure 4.3. Instrumentation for small scale connector tests.

(3251 mm (128 in.) from each end) in increments of 1,000 lbs until a moment, twice that which would occur in the unit under its own weight when it was lifted, was obtained. This magnitude of moment was selected to simulate a dynamic load that might occur when the specimen is moved. As shown in the photograph in Fig. 4.5, "line load" was transmitted to the specimen using a load frame anchored to the SEL tie-down floor. To ensure even distribution of the "line load" across the scarified concrete surface of the specimen, sand was placed between the specimen and the distribution beam. This test was repeated four times to ensure repeatability of the results.

All instrumentation was monitored and recorded using a computer controlled DAS. Loads applied to the specimen were monitored at both load points using load cells. Instrumentation on this PCDT was the same as used in the model bridge which is described in Sec. 4.4.

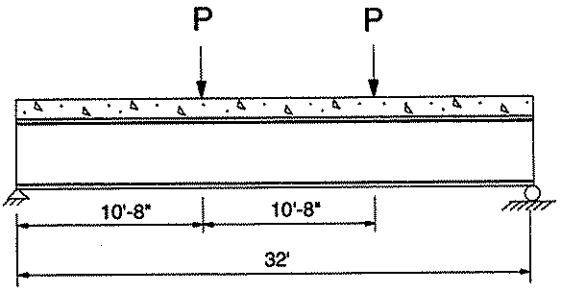

Figure 4.4. Schematic of "handling strength" test.

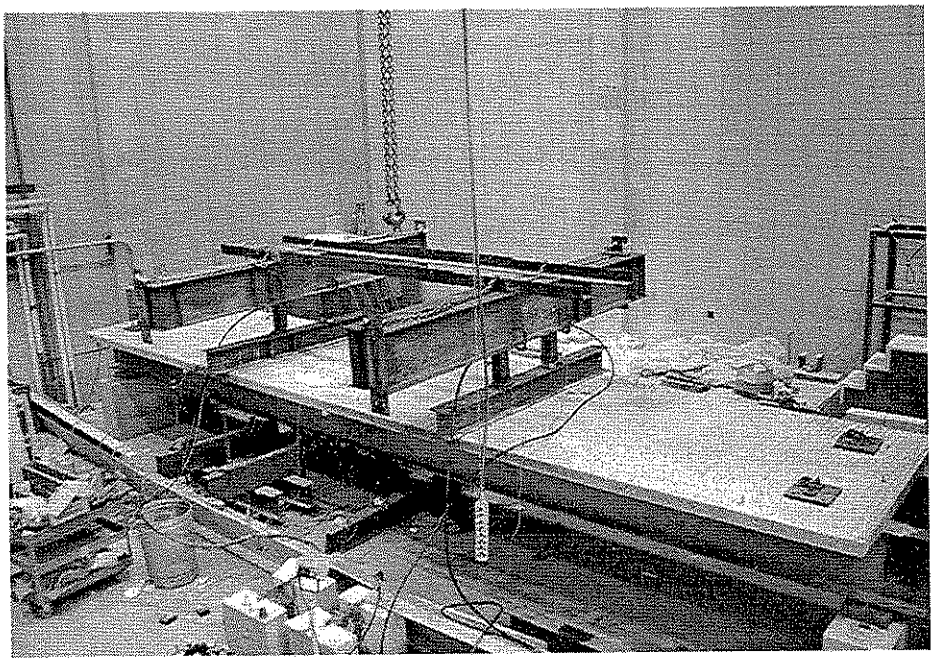

Figure 4.5. Photograph of "handling strength" test.

4.4 Model Bridge Tests

4.4.1 PCDT Units Only

As noted in Chp. 3, the model bridge was constructed and initially tested with only the PCDT units in place. Tests were completed in this configuration to determine the number of

connections between adjacent PCDT units required to obtain the desired lateral load distribution and to withstand construction loads. A total of 16 connectors were precast (see Fig. 3.22) into one or both edges of the PCDT unit depending on its location in the model bridge. The location of the connectors in the four series of tests is shown in Fig. 4.6. As described in Chp. 3, the model bridge was simply supported with a pin and roller arrangement. Testing started with three welded connections along each joint (Series 3 - Fig. 4.6a), two additional connectors were then welded along each joint (Series 5 - Fig. 4.6b) and the model re-tested. Note in this configuration as well as those that follow, the connections are not uniformly distributed along the interface between PCDT units being connected. However, the arrangements of connectors are symmetrical about the midspan of the model bridge. In the other two series of tests, there were seven (Series 7 - Fig. 4.6c) and nine (Series 9 - Fig. 4.6d) connectors. The same procedure was used in the testing of each of the four connector arrangements. Load was applied at each of the 16 load points shown in Fig. 4.7a in increments of 4,450 N (1,000 lbs) until 71,170 N (16,000 lbs) was reached. Instrumentation used in the bridge model test is also shown in Fig. 4.7. As shown in Fig. 4.7a, a total of 12 sections in the model bridge were instrumented with both steel and concrete strain gages; all gages were oriented to measure longitudinal strains. Each beam of the PCDT units was instrumented at two sections, at mid-span and at the quarter span, with five strain gages at each section. A concrete strain gage was located on the top surface of the PC concrete directly above the steel beam (see Fig. 4.7b). Steel strain gages were mounted at four locations: two on the bottom surface of the upper flange, one at mid-height of the web and

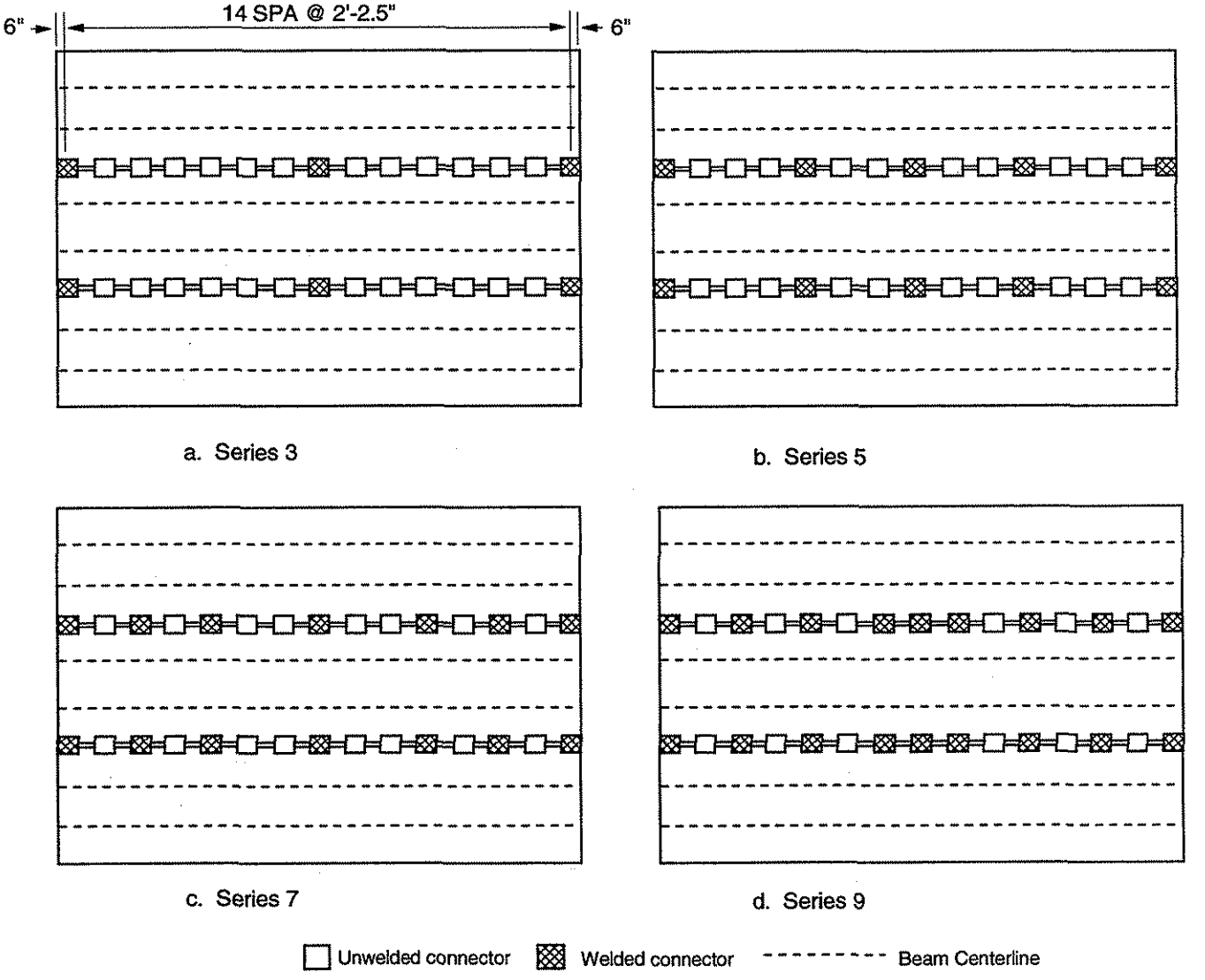

Figure 4.6. Location of connections in model bridge tests.

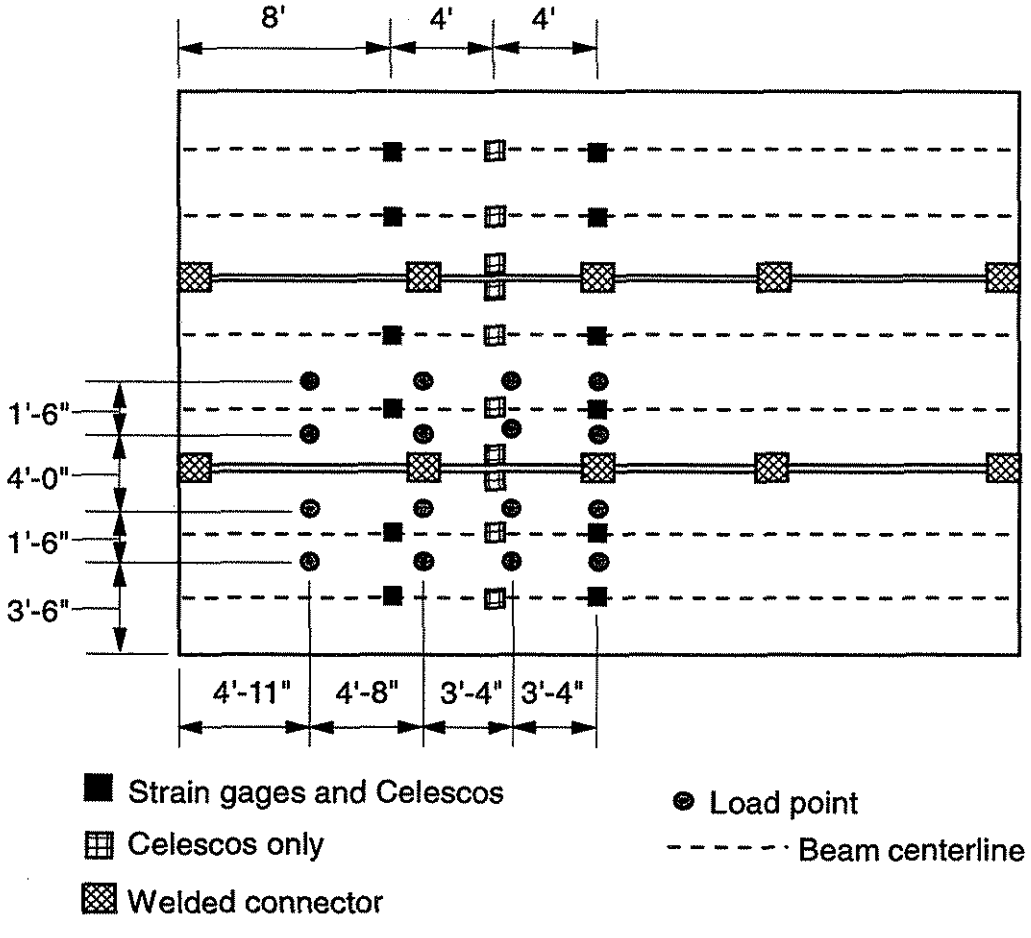

a. Location of instrumentation - plan view

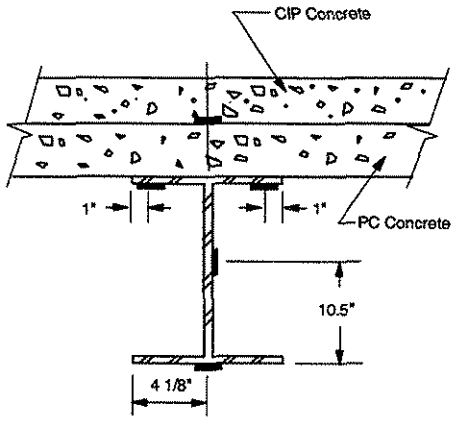

b. Location of strain gages in cross-section

Figure 4.7. Instrumentation used in model bridge.

one on the bottom surface of the bottom flange. Strains measured by the two strain gages on the top flange were essentially the same, thus an average of these two strains is used in reporting the data in Chp. 6.

Deflections were monitored at three locations on each of the six steel beams in the model bridge. The Celescos were located at mid-span, quarter span, and at the three-eighths span (see Fig. 4.7a). Additionally, at the three-eighths span section (3,570 mm (12 ft) from the end) the deflection instrumentation was positioned so that differential movement between adjacent PCDT units could be monitored. This location was selected because it was thought this is where the greatest differential movement between adjacent PCDT units would occur.

4.4.2 CIP Portion of Deck in Place

This phase of testing was completed for several reasons: (1) to determine the contribution of the CIP concrete and reinforcement on load distribution, (2) to determine the effect that diaphragms and diaphragm position have on load distribution, and (3) to determine the behavior and strength of the bridge system.

As will be shown in Chp. 6 (see Sec. 6.3.1), five connections (Series 5 - Fig. 4.6b) between PCDT units provided the desired load distribution. Thus, the bridge model was returned to this configuration prior to pouring the CIP portion of the deck. With the CIP portion of the deck in place, the model bridge was tested using exactly the same procedure (load applied at 16 different locations, in 4,450 N (1,000 lbs) increments, etc.) that was used in the testing of the model bridge with only the connected PCDT units (i.e., no CIP concrete). Details of this testing procedure were presented in the previous section (Sec. 4.4.1). Since the strength of the model bridge with the CIP is greater than when only the PCDT's were present,

the maximum applied load was increased to 142,340 N (32,000 lbs). To determine the effect of diaphragms on the behavior of the bridge and on load distribution, diaphragms were installed as described in Chp. 3 at two positions: mid-height of the web (see Fig. 3.21a) and directly under the concrete deck (see Fig. 3.21b). For each diaphragm position, load was once again applied at the 16 load locations shown in Fig. 4.7a in 4,450 N (1,000 lbs) increments up to a maximum of 142,340 N (32,000 lbs).

At this time, the behavior of the bridge under overload conditions was investigated. All diaphragms were removed and loads were applied to the model in two different configurations. In Overload Test 1, shown in Fig. 4.8a, load was applied at four points. Load was applied to the model bridge in 1,110 N (250 lbs) increments at each Point 1 and 4,450 N (1,000 lbs) at each Point 2 until a total load of 448,400 N (100,000 lbs) was on the bridge. This magnitude of load is 2 1/2 times a legal H20 truck loading (177,920 N (40,000 lbs)). Note the ratio of load at Point 1 and Point 2 was selected to simulate the ratio of front axle load to rear axle load (that is, 1:4). After each load increment, strains and deflections were recorded using the computer controlled DAS.

In Overload Test 2 shown in Fig. 4.8b, load was applied at two points in the same manner as described for the four point test. However, load was only applied to a maximum magnitude of 177,920 N (40,000 lbs).

To determine the contribution of the bottom plates in the connections between the PCDT units, these ten plates were removed and the model bridge was re-tested using the procedure previously described (load applied at 16 locations, 4,450 N (1,000 lbs) increments, etc.). In these tests, a maximum load of 142,340 N (32,000 lbs) was applied at each location.

The final tests on the bridge were without the bottom cover plates with the bridge being subjected to the two overload conditions previously described (see Fig. 4.8). A total load of 756,000 N (170,000 lbs) was applied in Overload Test 1 and 659,150 N (147,000 lbs) was applied in Overload Test 2. Strain and deflection measurements were recorded thoughout these tests also.

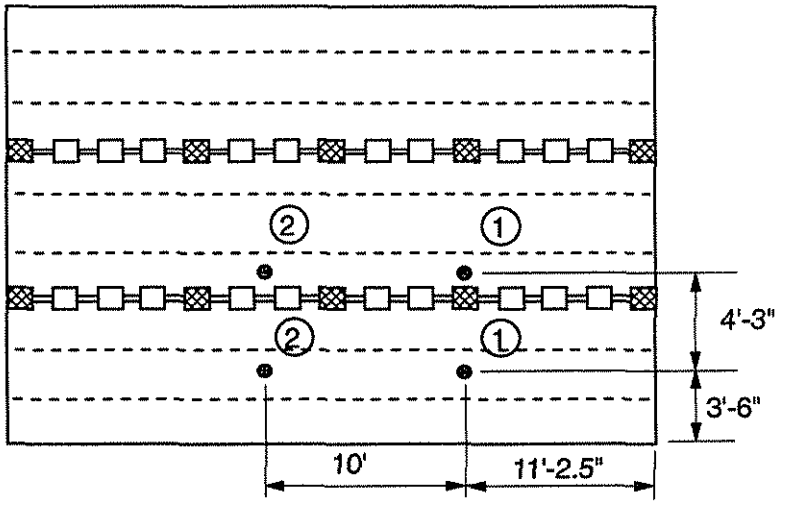

a. Overload test 1

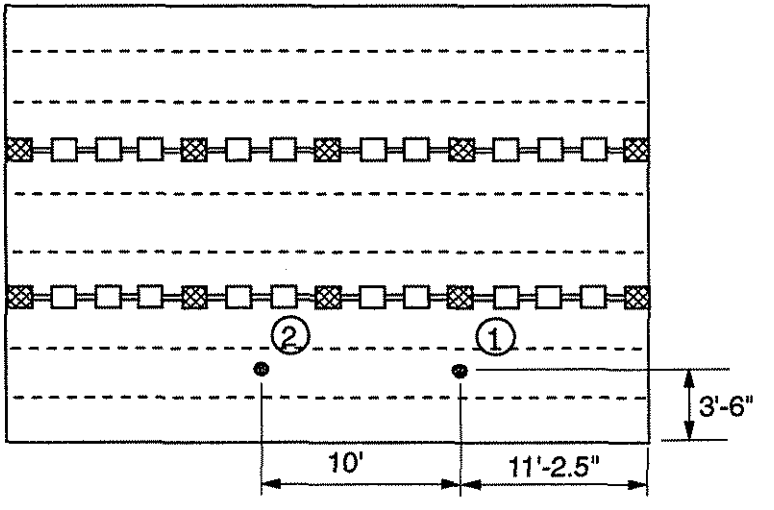

b. Overload test 2

Figure 4.8. Location of loading points used in overload tests.

5. FINITE ELEMENT MODELS

One of the primary objectives of this research was to determine the structural behavior for this bridge system. To predict the structural behavior of this bridge system, a finite element model (FEM) was developed and validated with the data from the experimental portion of this investigation. There are a variety of finite element software packages available at ISU, but due to the simplicity of its graphic user interface and the relative ease in which results can be accessed, the ANSYS 5.1 (11) finite element package was used. This package has a large number of different types of elements that allow many different types of analyses to be completed. The three FEM's that were developed, as well as the various elements used, are presented in the following sections.

5.1 Element Types

The FEM's utilize four different types of elements to model the components in the bridge system. Many of the elements are utilized in a number of different situations to model different parts of the bridge; these different applications are discussed in Sec. 5.2. The element types are described in the ANSYS 5.1 Users Manual (11).

5.1.1 BEAM4 Element

From the ANSYS 5.1 Users Manual:

> "BEAM4 is a uniaxial element with tension, compression, torsion, and bending capabilities. The element has six degrees of freedom at each node; translation in the nodal x, y, and z directions and rotations about the nodal x, y, and z axes."
>
> "The geometry, node locations, and coordinate system are shown (see Fig 5.1). The element is defined by two or three nodes, the cross-sectional area, two area moments of inertia (IZZ and IYY), two thicknesses (TKY and TKZ), an angle of rotation about the element x-axis, the torsional moment of inertia, and the material properties."

"The beam must not have zero length or area. The moments of inertia, however, may be zero if large deflections are not used. The beam can have any cross-sectional shape for which the moments of inertia can be computed. The stresses, however, will be determined as if the distance between the neutral axis and the extreme fiber is one-half of the corresponding thickness."

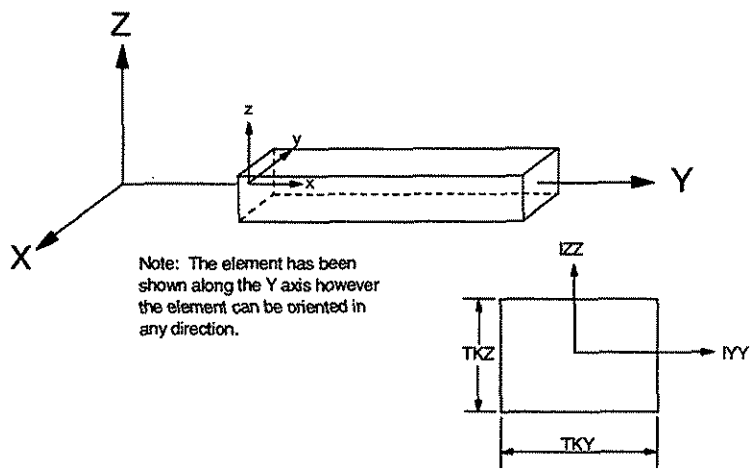

Figure 5.1. Geometry of BEAM4 element.

5.1.2 LINK8 3-D Spar Element

From the ANSYS 5.1 Users Manual:

"LINK8 is a spar which may be used in a variety of engineering applications. Depending on the application, the element may be thought of as a truss element, a cable element, a link element, a spring element, etc. The three-dimensional spar element is a uniaxial tension-compression element with three degrees of freedom at each node: translations in the nodal x, y, and z directions. As in a pin-jointed structure, no bending of the element is considered."

"The geometry, node locations, and the coordinate system for this element are shown (see Fig. 5.2). The element is defined by two nodes, the cross-sectional area, an initial strain, and the material properties."

"The spar element assumes a straight bar, axially loaded at its ends, and of uniform properties from end to end. The length of the spar must be greater than zero so nodes i and j must not be coincident. The area must be greater than zero. The displacement function assumes a uniform stress in the spar."

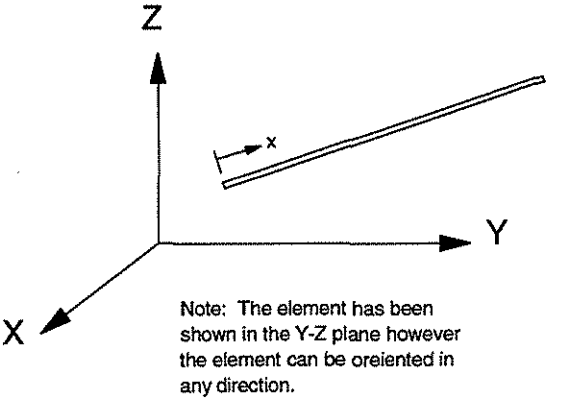

Figure 5.2. Geometry of LINK8 element.

5.1.3 BEAM44 3-D Tapered Unsymmetric Beam Element

From the ANSYS 5.1 Users manual:

"BEAM44 is a uni-axial element with tension, compression, torsion, and bending capabilities. The element has six degrees of freedom at each node: translations in the nodal x, y, and z directions and rotations about the nodal x, y, and z axes (see Fig. 5.3). The element allows different unsymmetrical geometry at each end and permits the end nodes to be offset from the centroidal axis of the beam."

There are options with ANSYS that allow element stiffness releases at the nodes in the element coordinate system. Releases should not be such that that free-body motion could occur.

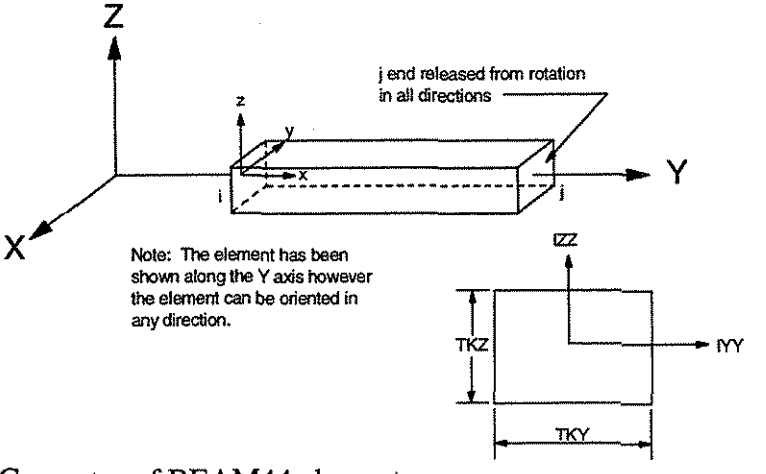

Figure 5.3. Geometry of BEAM44 element.

5.1.4 SHELL63 Elastic Shell Element

"SHELL63 has both bending and membrane capabilities. Both in-plane and normal loads are permitted. The element has six degrees of freedom at each node: translations in the nodal x, y, and z directions and rotations about the nodal x, y, and z axes."

"Zero area elements are not allowed. This occurs most often whenever the elements are not numbered properly. Zero thickness elements or elements tapering down to zero thickness at any corner are not allowed."

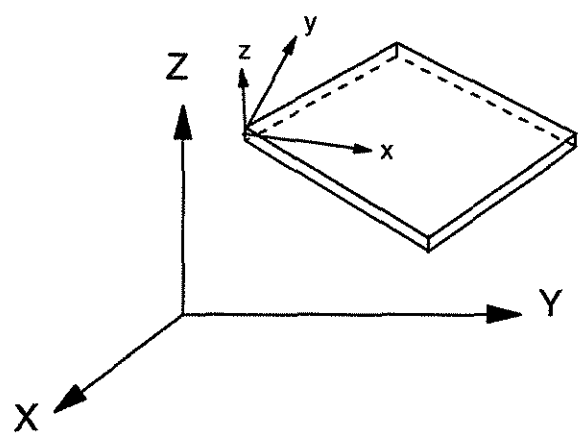

Figure 5.4. Geometry of SHELL63 element.

5.2 Description of FEM Geometry and Material Properties

Three finite element models were developed to model the structural response of three different bridge systems. Model 1 was developed to model the bridge system described in Chp. 3 when only the PC concrete deck was in place; Model 2 of the bridge system described in Chp. 3 included the CIP deck. Model 3, with a continuous deck, was developed to simulate a laterally continuous deck bridge.

5.2.1 Element Properties

The major components of the basic finite element model for a portion of the bridge structure is shown in Fig 5.5. Illustrated in Fig. 5.5a is an isometric view of the structure; a FEM of this structure is shown in Fig. 5.5b. This model forms the basis for all the bridge models that were developed. The properties used for each of the elements are the same for all three bridge models. The reasons for selecting the various element types, as well as the actual geometric and material properties used, are presented in the following sections.

5.2.1.1 Steel Beams

The steel beams were modeled with BEAM4 elements, which are prismatic 3-D flexural members. The element was assigned an area of 11,810 mm^2 (18.3 $in.^2$) a moment of inertia of 616 E6 mm^4 (1,480 $in.^4$) and a depth of 530 mm (21 in.). These are the properties of the W21x62 steel beams which were used in the model bridge. The shear deflection constant was conservatively set at 2.3 (since the actual value is unknown) and is based on the ratio of web area to total area.

The material properties for this element are those for steel. The Modulus of Elasticity used was 200,000 Mpa (29,000,000 psi) with a Poisson's ratio of 0.3.

5.2.1.2 Shear Connector Assembly

The shear connector assembly shown in Fig 5.5.b consists of two parts. The lower part of the shear connector assembly is modeled with BEAM44 elements; the geometric properties for this element are based on the spacing of the shear connectors and the geometry of the web of the steel beams. Shear connector area is calculated as the average

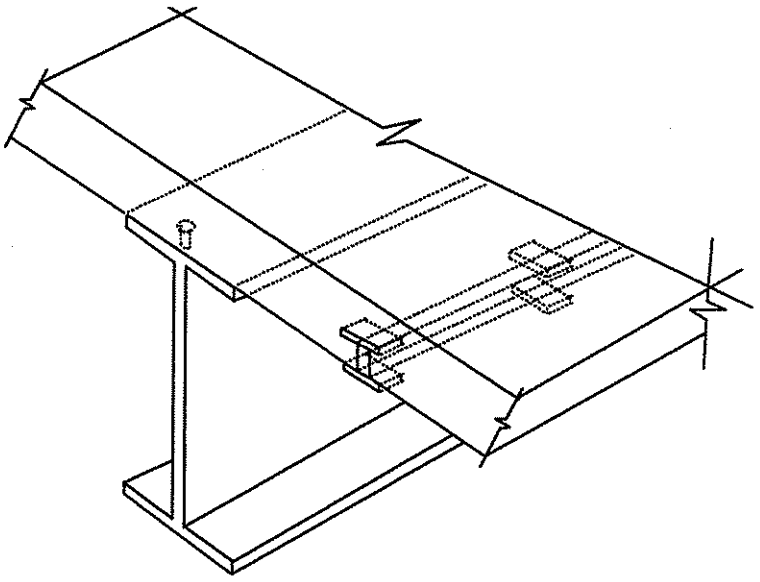

a. Isometric view of partial structure

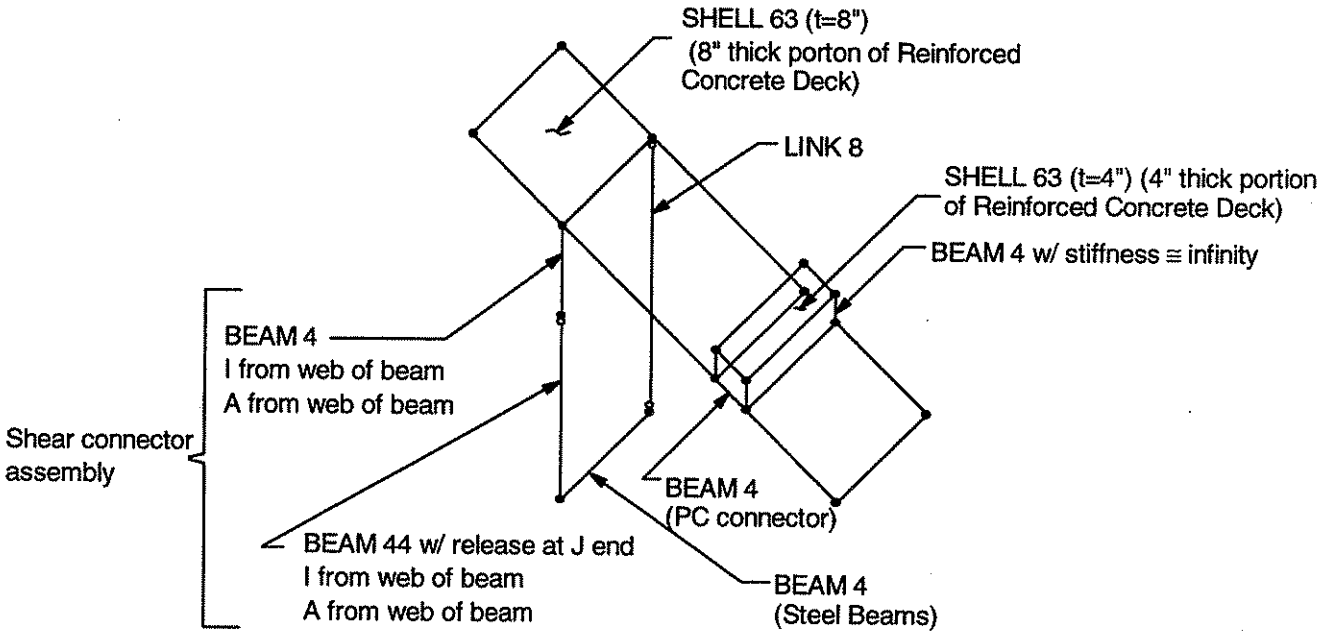

b. FEM of structure

Figure 5.5. Basic finite element model (Model 2).

spacing of the adjacent shear connectors times the web thickness. The moment of inertia is calculated for this same section about an axis perpendicular to the longitudinal axis of the steel beam (12). The area is 6,190 mm^2 (9.6 $in.^2$) and the moment of inertia is 192E6 mm^4 (460.8 $in.^4$). Upper ends of the BEAM44 elements are released to rotation. The release at the j end at the location of the deck-top flange interface is based on work completed by Dunker (12). Using this type of element, model shear connector slip and shear connector forces were directly obtained. The material properties used are for steel as given previously.

The top portion of the shear connector assembly consists of BEAM4 elements with the same geometric properties as the BEAM44 element without rotation release at either end. Again, the material properties used are for steel. The selection of this element plus the BEAM44 element correctly models the behavior of the shear connectors used in the model bridge.

At locations where the deck and beams each had nodes with the same x and y coordinates (as a result of meshing of the elements), LINK8 elements were used. The properties for this element are the area used in the shear connector assembly (6,190 mm^2 (9.6 in^2)) with steel material properties. The purpose of using this element was to ensure that the deck and the beams are acting as a unit (i.e., the deflection of the deck and the beams at the same x and y coordinates are the same).

5.2.1.3 Reinforced Concrete Deck Assembly

The concrete deck assembly for Model 1 consisted of three deck slab panels (one panel per unit). Individual panels were separated by a 51 mm (2 in.) gap as mentioned in Chp. 3 to simulate extremely poor construction practice.

Modeling the reinforced concrete deck in Model 2 was difficult. In Model 2, there were two deck thicknesses - 204 mm (8 in.) PC plus CIP concrete at all locations except at the joints between the PCDT units where the depth was only 102 mm (4 in.) (i.e., the depth of CIP concrete). Modeling the variation in deck thickness required the use of three types of elements. Obviously, the two portions of the deck are modeled with SHELL63 elements with the appropriate thickness of either 203 mm (8 in.) or 102 mm (4 in.) with the element defined at the elevation of the neutral axis. The problem is making the two different thickness decks act together. At the point where the thickness changes from 203 mm (8 in.) to 102 mm (4 in.) (that is, the longitudinal joint between PCDT units) the rotation and deflection compatibility needs to be enforced. To accomplish this, BEAM4 elements with an area and moment of inertia of approximately infinity were used.

The material properties used for the concrete deck assembly are as follows. For the actual deck (SHELL63 elements), a weighted average of the Modulus of Elasticity of the reinforcing steel and the concrete based on the percentage of each was used. In calculating this weighted average E_s= 200,000 MPa (29,000,000 psi) and $E_c = 5{,}000*(f'_c)^{0.5}$ $(57{,}000*(f'_c)^{0.5})$ were used. The Poisson's ratio of the deck was selected to be 0.15 based on typical published material properties. The "infinite" stiffness BEAM4 element was assigned the Modulus of Elasticity of steel.

5.2.1.4 PC Connection Detail

The connection detail developed in the laboratory was modeled with BEAM4 elements with the moment of inertia and area of the connection detail (I = 56.8 E6 mm^4 (131.6 $in.^4$), A = 5,030 mm^2 (7.8 $in.^2$)). The moment of inertia is calculated for the two plates of the connection detail described in Chp. 3 for transverse bending of the bridge

about the mid-depth of the PC deck. Area of this element is the area of the two plates in the transverse direction of the bridge; material properties are that of steel. The FEM model was developed so that any number of elements representing the PC connections could be inserted at essentially any location.

5.2.2 Bridge Models Using Finite Elements

The finite element model of the PC concrete deck with connections (Model 1) that was developed is shown schematically in Fig 5.6. It consists of the BEAM4, LINK8, BEAM44, and SHELL63 elements previously described. The difference between this and the basic model is that there is only one deck thickness (102 mm (4 in.)) as there is no CIP concrete. The material and geometric properties are the same as the elements described as the basic model. Model 2 utilizes the properties and conditions presented for the basic model as shown in Fig. 5.5. The model used to simulate typical laterally continuous bridge decks (Model 3) is shown in Fig. 5.7. The difference between this model and the PC concrete only model (Model 1) is simply that the deck thickness is a constant 203 mm (8 in.) throughout and there are no PC connectors.

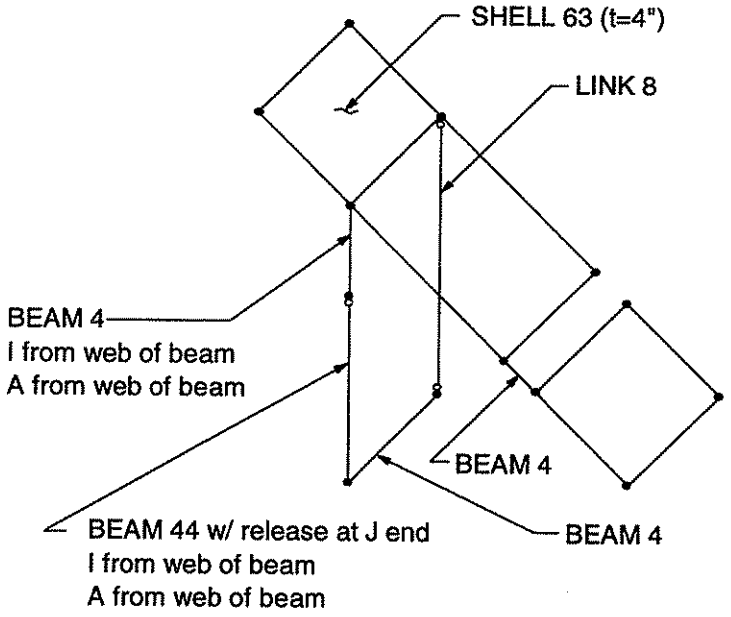

Figure 5.6. Finite element model with PC deck only (Model 1).

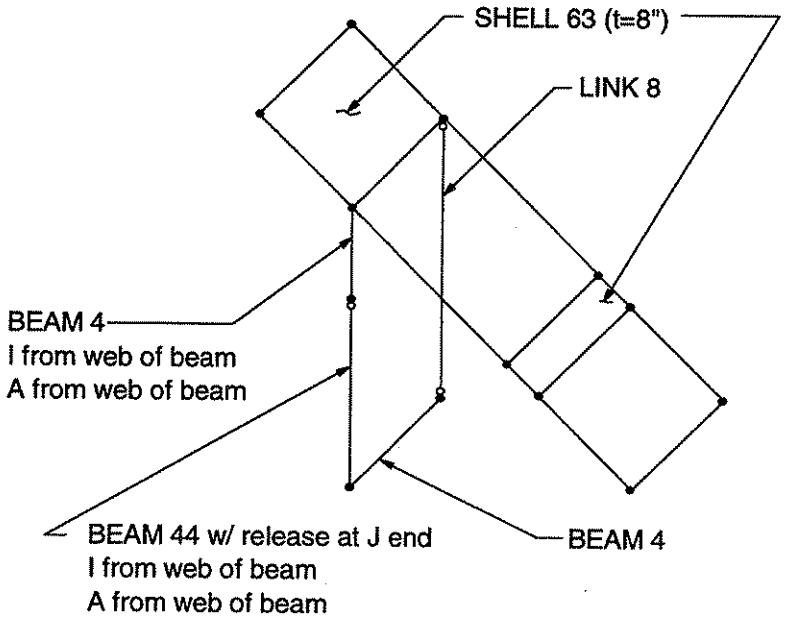

Figure 5.7. Finite element model of laterally continuous bridge system (Model 3).

6. EXPERIMENTAL AND ANALYTICAL RESULTS

6.1 Experimental Results: Small Scale Connector Tests

Small scale connector tests consisted of testing reduced scale bridge deck specimens with various connector assemblies, as described in Chp. 4, to: (1) determine the type of connection that could be practically implemented, (2) investigate the structural response and strength of the different connections, and (3) obtain behavior data of the connection details for validation of a FEM of the connection.

Constructing these small scale units provided insight into the feasibility of each of these types of connections. The bolted connection detail was difficult to construct because the conduits used for forming the holes were not stable enough to withstand loads imposed during placement of the concrete; they tended to move laterally as well as rotate. Thus, this connection was abandoned; if the desired bolt hole location and alignment could not be obtained in the small scale specimens under laboratory conditions, it would be difficult to obtain the required placement in the full scale PCDT units in the field. The construction of the second connection (see Fig. 3.1) was significantly easier; this connection could be fabricated in the field with minimal difficulty. It should be noted that in all of the specimens tested the weld failed in only one specimen. This occurred in one of the specimens after the ultimate load had been reached and excessive deformation had taken place. The compressive strength of the PC concrete in Specimens 1 and 2 (see Fig. 4.1) during testing was 37,920 kPa (5,500 psi). For Specimens 3 and 4, (see Fig. 4.1) the PC portion had a compressive strength of 39,990 kPa (5,800 psi) and the CIP portion had a compressive strength of 36,540 kPa (5,300 psi).

The moment-deflection curves at the centerline for the two specimens with only the PC portion of the deck in place are shown in Fig. 6.1. One specimen (Specimen 2) had top and bottom connector plates while the other one (Specimen 1) only had a bottom plate connector plate (see Fig. 4.1). Moments were calculated at mid-span from the specimen geometry and the applied load. This was done since the load in Specimens 1 and 2 was applied 152 mm (6 in.) off center and at the centerline in Specimens 3 and 4. To be able to compare the capacity of the connections with and without the CIP it was necessary to calculate the moment at the centerline rather than simply compare applied loads. As can be seen in this figure, the specimen with only the bottom plate (Specimen 1) was significantly less stiff than the specimen with top and bottom plates (Specimen 2). Of

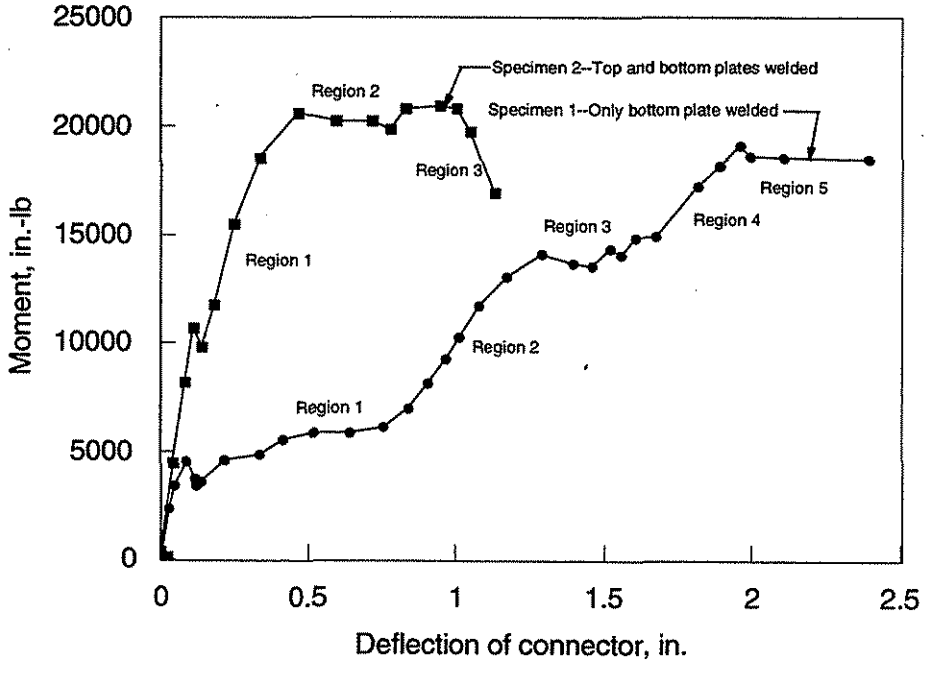

Figure 6.1. Moment-deflection curve of small scale specimens without CIP deck.

particular interest in Specimen 1is the fact that there are three locations (Regions 1, 3, and 5) where the deflection continued to increase without an increase in load. The most likely reason for this behavior is described in the following paragraph.

After welding the bottom plates to the flanges of the channels, there was a gap of varying width from 0 mm (0 in.) (i.e., flush) to 51 mm (2 in.) along the adjoining faces of the panels. It is obvious that during construction of the PC connection in the field the results may be significantly different than those in the laboratory. Realizing this, the small scale specimens were intentionally "poorly" constructed (i.e., an excessive gap between the specimens was constructed). This gap and plus its non-uniformity explains the first two horizontal regions (Regions 1 and 2) shown on the load-deflection curve. Region 1 represents the initial deflection of the specimen due to bending of the welded plate. During this phase of loading, the load was carried only by the plate which bent about its neutral axis. After the plate had reached its flexural strength, the specimen began to deflect significantly without an increase in the load due to yielding of the plate. During testing, it was observed visually and by monitoring the load that when the specimen had sufficiently deflected so that the faces of the adjoining panels were in contact, the specimen had additional strength (i.e., the concrete in adjoining panels which was in contact provided a compressive force and the steel plate provided a tensile force; these two forces thus provided flexural resistance.). This mechanism resulted in the second portion of increasing load with deflection (Region 2). During this time of increasing moment capacity, it is hypothesized that some of the internal forces in the plate (i.e., those near the top surface of the plate) changed from compression to tension thereby increasing the specimen's ability to carry moment. The second region of increasing deflection

without an increase in load (Region 3) is explained by the fact that when the units did come into contact, the contact was not continuous across the full transverse width of the specimen. As previously noted, "poor" construction of the specimens resulted in a gap of varying widths between the units. The second constant moment region (Region 3) is thought to be the result of some additional extreme fiber yielding which began after redistribution of the internal forces. This continued until the faces of the units were in full contact whereby the stiffness of the system changed again. The moment on the specimen again began to increase until yielding of the full specimen occurred (Region 5).

The moment-deflection curve for Specimen 2 is a typical load-deflection response. The moment was resisted consistently until yielding of the specimen occurred whereby the specimen failed. During loading (Region 1) the load is resisted by the compressive force developed in the top plate and the tensile force developed in the bottom plate. The small decrease in Region 1 is due to some movement of the channel relative to the concrete. In Region 2, the top and bottom plates begin to yield and the ultimate moment is reached. In Region 3, significant necking in the bottom plate has occurred and the area resisting the loads is significantly reduced.

It is interesting to note that the ultimate strength of the two specimens is essentially the same. However, Specimen 1 (with only the bottom connection plate) reached that load at a deflection over twice that of Specimen 2. Connected PCDT units without the CIP concrete will only be subjected to construction loads. Prior to subjecting the bridge to traffic loading, the CIP concrete will be added. Thus, the small scale specimen tests just described (only PC concrete) are temporary and only occur during construction of the bridge. Also, when the CIP concrete is added, the gap between units

previous described will be essentially eliminated by the CIP concrete which will fill these gaps.

Shown in Fig. 6.2 is the moment-deflection curve for the small scale specimens (Specimens 3 and 4) with the CIP portion of the deck added. It was originally thought that the connection detail would perform satisfactorily with only the welded bottom plate (Specimen 3) because the CIP concrete would resist compression similar to the top plate. As is evident in this figure, this is not the case. Specimen 3 did not perform nearly as satisfactorily as the one with the top and bottom plates (Specimen 4). This is primarily due to the fact that without the top plate, the connection was allowed to rotate much more freely. It is thought that this additional rotation caused the reinforcement welded to the channel to yield under large loads. The sudden drop in the load being carried in Specimen

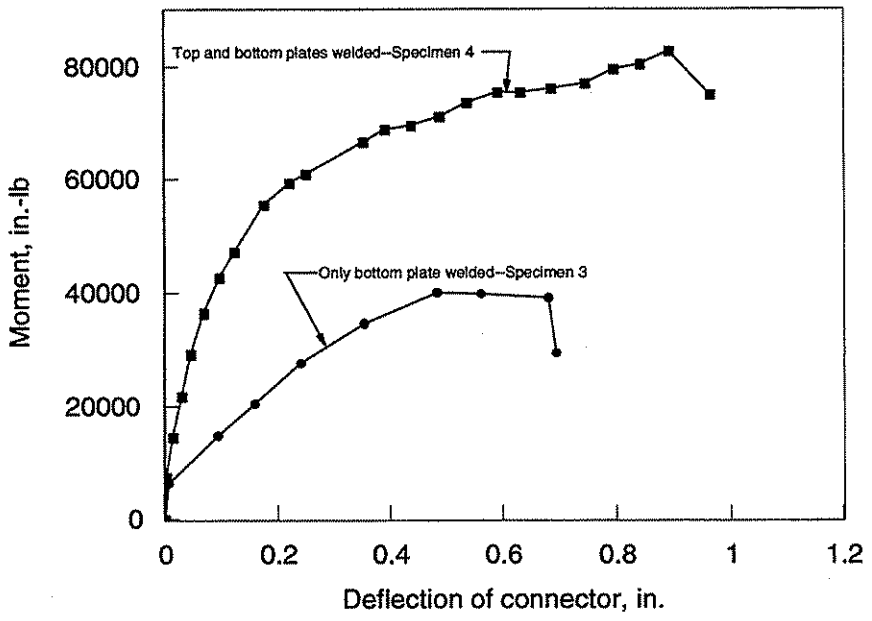

Figure 6.2. Moment-deflection curve of small scale specimens with CIP deck.

3 is attributed to the fact that one of the reinforcing bars welded to the channel broke free causing a sudden change in the specimen's properties.

For the Specimens 3 and 4, it was found that the controlling parameter for the connection detail was strength rather than deflection. The strength Specimen 4 is over two times that of Specimen 3. Based on this and the fact that construction of the two plate detail required very little additional effort (the hardest part of installing the connection is the overhead welding of the bottom plate), it was decided to proceed with the connection that had top and bottom plates (Specimen 4).

Only the deflection data at midspan (Figs. 6.1 and 6.2) is presented in this report. The strain data monitored in the bottom steel plates led to the same conclusions as those presented previously. Deflection instrumentation and strain gages at the quarter points were installed for detecting any asymmetrical behavior in the specimens. For specimens with only the PC concrete, an asymmetric behavior was noted as one would expect due to the eccentricity of the applied load. Symmetry was observed in both strain and deflection data obtained during testing of the full-depth specimens (i.e., PC plus CIP).

The strength of Specimen 3 is approximately twice that of Specimen 1 whereas the strength of Specimen 4 is approximately four times that of Specimen 2. This can be attributed to the shift in the location of the neutral axis due to the additional steel on the tension side.

6.2 Experimental Results: "Handling Strength" Test of a Single Unit

The "handling strength" tests of a single PCDT unit consisted of testing a 9,750 mm (32 ft) long full scale specimen; see Chp. 3 for a description of the specimen and Chp. 4 for details of the test setup and instrumentation employed. This type of testing was

completed to determine: (1) the "handling strength" of the PCDT units during erection, (2) the amount of composite action obtained between the PC concrete and the steel beams, and (3) the response of PCDT units to load for FEM verification.

Shown in Fig. 6.3 is the strain and deflection response of the specimen during one of the four "handling strength" tests. Note that the loads plotted are the loads at one load point (i.e., the total load on the specimen is twice this amount). Strains are shown (Fig. 6.3a) at the centerline as well as at the quarter point (Fig. 6.3b). Shown in each graph is the strain at four locations on the cross section: top of PC concrete, bottom surface of the top beam flange, mid-height of the web, and on the bottom surface of the bottom beam flange. The data, in all cases, shows a linearly increase in strain with load. A maximum strain of -30 MII and 76 MII was measured in the concrete and steel, respectively. In Fig 6.3c, the linear load-deflection curve indicates that the PCDT unit underwent elastic deformation as shown in Figs 6.3a and 6.3b. It should be noted that although the data are not presented here, the deflections at the quarter points exhibited the same response. Deflections measured at the edges of the cross-section indicated that no "tilting" of the PCDT unit occured.

Shown in Figs. 6.3 d and e is the strain responses which occured at various increments of load at the centerline (Fig. 6.3d) and quarter point (Fig. 6.3e). Note that the loads in these figures are also for one load point. The linear strain distribution at the two section for the three load levels shown in these figures clearly indicates the composite action between the concrete and steel. The theoretical location of the neutral axis (determined using the geometry and modulus of elasticity of each material) and the

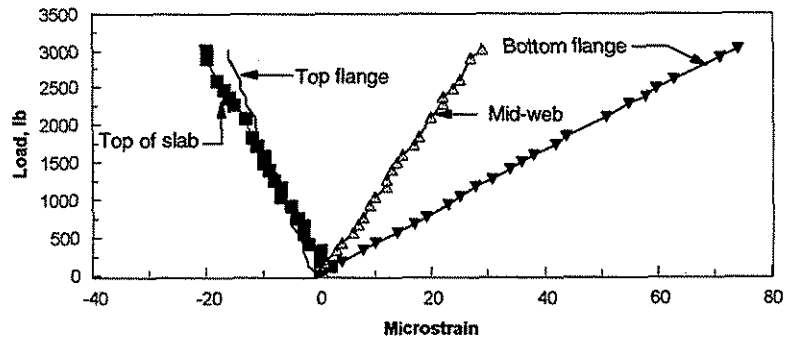

a. Strain at centerline

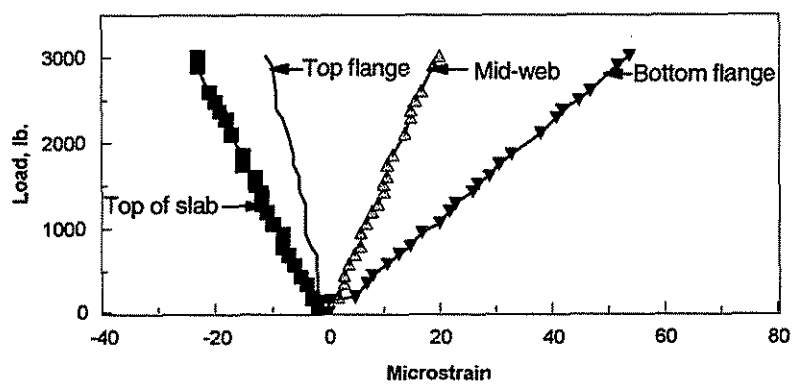

b. Strain at quarter point

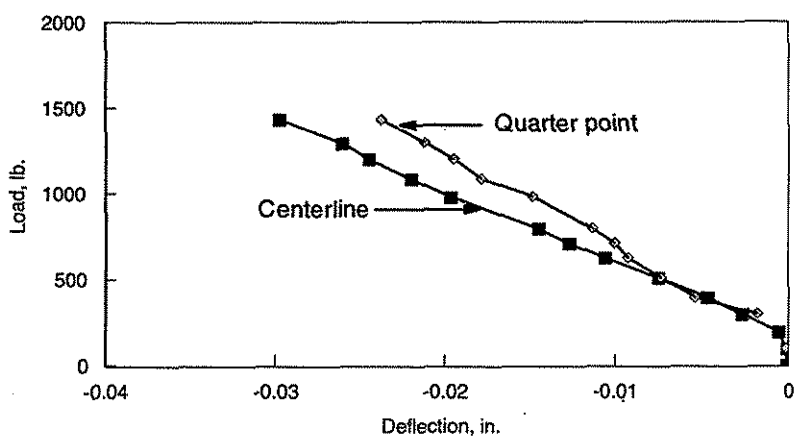

c. Deflection

Figure 6.3. Results from "handling strength" tests.

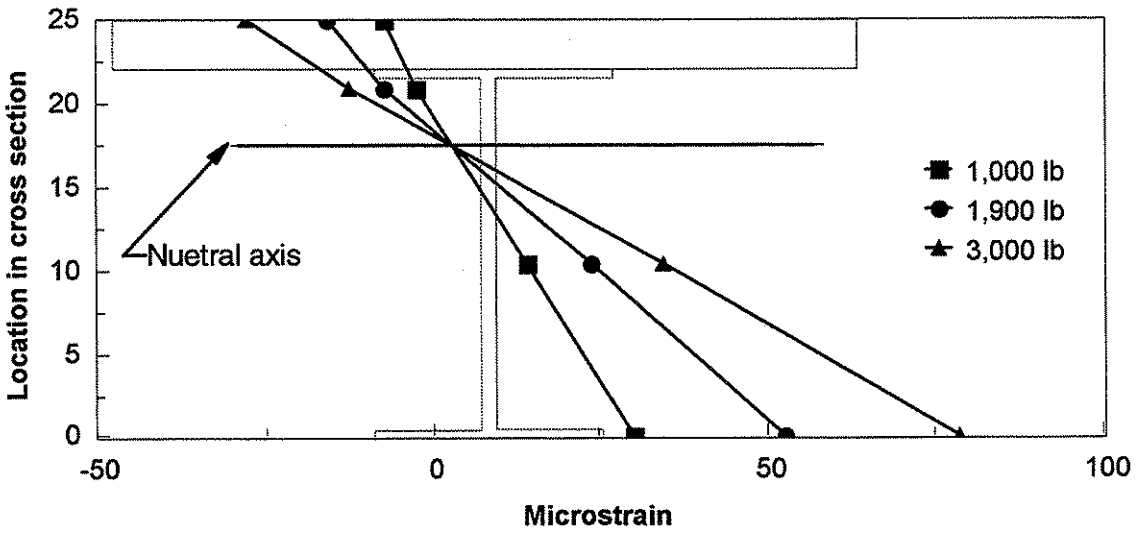

d. Strain profile at the centerline

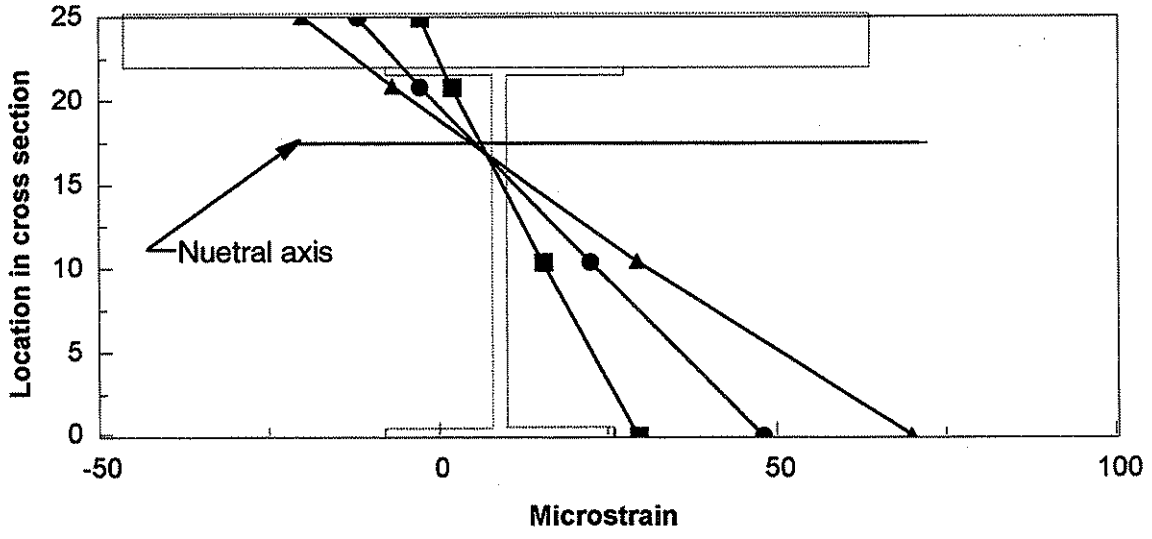

e. Strain profile at quarter point

Figure 6.3. Continued.

experimental location are nearly the same. This indicates that the welded shear studs are effectively transmitting the shear forces between the steel beams and the concrete deck. The compressive strength of the concrete used in this PCDT unit during testing was 37,920 kPa (5,500 psi). The level of strain in the steel and concrete clearly shows that the PCDT units have sufficient strength to resist the dynamic loads that will occur during placement of the units. Additionally, it should be noted that prior to testing, the PCDT unit was moved in the SEL using the overhead crane without damaging the PCDT unit. However, since the gearing in the SEL crane is low, the dynamic forces did not approach those a typical crane would impart during movement of the units.

6.3 Full Scale Model Bridge Tests

A total of 132 tests were performed on the model bridge. The breakdown of these tests is as follows: 64 on the bridge without the CIP deck, 68 on the bridge with the CIP deck, 128 service load tests, and 4 ultimate load tests. The full scale model bridge tests consisted of testing a 9750 mm (32 ft) simple span bridge specimen with a 6400 mm (21 ft) wide deck (see Chp. 4). This testing was completed for several reasons: (1) to determine the contribution of the CIP concrete in distributing live loads, (2) to determine the effect that diaphragms and diaphragm positioning have on load distribution, and (3) to determine the behavior and strength of the bridge system.

The location of the load points used in testing the model under the various conditions is shown in Fig. 6.4. These load points were selected so that load could be applied at various longitudinal sections (Sec. 1, Sec. 2, etc. in Fig. 6.4) and at various

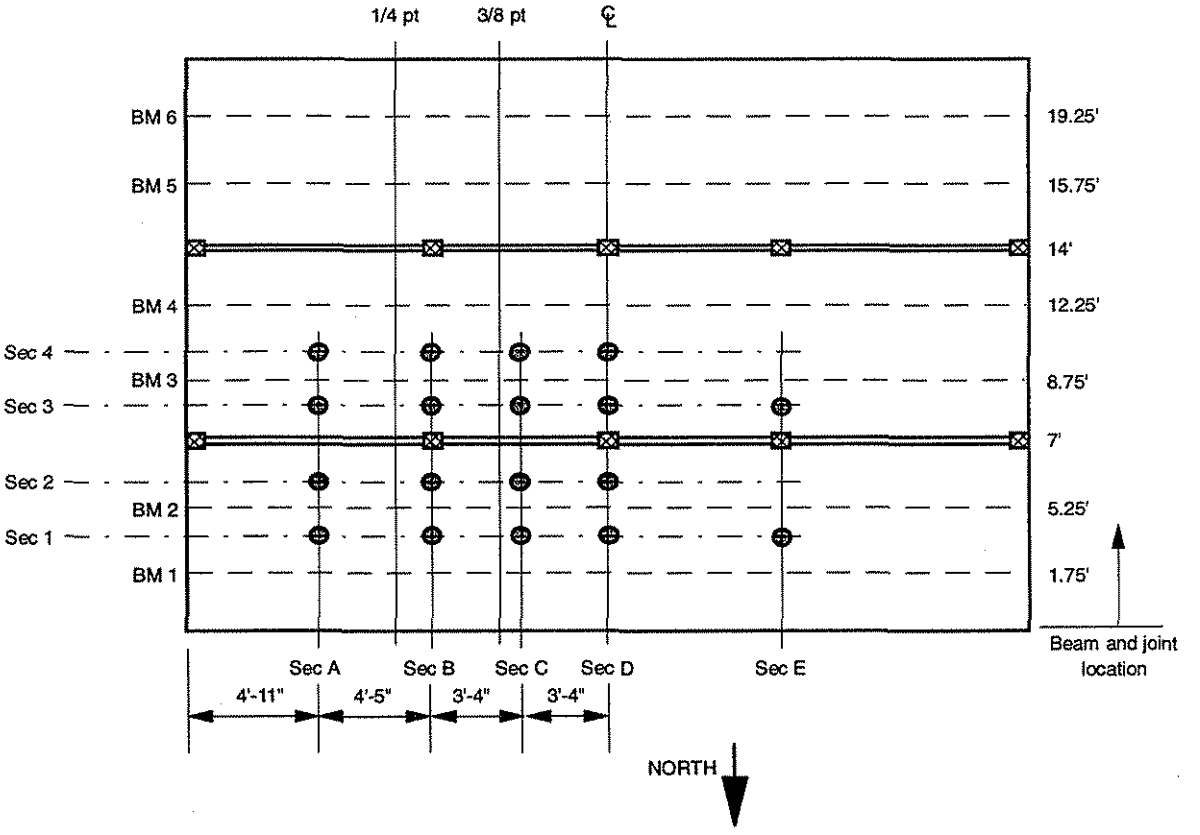

Figure 6.4. Location of load points.

transverse sections (Sec. A, Sec. B, etc. in Fig. 6.4). These load points made it possible to apply load at various distances from the PC deck connectors. In the following discussion, load points are given a letter/number designation. For example, Load point B3 indicates that load was applied at transverse Sec. B and longitudinal Sec. 3. Load point D3 indicates load was applied at transverse Sec. D and longitudinal Sec. 3, etc. The only load points used in the service load tests are A1 through A4, B1 through B4, C1 through C4, and D1 through D4. The load points E1 and E3 were only utilized in the overload tests. Note that the six steel beams in the bridge model have been identified as BM1, BM2, etc. in Fig. 6.4. These beam numbers are used in subsequent figures to identify the beam being

referenced. In some of the subsequent figures, data are referenced to the distance from the north edge of the bridge model. In these figures, data at the joints between adjacent PCDT units is presented that was not at a steel beam location. These distances are also given in Fig. 6.4.

6.3.1 Model Bridge Results: PC Deck Only

6.3.1.1 Experimental Results

As was previously noted, the model bridge was tested with only the connected PCDT units in place. Load was applied at the four locations on Sec. A- Sec. D (16 total load points) and varied from 0 N (0 lbs) to a maximum of 71,170 N (16,000 lbs). Strains and deflections (see Fig. 4.7 for locations) were recorded during each of these load cycles. As was described in Chp. 4 (see Fig. 4.6), the model bridge was tested with three, five, seven, and nine connectors in place. Representative results from these numerous tests are presented in the following figures.

Comparison of strains and deflections in the bridge with the various connector arrangements is presented with load being applied at two different load points (Points B1 and C3) are presented in Figs. 6.5 - 6.8. As is evident in these figures, the strain data and deflection data curves have very nearly the same shape and infer similar behavior. Based on this fact, the only data presented in the remainder of this report will be the deflection data at three locations: centerline, quarter point, and the 3/8 point.

The influence of the four arrangements of connectors (three, five, seven, and nine connectors) is illustrated in Figs. 6.9 - 6.11 (see Fig. 4.6 for the location of the connectors). Although there is some variation in the load applied (actual load applied is

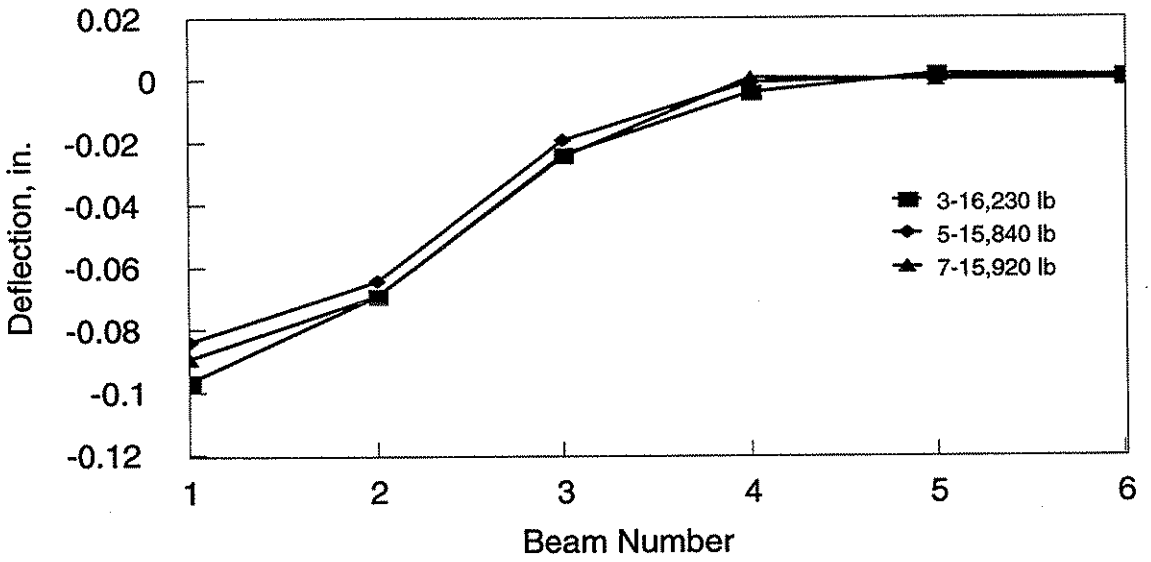

a. Deflection data

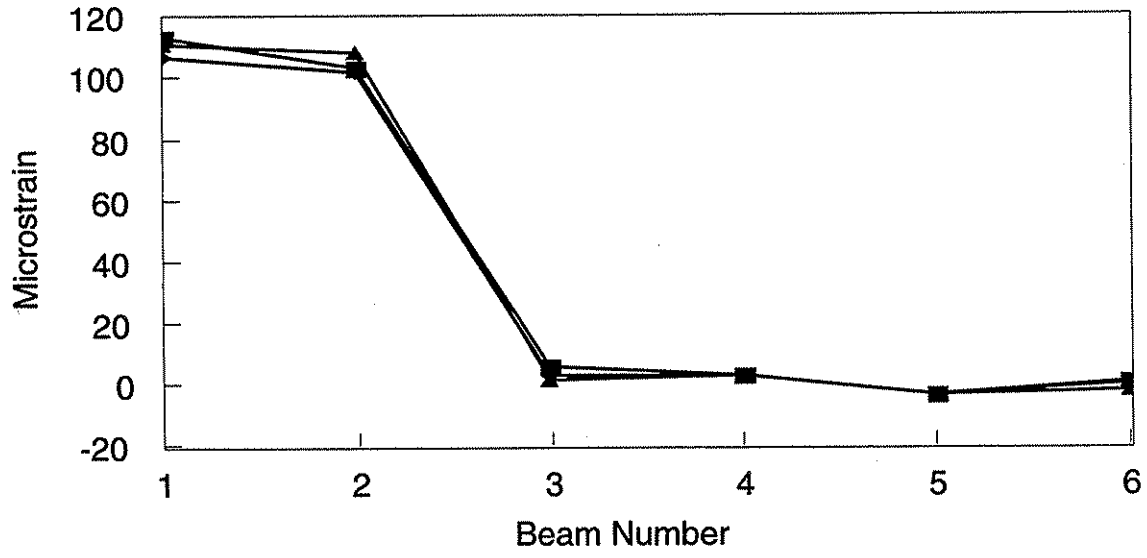

b. Strain data

Figure 6.5. Deflection and strain response at the centerline; load at point B1.

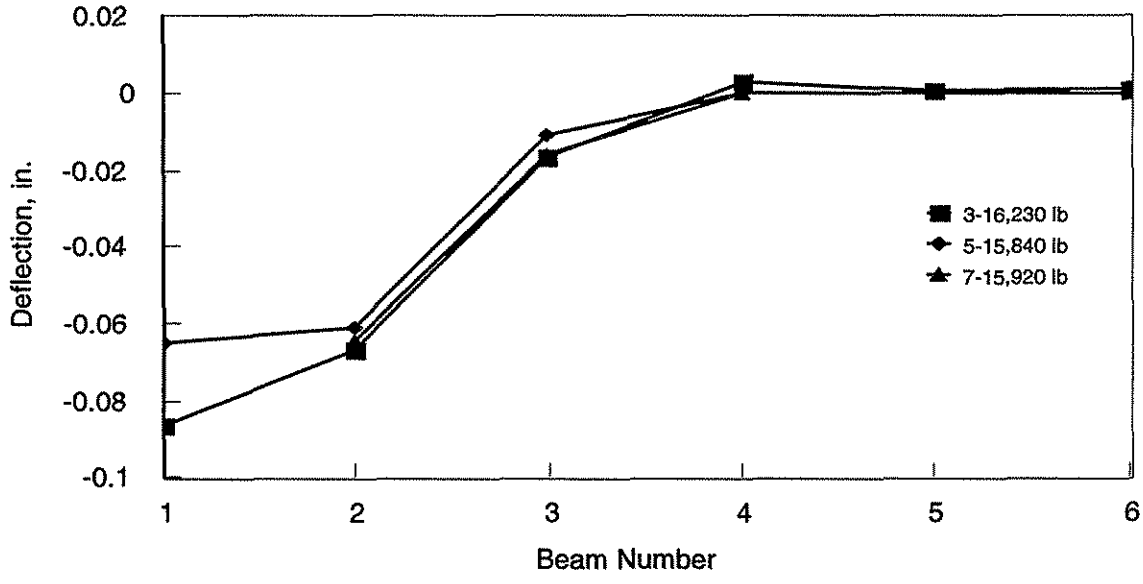

a. Deflection data

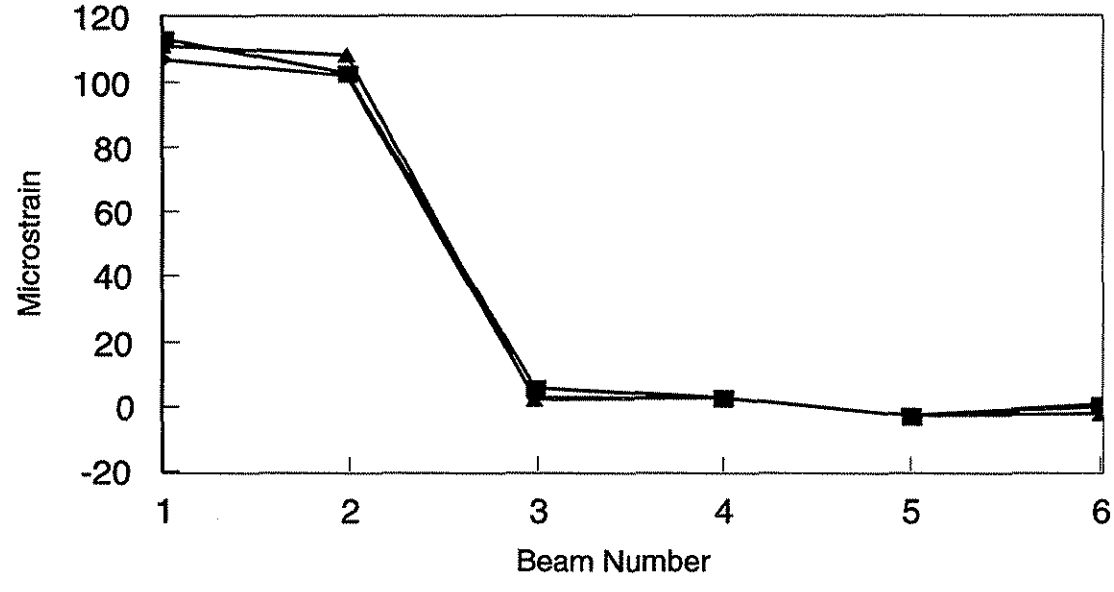

b. Strain data

Figure 6.6. Deflection and strain response at the quarter point; load at point B1.

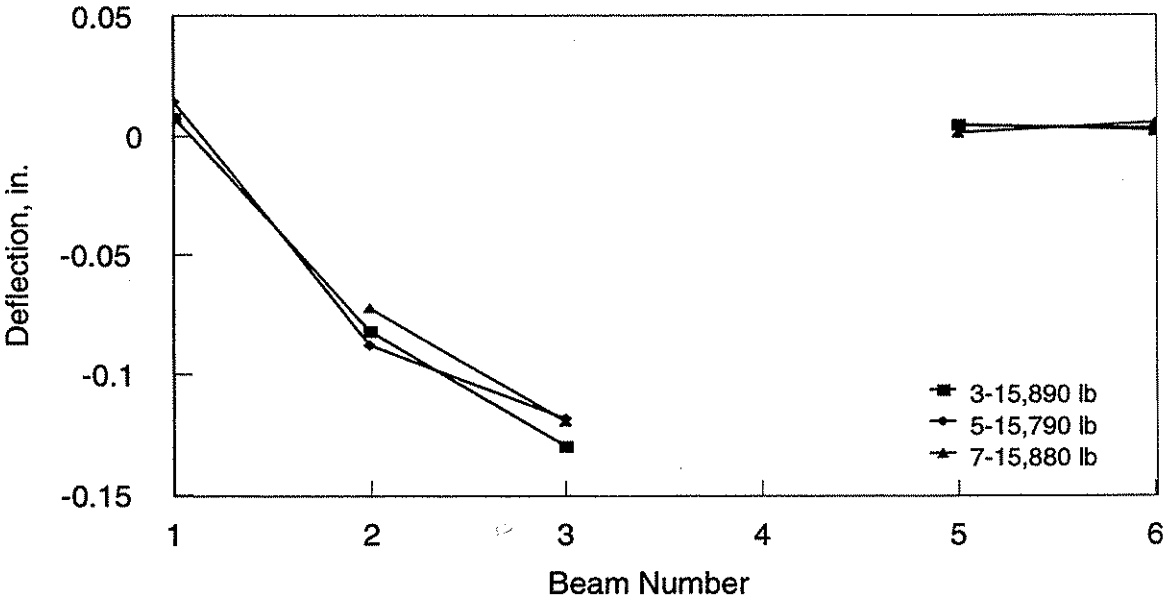

a. Deflection data

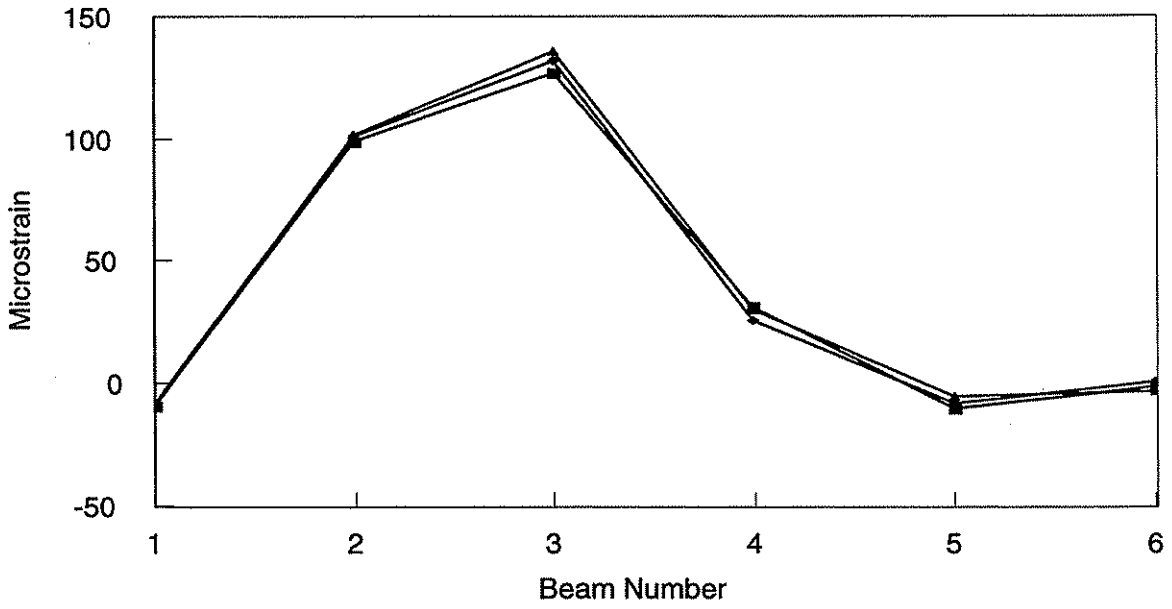

b. Strain data

Figure 6.7. Deflection and strain response at the centerline; load at point C3.

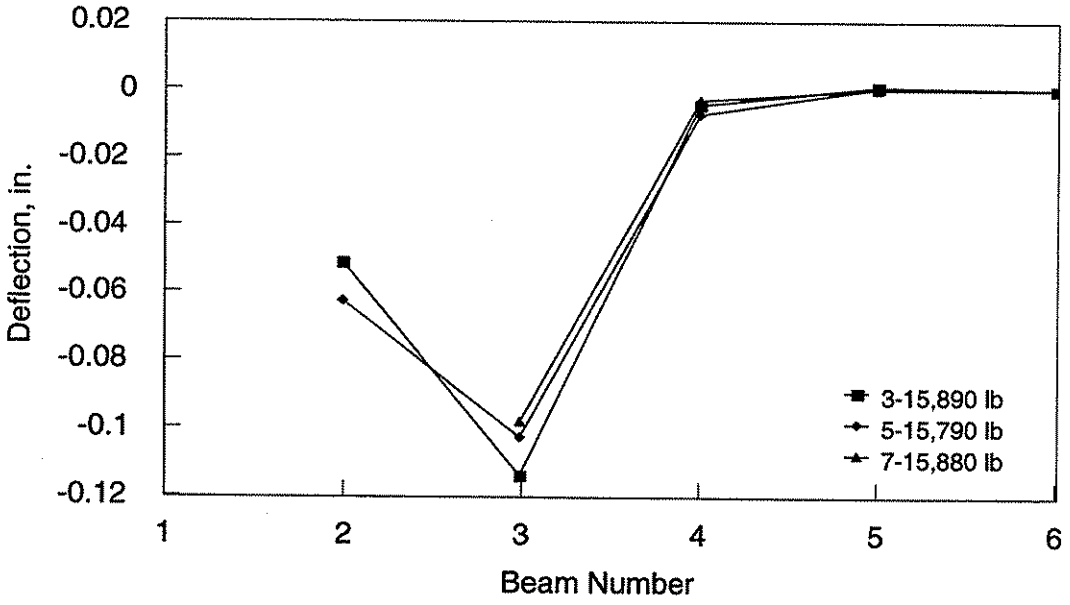

a. Deflection data

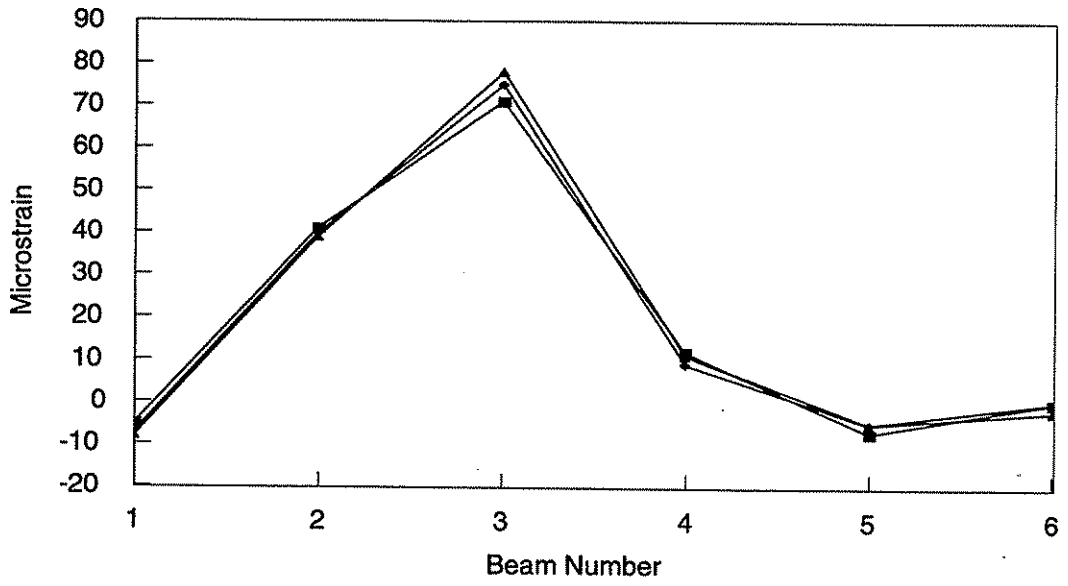

b. Strain data

Figure 6.8. Deflection and strain response at the quarter point; load at point C3.

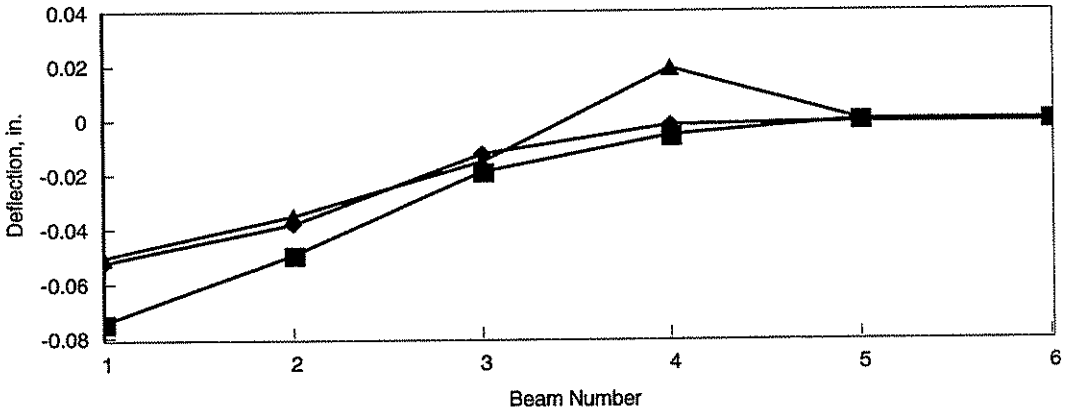

a. Centerline

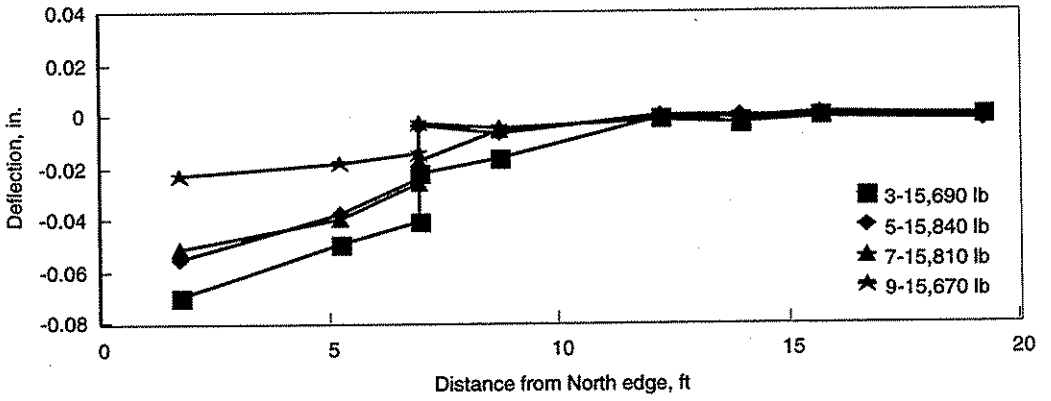

b. 3/8 point

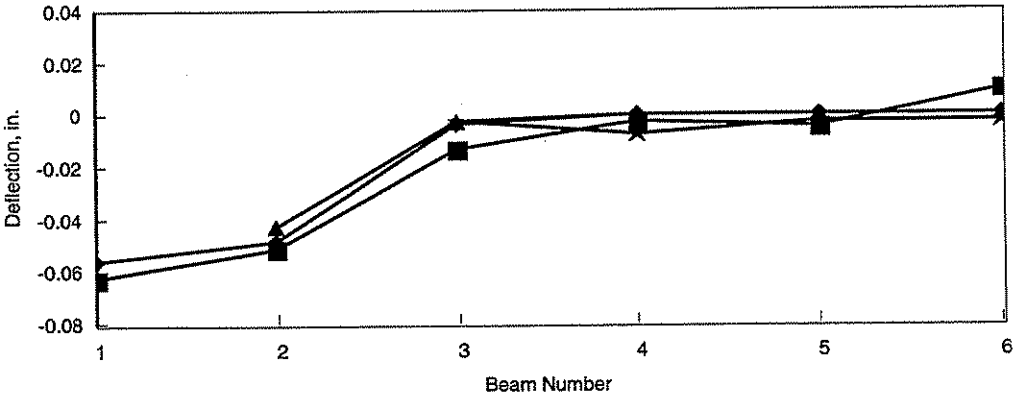

c. Quarter point

Figure 6.9. Influence of connector arrangement on bridge deflections; load at A1.

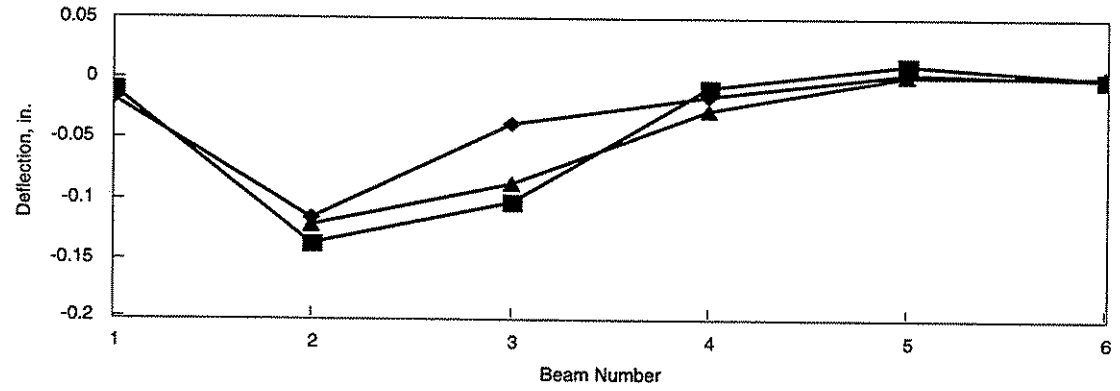

a. Centerline

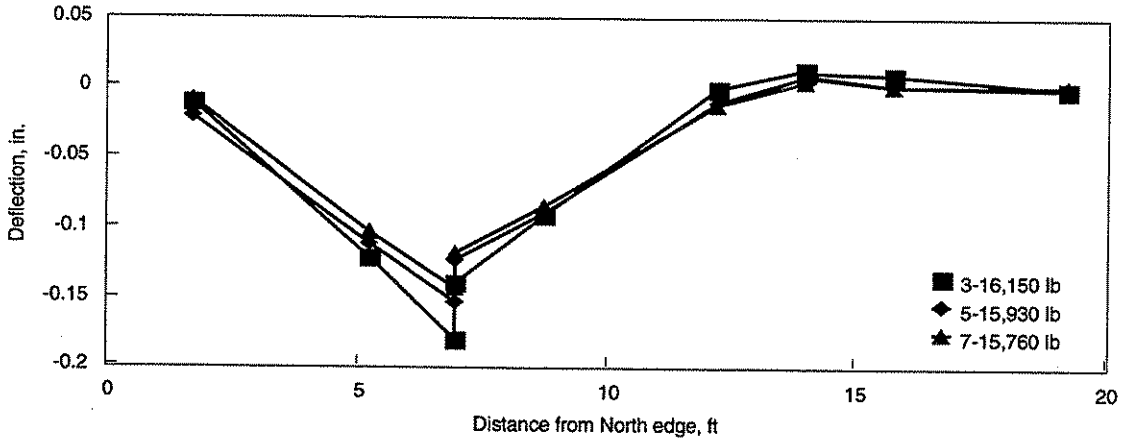

b. 3/8 point

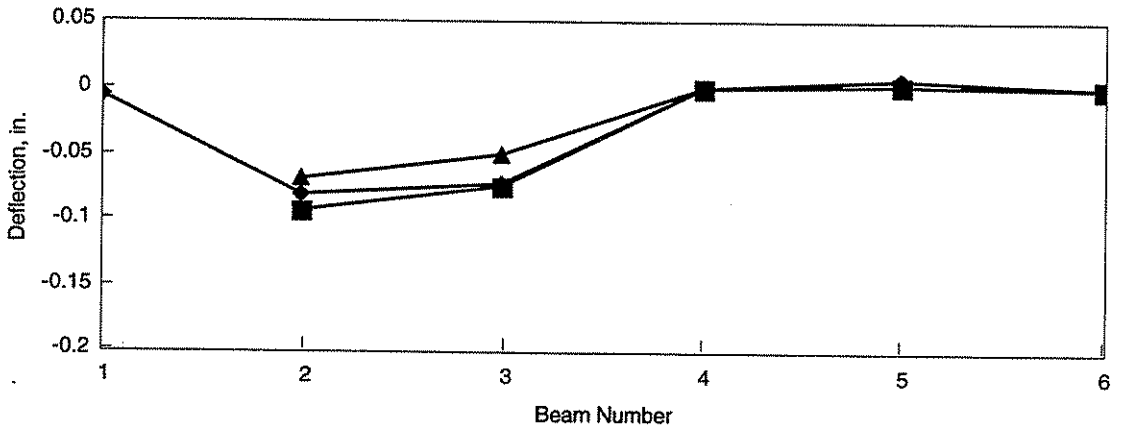

c. Quarter point

Figure 6.10. Influence of connector arrangement on bridge deflections; load at D2.

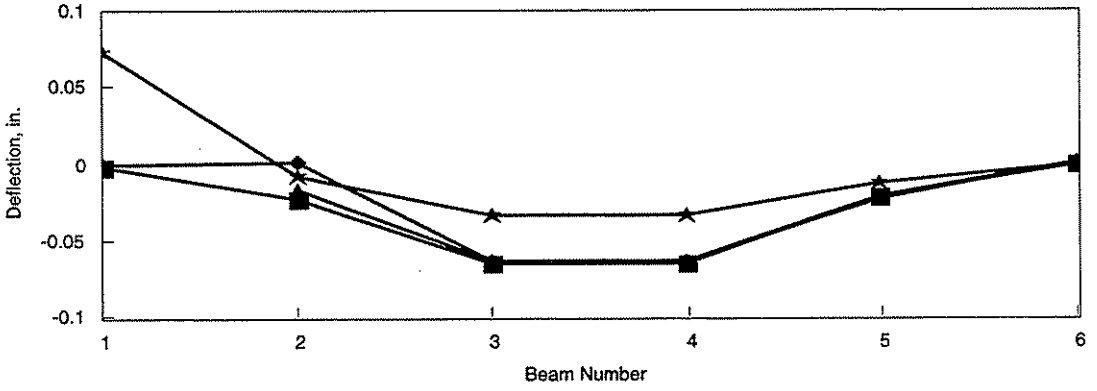

a. Centerline

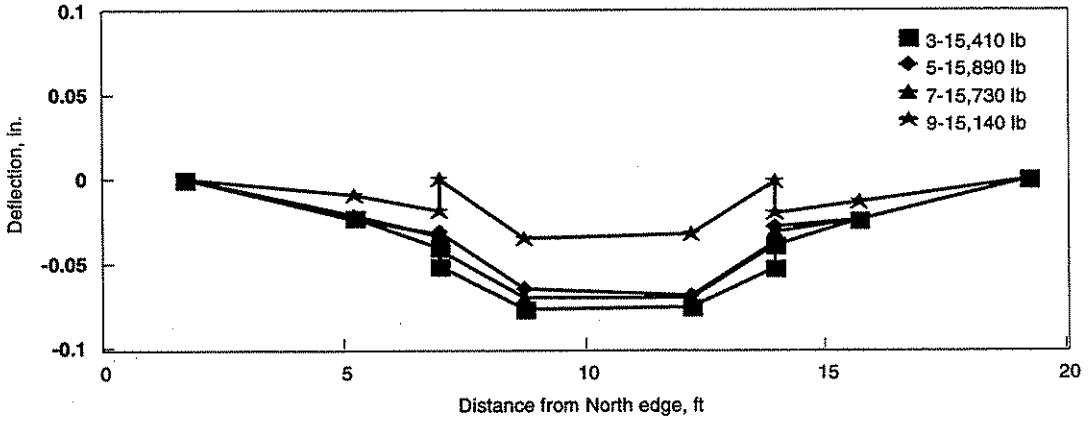

b. 3/8 point

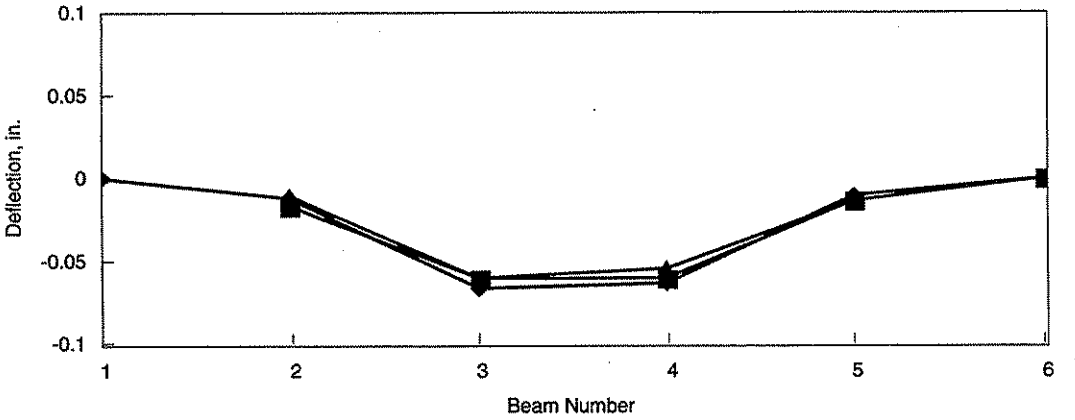

c. Quarter point

Figure 6.11. Influence of connector arrangement on bridge deflections; load at B4.

given in each figure), a nominal magnitude of 71,170 N (16,000 lbs) was applied. In these figures, three representative load points (Points A1, D2, and B4) are presented.

As was previously noted, load was applied at the 16 load points identified in Fig. 6.4 for each of the four connector arrangements. Data in these three figures are representative of the data that were collected. Note the three load points selected for presentation are at different distances from the individual connectors in the four connector arrangements as one would have in an actual bridge.

Deflections in these three figures indicate, as one would expect, the more connectors the better the lateral load distribution. As illustrated in Fig. 6.9, the connector arrangement has minimal influence on the deflections at the centerline (Fig. 6.9a) and quarter point sections (Fig. 6.9c). Greater differences are observed at the 3/8 point (Fig. 6.9b) section as a result of this section being further from the connectors. Thus, there is more differential deflection between the two PCDT units causing the difference in response.

This same general behavior is exhibited in Fig. 6.10. In Fig. 6.10a, one observes atypical deflections for Beam 3 with the five connector scheme. The cause of this abnormality is not known and can most likely be attributed to a deflection transducer that was not properly vertically aligned.

In Fig. 6.11, one observes the same behavior for the three, five, and seven connector schemes but a markedly different response for the nine connector scheme. The atypical deflection pattern is due to the fact that the nine connector spacing adds a connector very close to Load point B4 whereas the other connector arrangements did not.

Thus, the arrangement of PC connectors influences the global as well as local behavior of the bridge system.

Review of the deflections in these figures indicates that, in general, the number of connectors has minimal effect on the resulting deflections and thus minimal effect on the lateral load distribution. An exception to this observation is illustrated in Fig. 6.9a where the 9 connector arrangement is seen to provide significantly better lateral load distribution.

Reflective cracking in the CIP deck is dependent on controling of differential deflection between the adjacent PCDT units. There are three ways to control this reflective cracking. First, providing a substantial number of PC deck connectors which would provide more lateral continuity between adjacent PCDT units therefore reducing the amount of differential deflection. Second, provide adequate reinforcement in the slab. This would add strength to the CIP concrete and therefore be more resistant to reflective cracking. The third possibility is a combination of these two, PC deck connectors and CIP deck reinforcement. Data referenced in Figs. 6.9 - 6.11 indicated that connectors can provide the desired lateral load distribution. Reinforcement in the CIP portion of the deck will also provide lateral load distribution and provide resistance to reflective cracking. It appears the best connection arrangement is a combination of the two; data verifying this statement is presented in the following sections.

The results from these series of connector tests indicate that the five connector arrangement did improve the distribution relative to the three connector scheme. However, there was minimal improvement in lateral load distributin when the seven and nine connector arrangements were used. The small improvement with seven and nine connectors suggests it is not worth the extra cost and labor required to install them. Thus,

it was determined that five connectors would provide the desired lateral load distribution for this model. Note the number of connectors required is a function of bridge length. Although five connectors provided the desired lateral load distribution in the laboratory model bridge, the number of connectors required in longer bridges has yet to be determined.

6.3.1.2 Verification of Analytical Results

Representative samples of the analytical and experimental deflections in the PCDT units with various connector arrangements are presented in Figs. 6.12 - 6.18. In Fig. 6.12 - 6.14, the nominal service load of 71,170 N (16,000 lbs) is applied at Load Point C1. Results are presented in Figs. 6.12, 6.13, and 6.14 for three connectors, five connectors, and seven connectors, respectively. Similar results are presented in Figs. 6.15 - 6.18 where the nominal 71,170 N (16,000 lbs) load is applied at Load Point C2. In this group of figures, four connector arrangements are given; three connectors (Fig. 6.15), five connectors (Fig. 6.16), seven connectors (Fig. 6.17), and nine connectors (Fig. 6.18). In these figures, since loading is at Section C (Load points C1 and C2), one would expect more significant displacement at the 3/8 point section (part b in each of these figures) since it is closer to the applied load. In reviewing these figures, one observes very good agreement between the analytical and experimental results. The exception to this statement is at the 3/8 point section (part b in these figures) at the edge between PCDT Unit 1 and PCDT Unit 2, 2,130 mm (7 ft) from the north edge of the model bridge (see Fig. 6.4). At this location, one observes a differential displacement which decreases as the number of connectors increases. The decrease in differential deflection with increase in

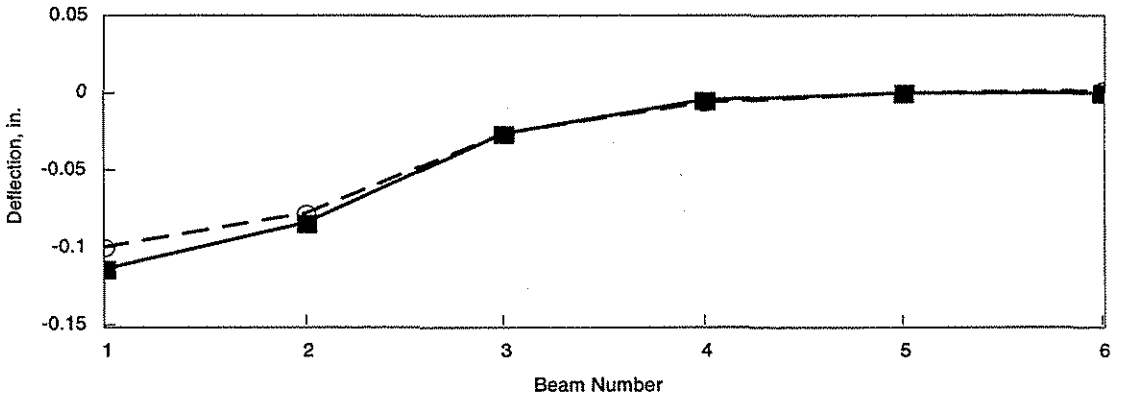

a. Centerline

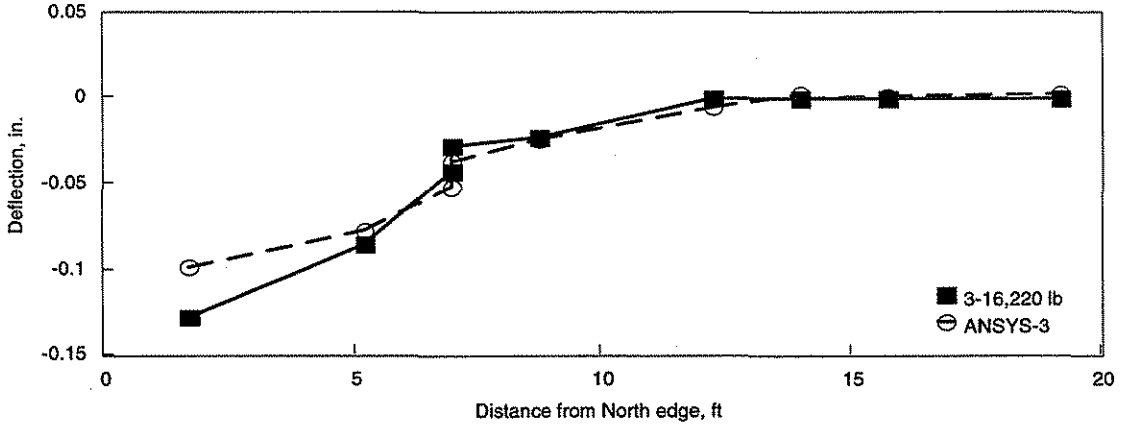

b. 3/8 point

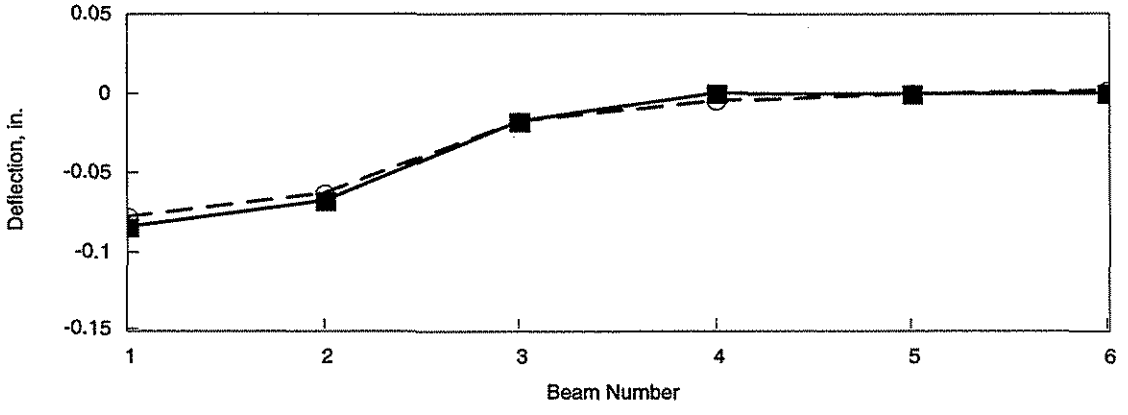

c. Quarter point

Figure 6.12. Experimental and analytical deflections in model bridge with three connectors; load at C1.

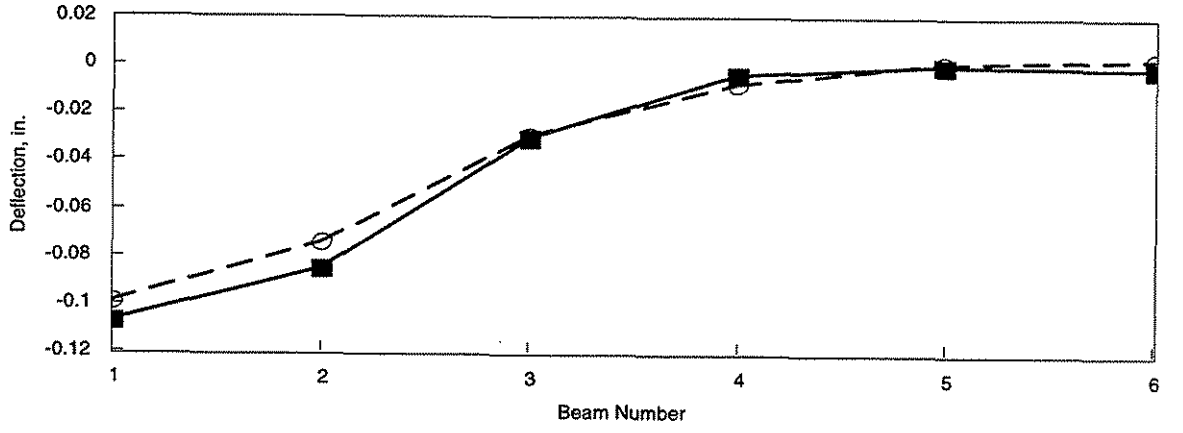

a. Centerline

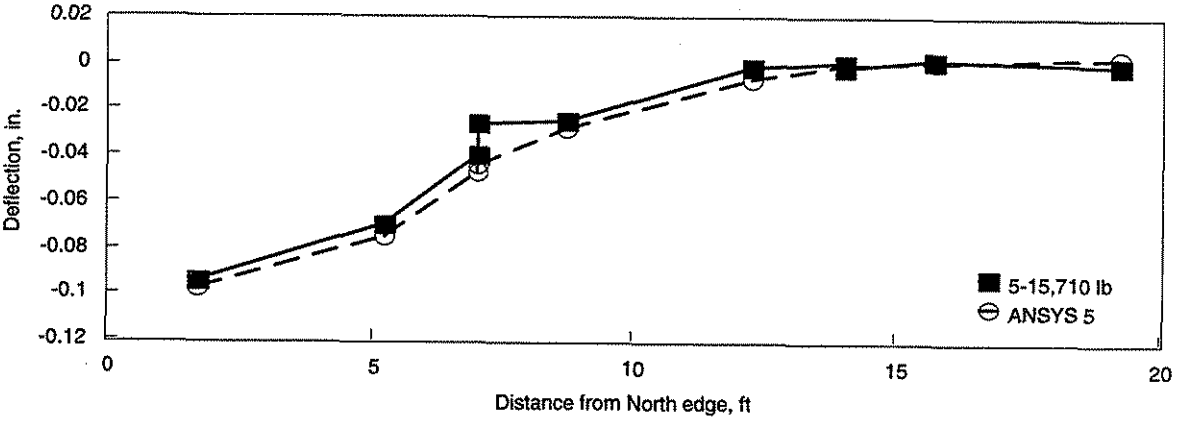

b. 3/8 point

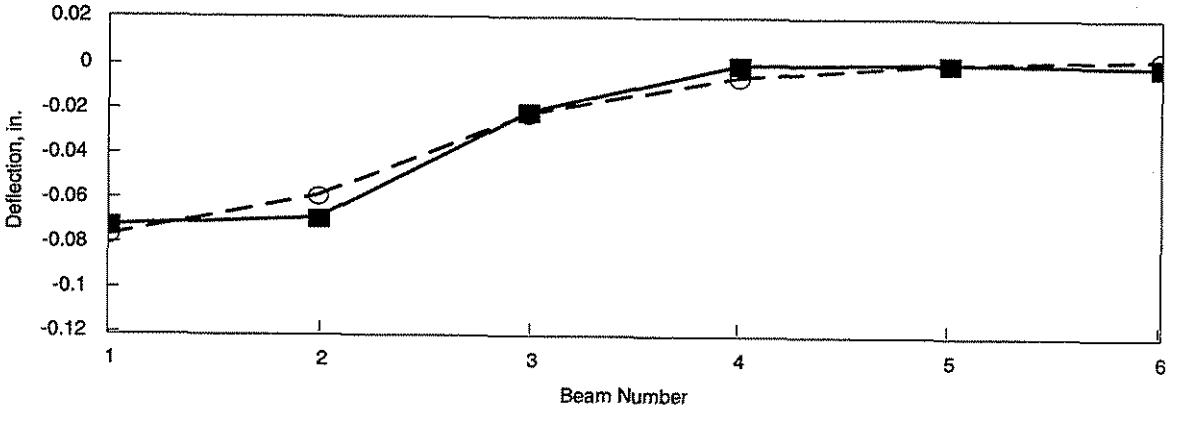

c. Quarter point

Figure 6.13. Experimental and analytical deflections in model bridge with five connectors; load at C1.

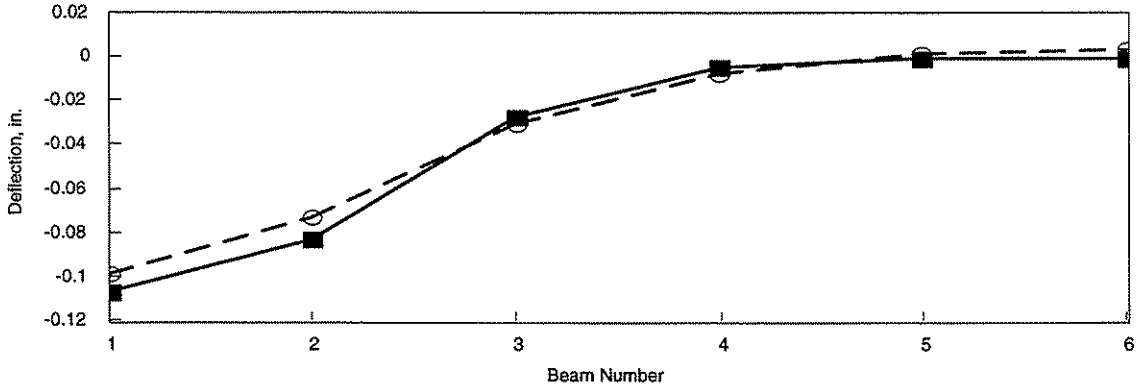

a. Centerline

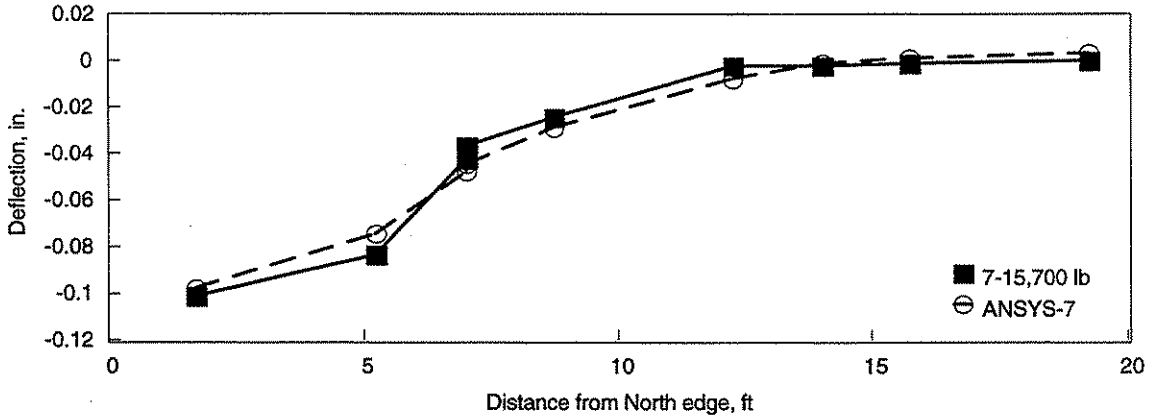

b. 3/8 Point

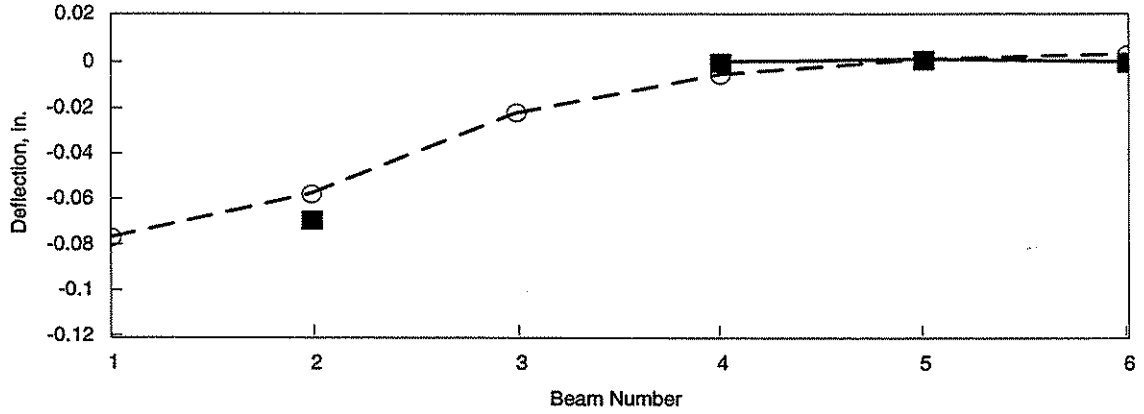

c. Quarter point

Figure 6.14. Experimental and analytical deflections in model bridge with seven connectors; load at C1.

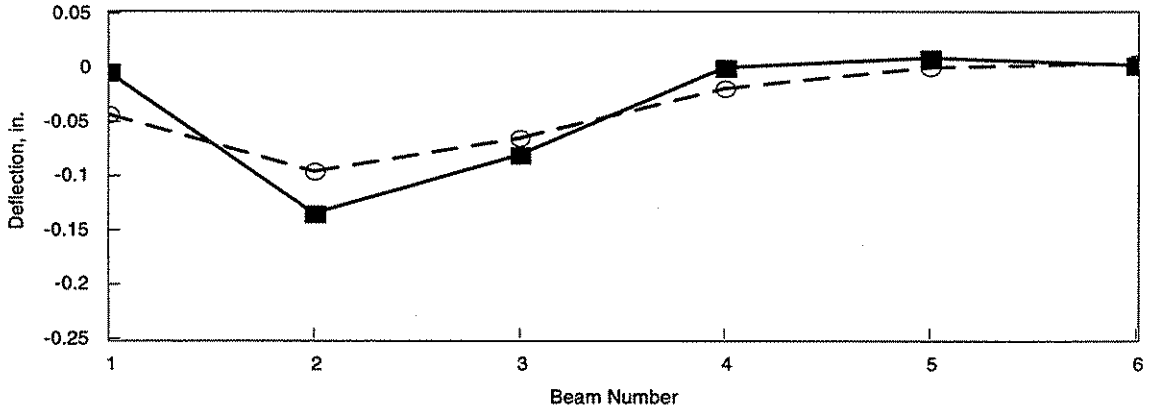

a. Centerline

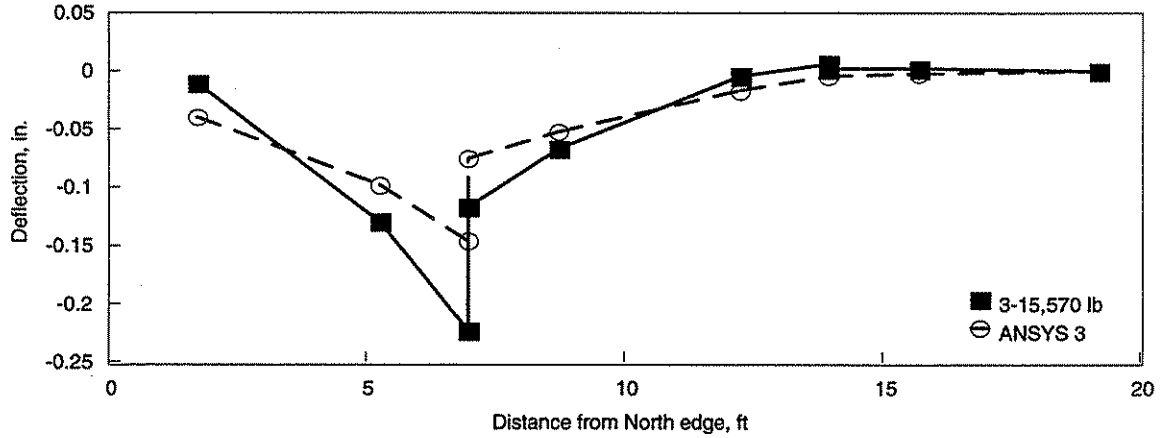

b. 3/8 point

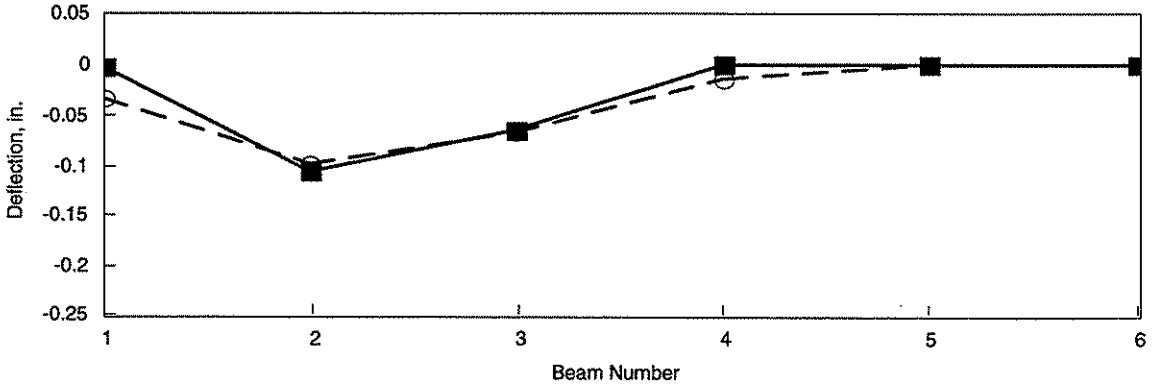

c. Quarter Point

Figure 6.15. Experimental and analytical deflections in model bridge with three connectors; load at C2.

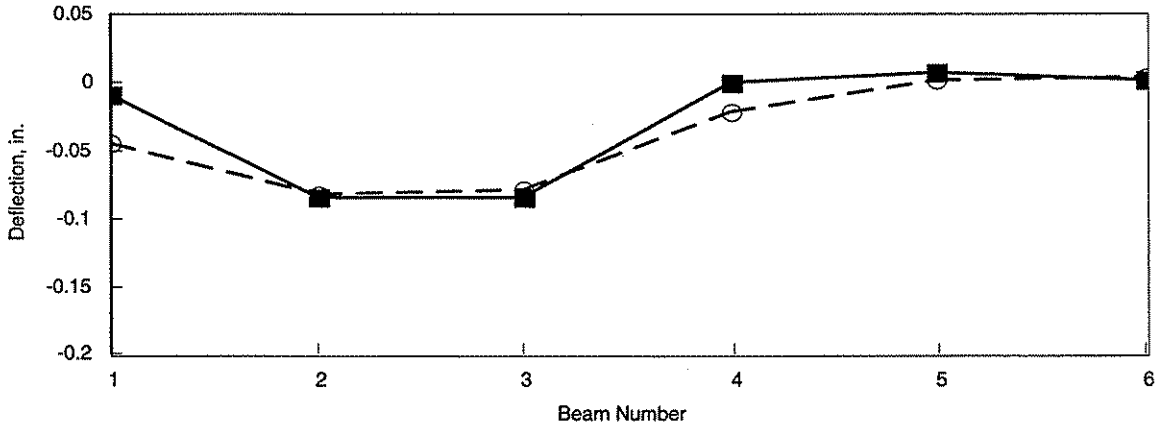

a. Centerline

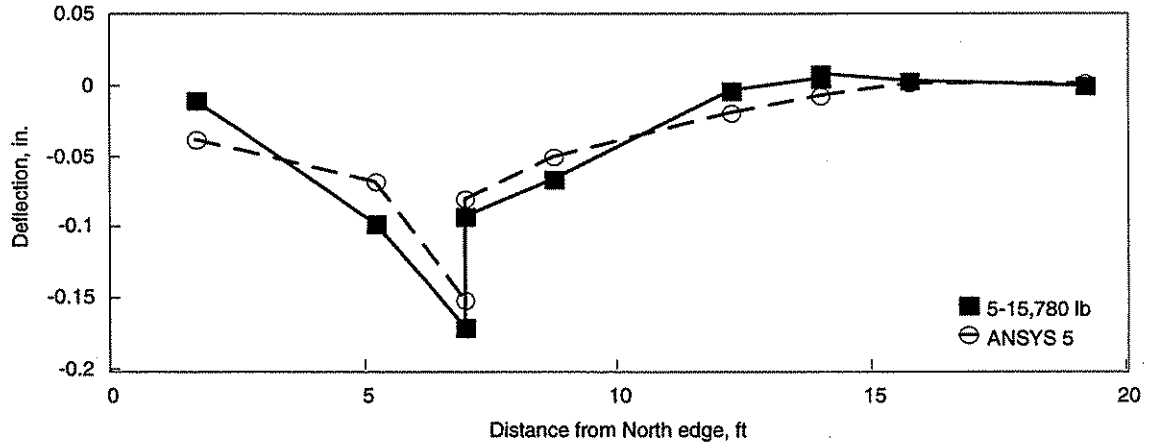

b. 3/8 point

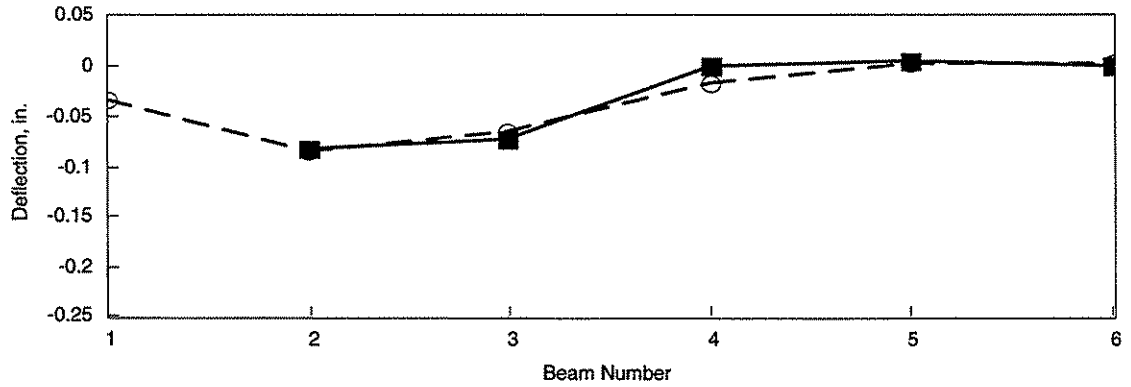

c. Quarter point

Figure 6.16. Experimental and analytical deflections in model bridge with five connectors; load at C2.

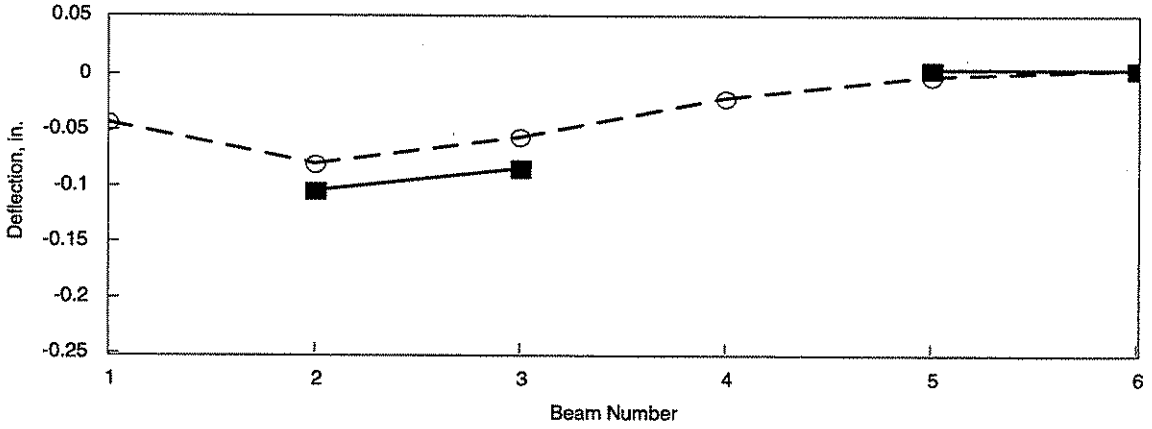

a. Centerline

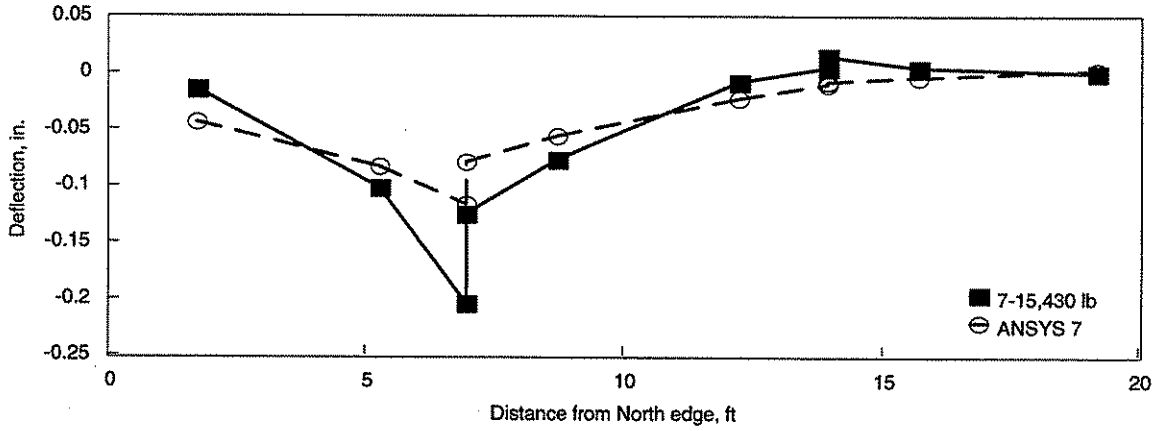

b. 3/8 point

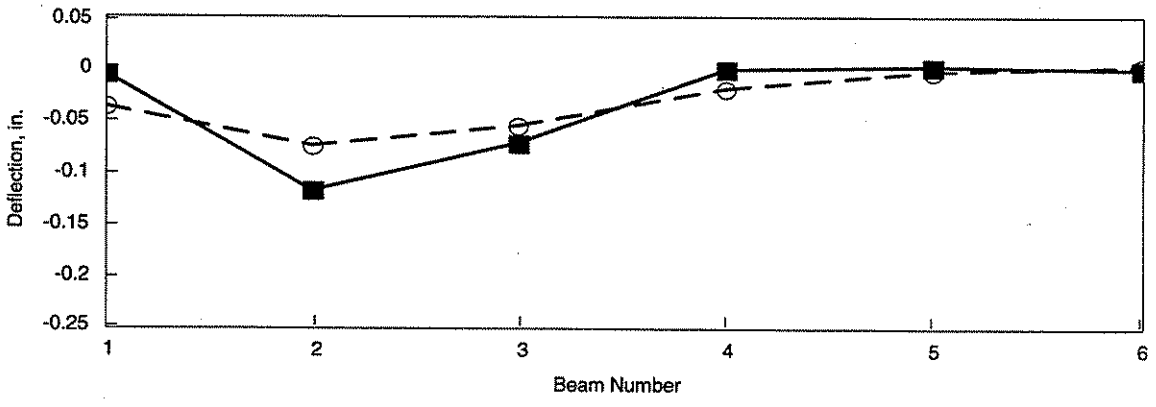

c. Quarter point

Figure 6.17. Experimental and analytical deflections in model bridge with seven connectors; load at C2.

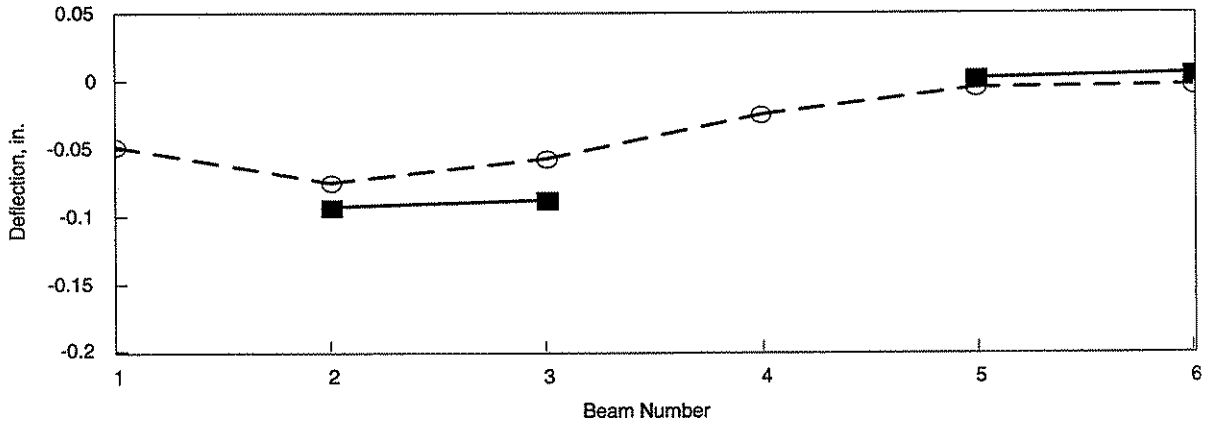

a. Centerline

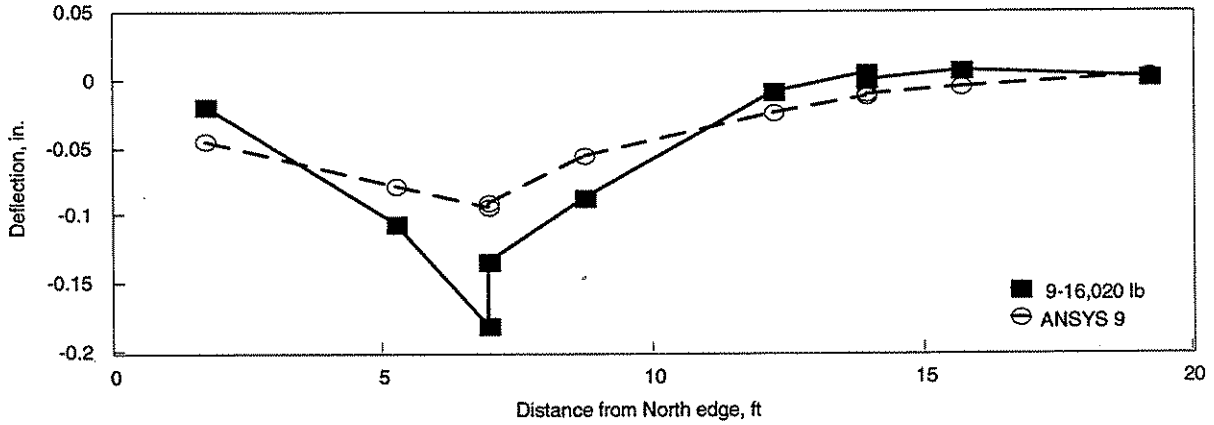

b. 3/8 point

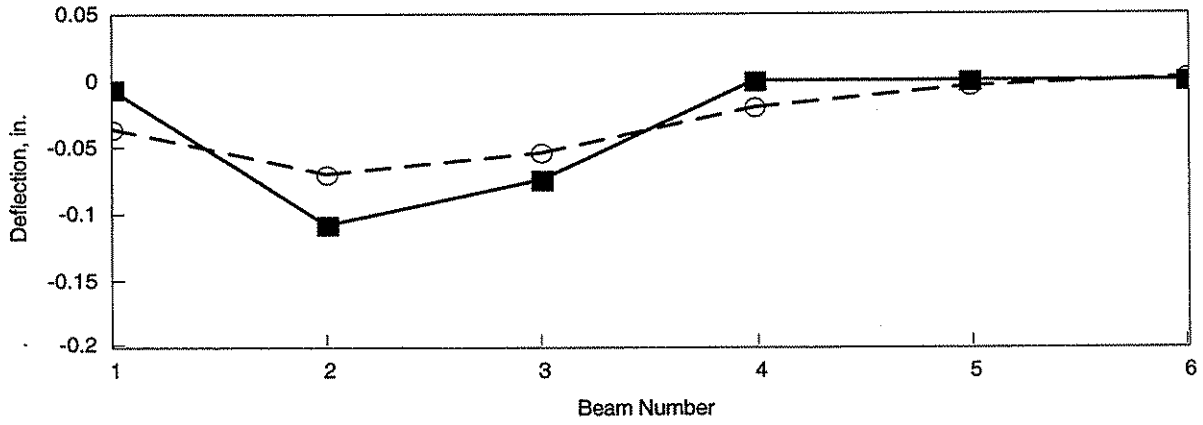

c. Quarter point

Figure 6.18. Experimental and analytical deflections in model bridge with nine connectors; load at C2.

number of connectors differs in the analytical and experimental results. The analytical model predicts that with load at C1 and seven connectors (Fig. 6.14) and with load at C2 and nine connectors (Fig. 6.18) the differential deflection is minimal. The experimental results in each of these cases however indicates the presence of differential displacement. This difference between the analytical and experimental results can be explained by the fact that in the analytical model, the PC connectors are idealized with fixed end conditions which in reality is not the case. They are somewhere between fixed and pinned - closer to fixed than pinned. This continuity difference can also explain why the analytical and experimental beam deflections nearest the joint differ by15%.

The fewer the connectors, the more apparent this modeling "error" (see Figs. 6.12 and 6.15). Thus, the difference between experimental results and analytical results is seen to decrease as the number of connectors increase.

In general, the analytical and experimental results are within 5 - 10% of each other; at a few locations, there is a 15% difference. The largest difference occurs at the interface between adjacent units. This difference is most likely the result connector fixity which was previously described and the fact that although the FEM assumes that the PCDT units are only connected at connector locations, there is some interaction at points where the common edges of the PCDT units are in contact. This contact is not constant along the common edges and is a function of variations in the construction of the units (i.e., small variations in the widths of the PC units). Due to the randomness of the contact points, it is not possible to model this interaction.

The results of these series of tests also lead to the conclusion that five connectors are appropriate in the model bridge. As previously noted, of the significant amount of data collected, only a very small representative amount has been presented here. The primary use of the remaining data was to validate the FEM that was developed. In general, this FEM gives excellent results. In a few isolated locations, the analytical and experimental results differ by approximately 15%. This difference was deemed acceptable since it is not possible to model the actual connector fixity and variable gaps (width and location) between adjacent PCDT units. The FEM for the bridge with only the PCDT units in place can be used to predict the behavior of the bridge system to construction loads and to various connector arrangements as well as for verification of the FEM for predicting the behavior in the complete bridge.

6.3.2 Experimental and Analytical Verification of Model Bridge with CIP Concrete

6.3.2.1 Model Bridge Without Diaphragms

After construction of the model bridge (i.e., CIP portion of deck added), - 203 mm (8 in.) total deck thickness and five connectors in place - six series of tests were completed. In the first series, there were no diaphragms; this configuration is referred to as ND in the following figures. To investigate the effectiveness of the CIP deck in transferring lateral loads, the model bridge was tested with the bottom plates of the connectors removed; this bridge configuration is referred to as NBP in subsequent figures. As was previously noted, a FEM was developed to predict the behavior of the ND bridge, that is the CIP concrete is continuous across the joints between adjacent PCDT units and the PCDT units are only connected at the connector locations (5 in this case). Analytical results from this FEM shall be designated as ANSYS in the following figures. In each of

the service load tests, a nominal load of 142, 340 N (32,000 lbs) was applied to the bridge at the previously described locations (see Fig. 6.4). Although there is some variation from this value indicated in the following figures, this value was used in all the analyses. This magnitude of load was selected to simulate the design wheel load normally used in the design of highway bridges.

Shown in Figs. 6.19 - 6.22 are the results of the testing of the bridge without diaphragms (ND) and without bottom plate (NBP) as well as the results from the finite element analysis for the bridge system under consideration. As is evident in these figures, when loading is along Sec. 1 - Load Point B1 (Fig. 6.19) and Load Point D1 (Fig. 6.20) and Sec. 3 - Load Point A3 (Fig. 6.22) there is excellent agreement between the analytical and experimental results. Also, removal of the bottom connector plate is seen to have minimal effect when the CIP concrete is in place. When loading is applied at Load Point D4 (Fig. 6.22), the contribution of the bottom plate is readily apparent. In this figure, there is good agreement between the analytical and experimental results with the bottom connector plates present. The fact that the deflections without the bottom connector plate (NBP) are almost twice those with the bottom connector plate (ND) indicates the importance of the bottom connector plate in this bridge system. The magnitude of the deflection with no diaphragms (ND) and without the bottom connector plate (NBP)is very small - less than 3 mm (0.1 in.) in most cases. Note the symmetrical response of the bridge illustrated in Fig. 6.22, which is for loading applied at D4 (see Fig. 6.4). This indicates that the retrofitted connection detail (see Sec. 3.5) used on the initially fabricated PCDT unit was structurally effective.

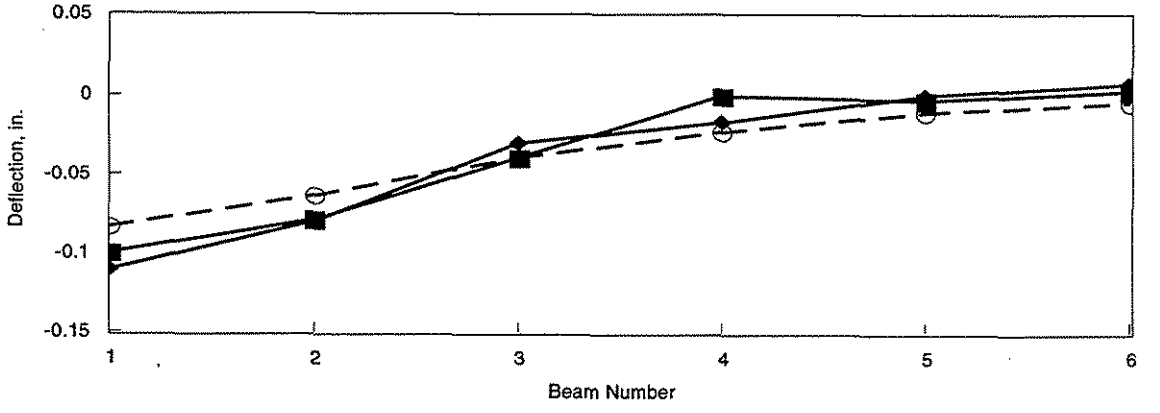

a. Centerline

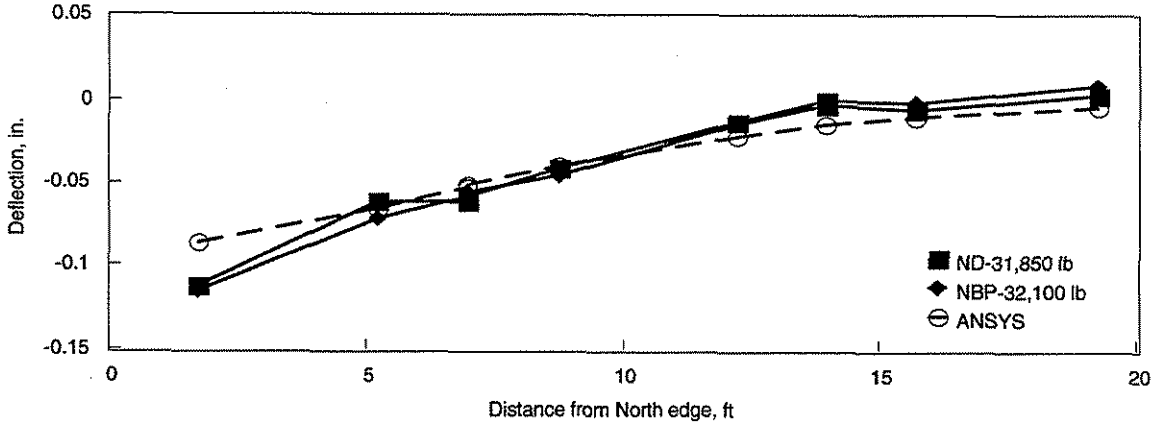

b. 3/8 point

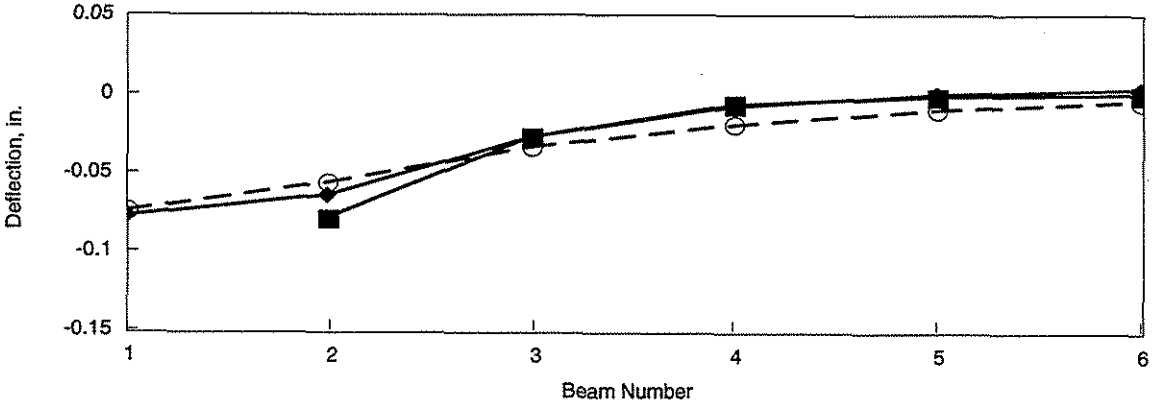

c. Quarter point

Figure 6.19. Experimental and analytical deflections: ND and NBP tests; load at B1.

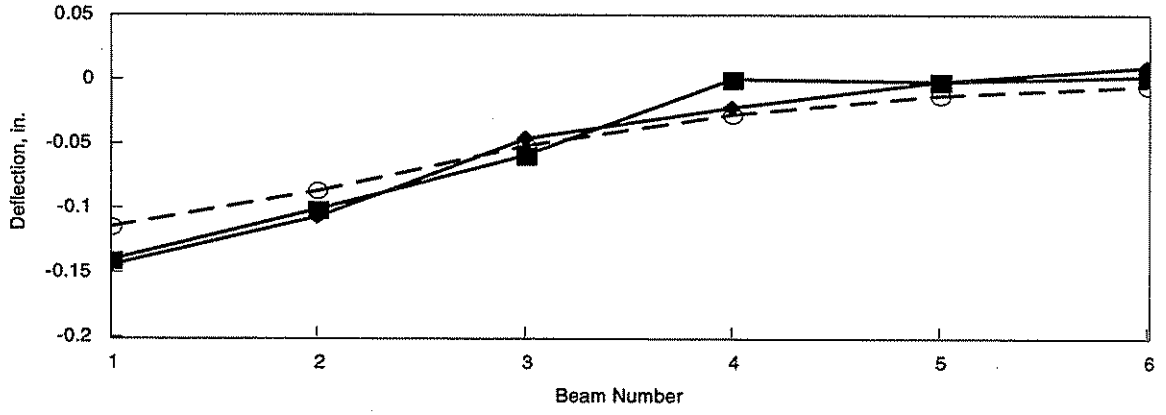

a. Centerline

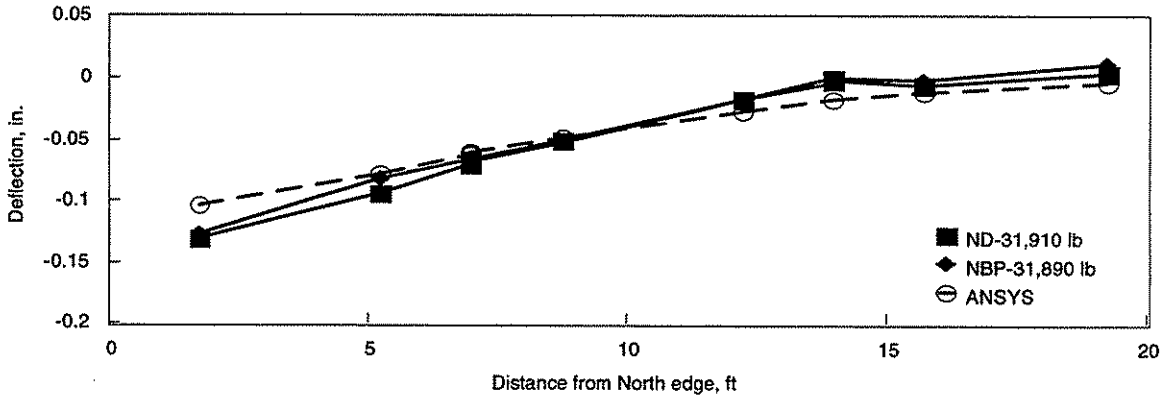

b. 3/8 point

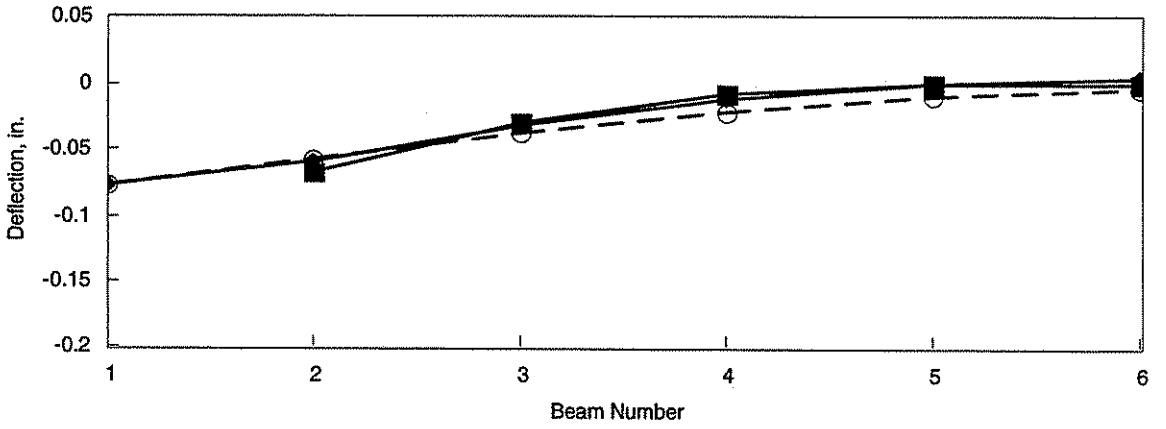

c. Quarter point

Figure 6.20. Experimental and analytical deflections: ND and NBP tests; load at D1.

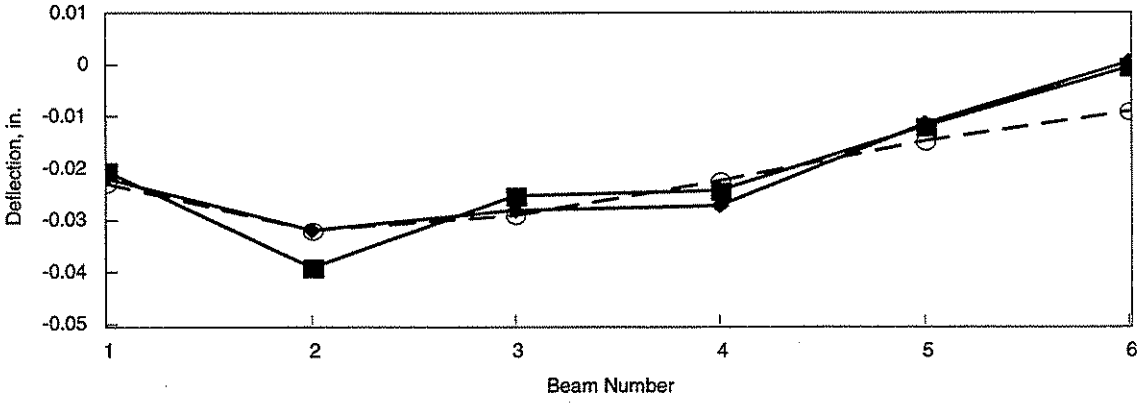

a. Centerline

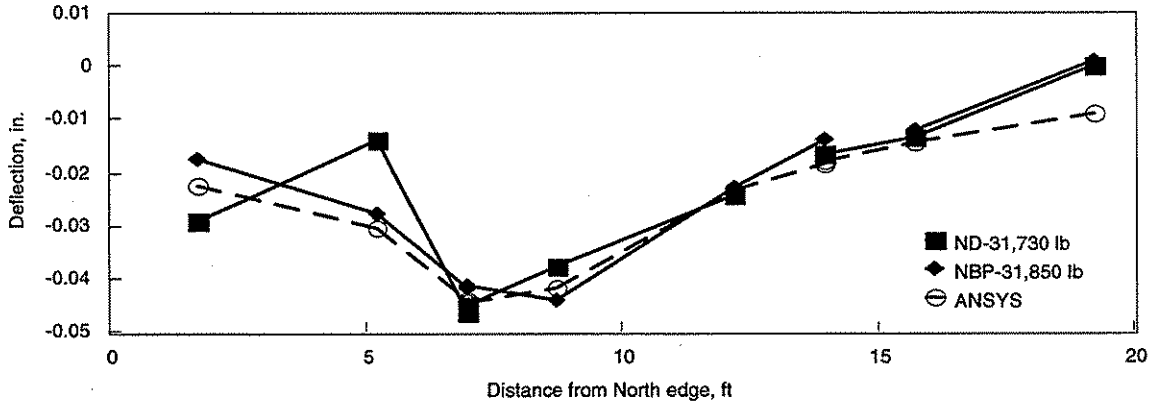

b. 3/8 point

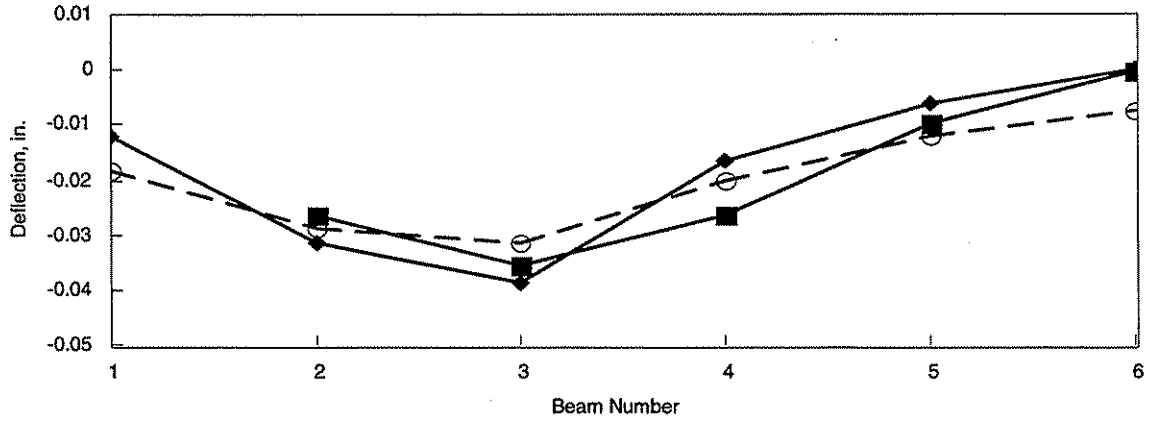

c. Quarter point

Figure 6.21. Experimental and analytical deflections: ND and NBP tests; load at A3.

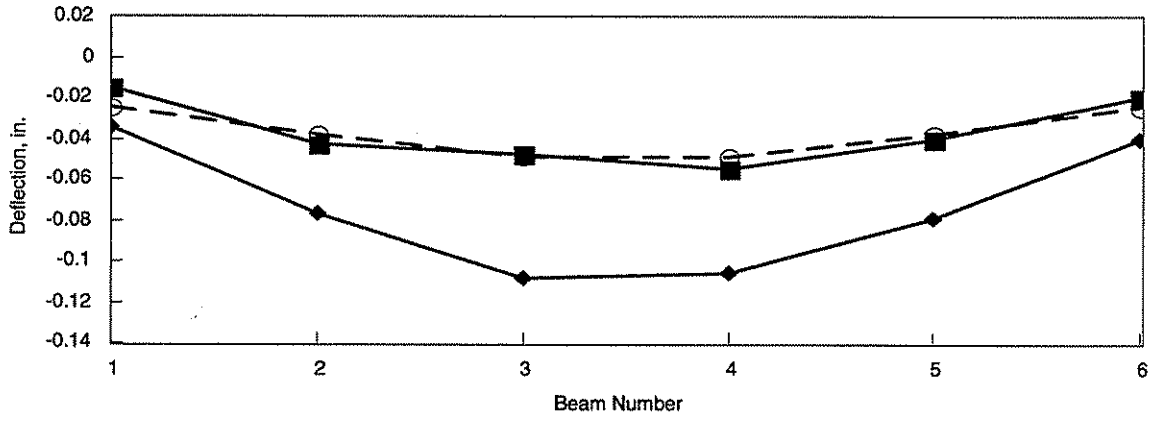

a. Centerline

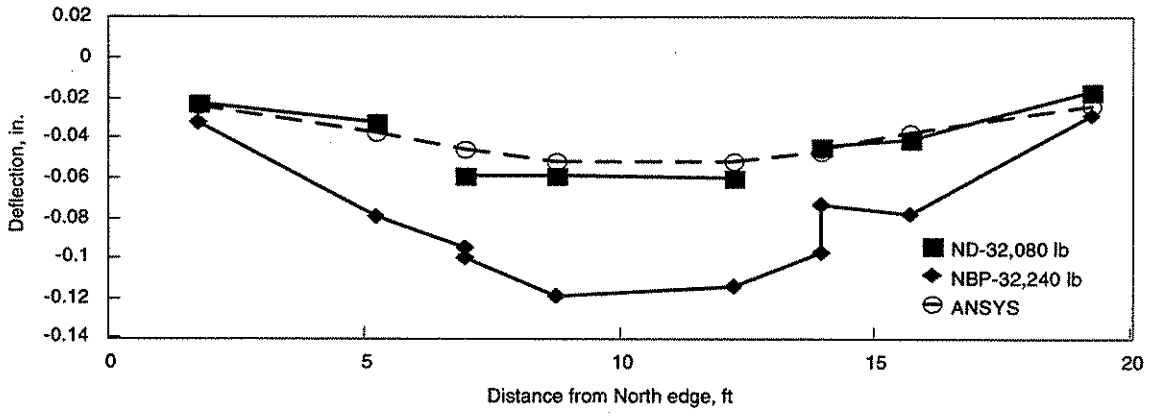

b. 3/8 point

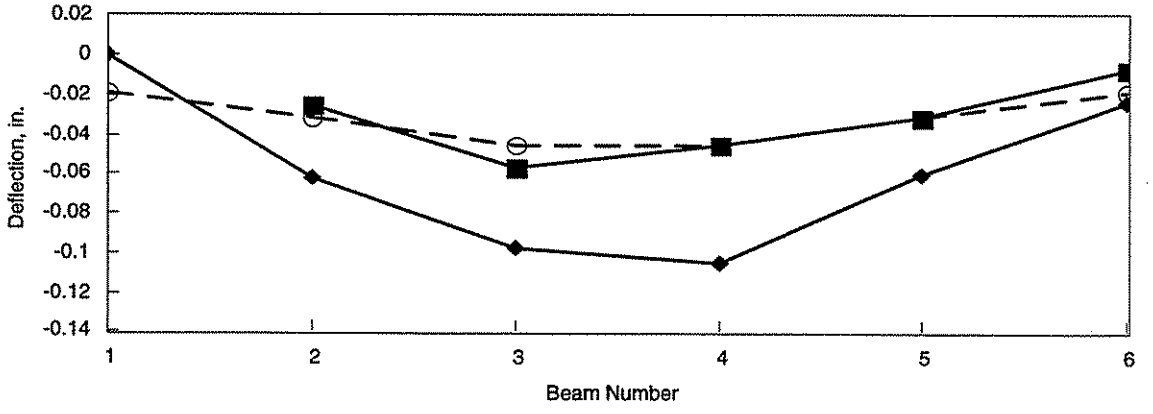

c. Quarter point

Figure 6.22. Experimental and analytical deflections: ND and NBP tests; load at D4.

6.3.2.2 Model Bridge with Diaphragms

Shown in Figs. 6.23 - 6.26 are the results of testing the model bridge with and without diaphragms. Note that during the diaphragms tests, the bottom plate of the connectors was in place. As shown in Fig. 3.14 the diaphragms are located at the 1/3 points of the span. When the diaphragms are at mid-web height of the beam webs (see Fig. 3.21a) the tests are designated as D1, and when the diaphragms are just below the concrete deck (see Fig. 3.21b) the tests are designated D2. In each of these figures, a nominal load of 71,170 N (32,000 lbs) has been applied to the model bridge. As in previous tests, only representative data are presented. Deflection data in these figures are from load being applied at four different load points B4 (Fig. 6.23), A1 (Fig. 6.24), A2 (Fig. 6.25), and D4 (Fig. 6.26). These point were selected for presentation as they are at different locations and distances from the diaphragms in the model bridge. As is evident in these figures, the diaphragms have minimal effect on the bridge's behavior. Deflection curves for the two cases with diaphragms (D1 and D2) are essentially the same as the case without diaphragms (ND). The only time the diaphragms reduced the deflections was when the load was applied close to the location of the diaphragms. This slight improvement is due to the fact that the diaphragms add a degree of transverse continuity to the two PCDT units. It should however be noted that less than a 10% improvement occurred in the most critical case. Therefore, it seems apparent that diaphragms are ineffective for load distribution. Typically, installation of diaphragms is very labor intensive - especially when placing them directly below the PC units (position D2). The added benefit of diaphragms has long been a point of discussion. From these results, it is

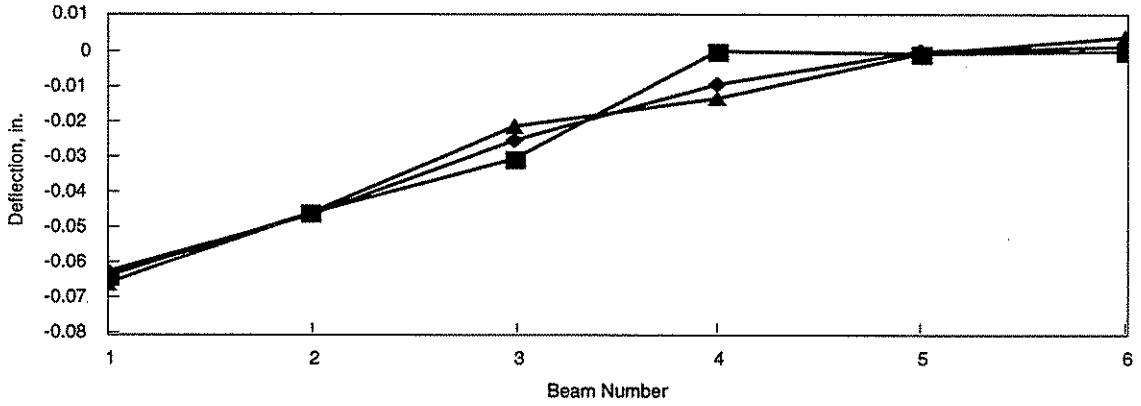

a. Centerline

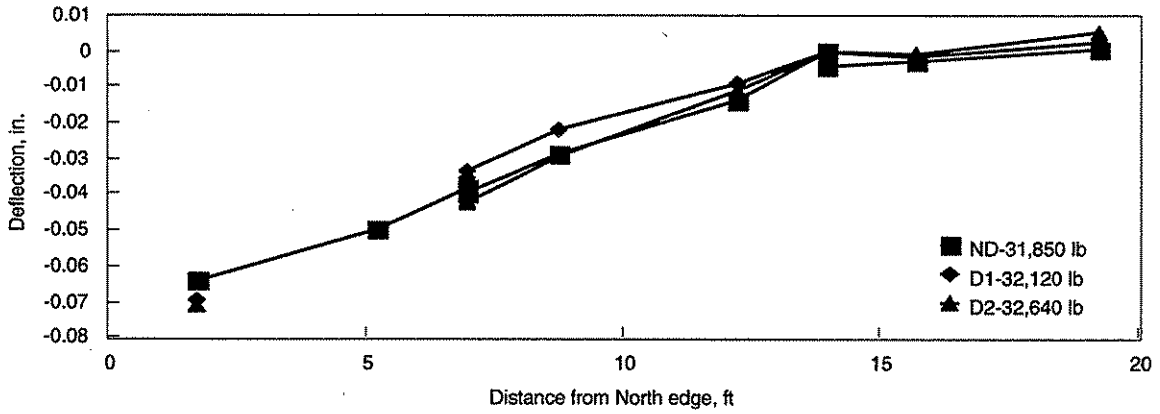

b. 3/8 point

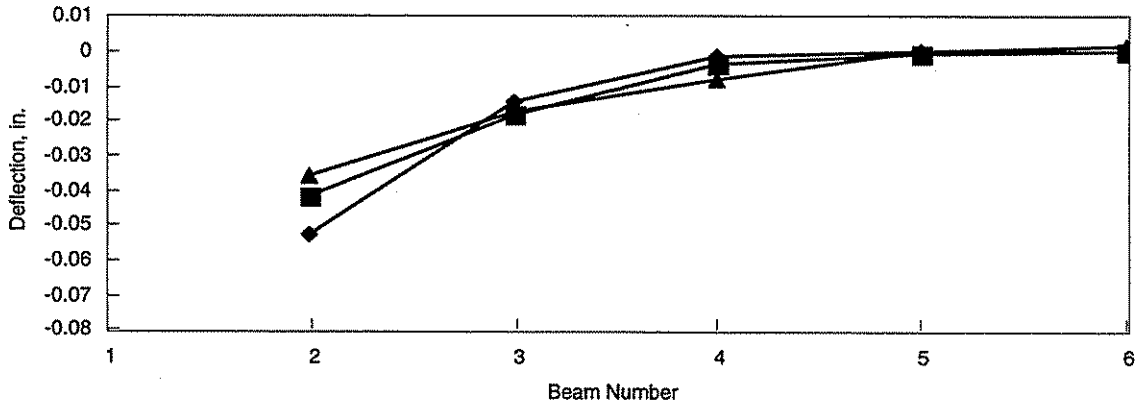

c. Quarter point

Figure 6.23. Model bridge deflections with and without diaphragms; load at B4.

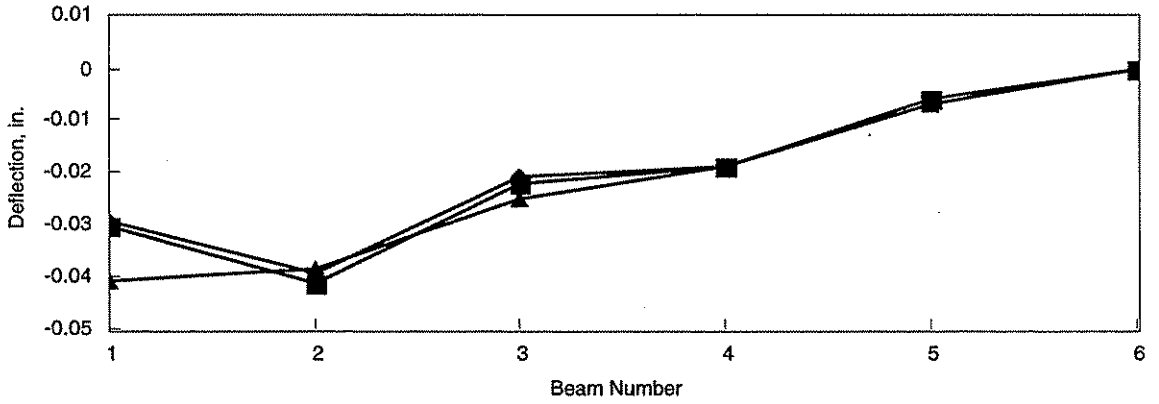

a. Centerline

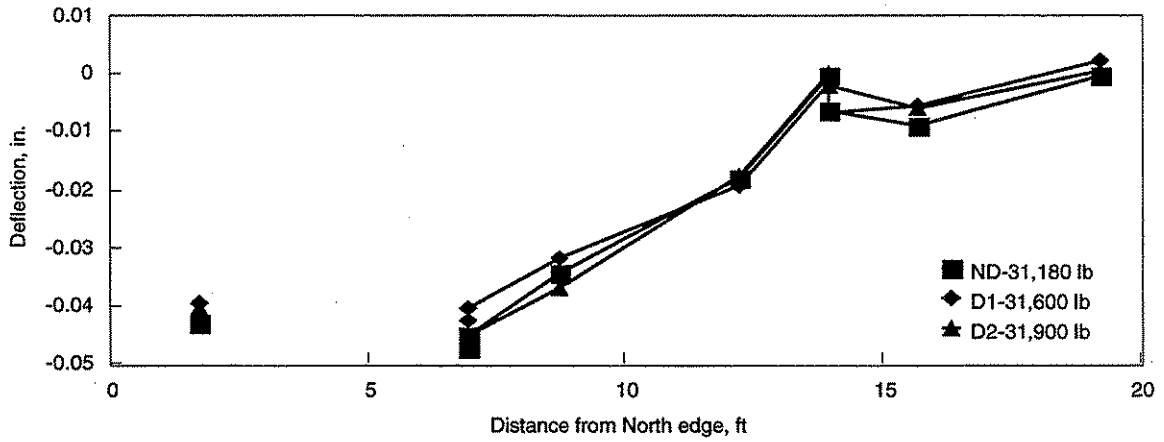

b. 3/8 point

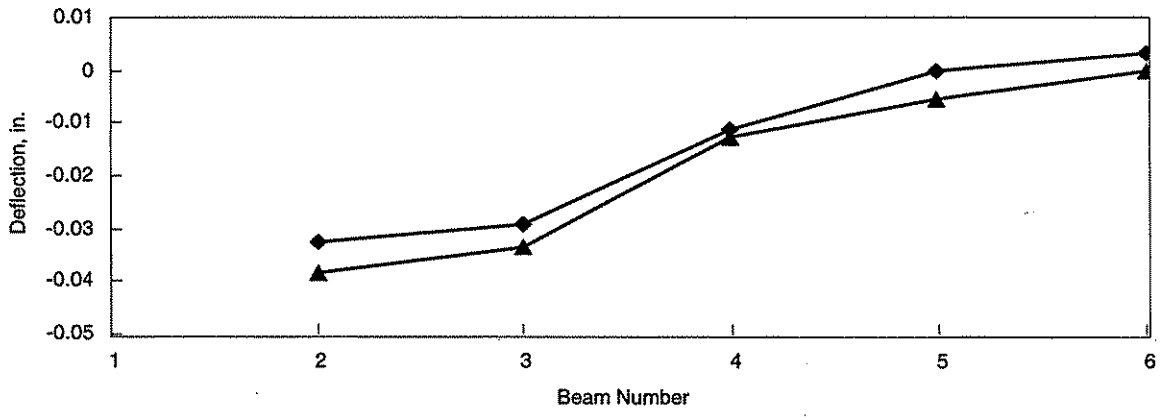

c. Quarter point

Figure 6.24. Model bridge deflections with and without diaphragms; load at A1.

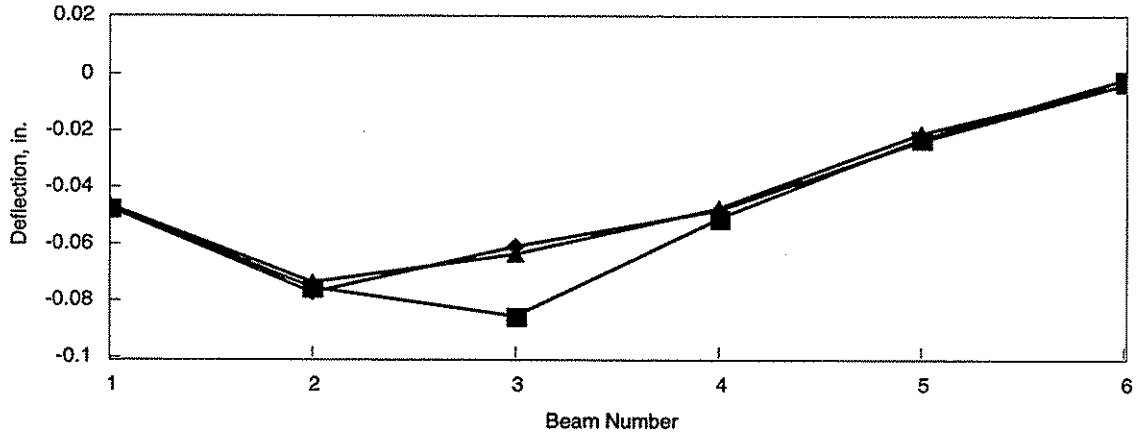

a. Centerline

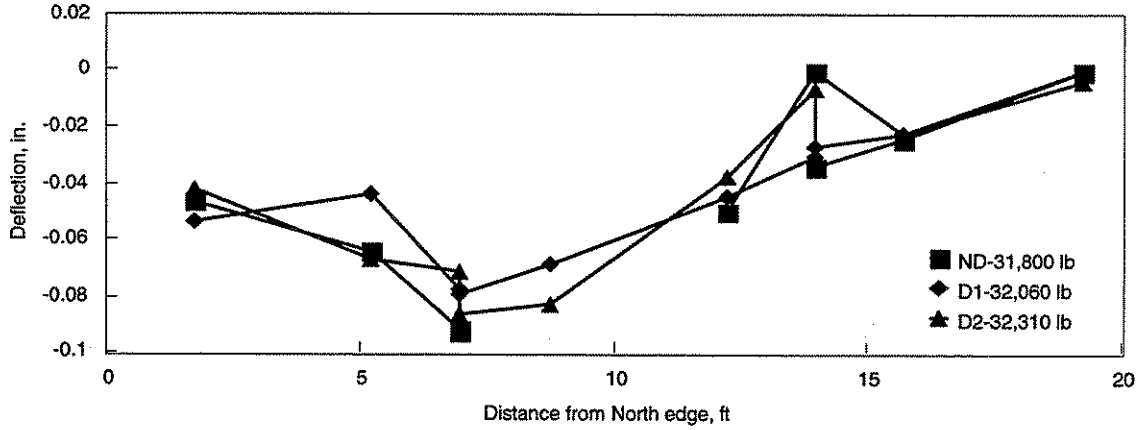

b. 3/8 point

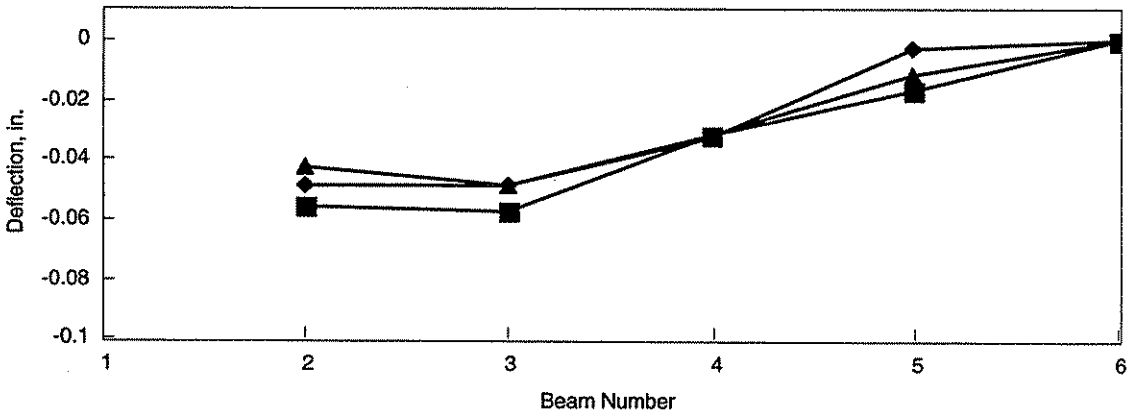

c. Quarter point

Figure 6.25. Model bridge deflections with and without diaphragms; load at A2.

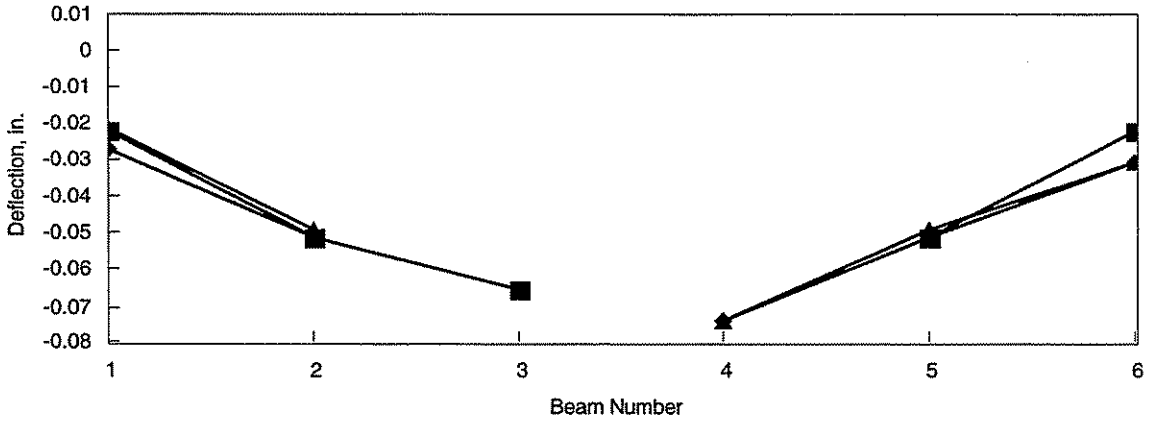

a. Centerline

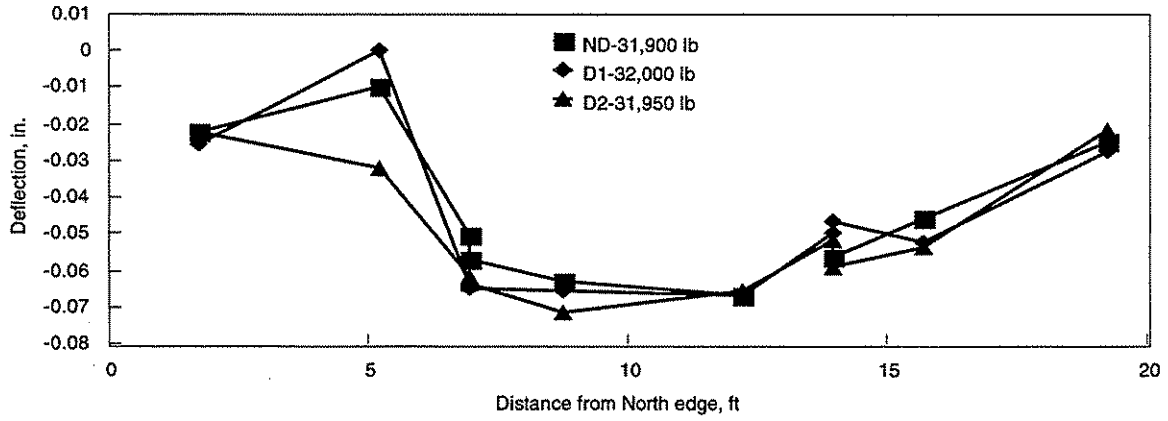

b. 3/8 point

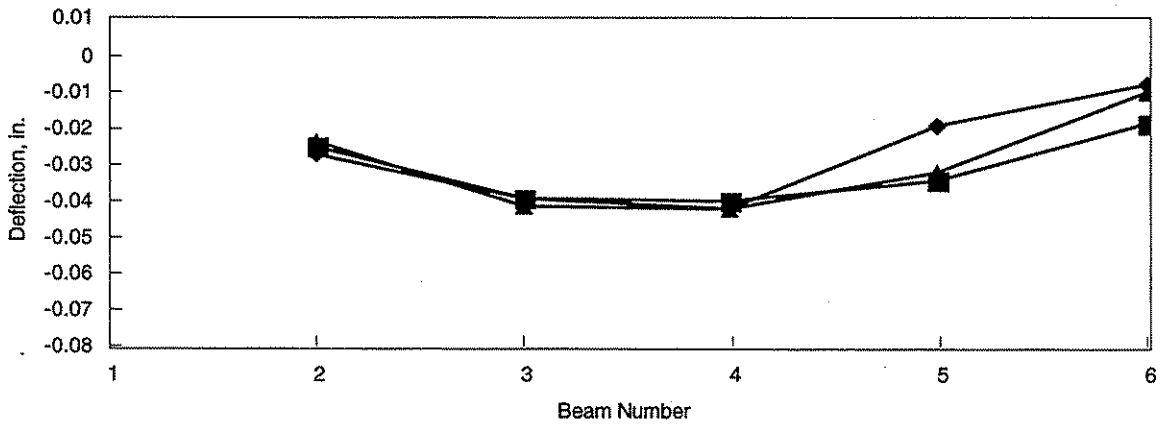

c. Quarter point

Figure 6.26. Model bridge deflections with and without diaphragms; load at D4.

obvious that the small improvement in lateral load distribution obtained from including diaphragms does not warrant the added costs of materials and labor required to install them.

In a previous Iowa DOT research project (HR-319) (13) interior diaphragms were determined to be ineffective in distributing vertical loads. In that investigation, the effectiveness of interior diaphragms in distributing vertical and horizontal loads in pre-stressed concrete stringer bridges was investigated. One of the conclusions of that study was that vertical load distribution is essentially independent of the type and location of intermediate diaphragms. Although the model bridge in this study contains steel stringers, the same ineffectiveness of the diaphragms in distributing vertical loads was determined.

6.3.2.3 Overload Tests of Model Bridge

Shown in Figs. 6.27 - 6.29 are the results of the overload tests where two load points were used (see Fig. 4.8b); note in these figures the sum of the two applied loads have been plotted. As before ND means no diaphragms, and NBP means no bottom plate. As is evident, there is no difference in the deflection of the bridge under the applied load with and without the bottom connector plates. This is obvious by the fact that the curves basically overlap at all load increments. This is consistent with the results previously presented. From the previous data, it was found that the only time this condition influenced the behavior of the model bridge was when load was applied at the center of the bridge. Since the four point load test (Fig. 4.8a) did not have a load at the center of the bridge, omitting the bottom connector plate was found to have no influence. These results have thus not been included in this report. As was previously noted, an attempt

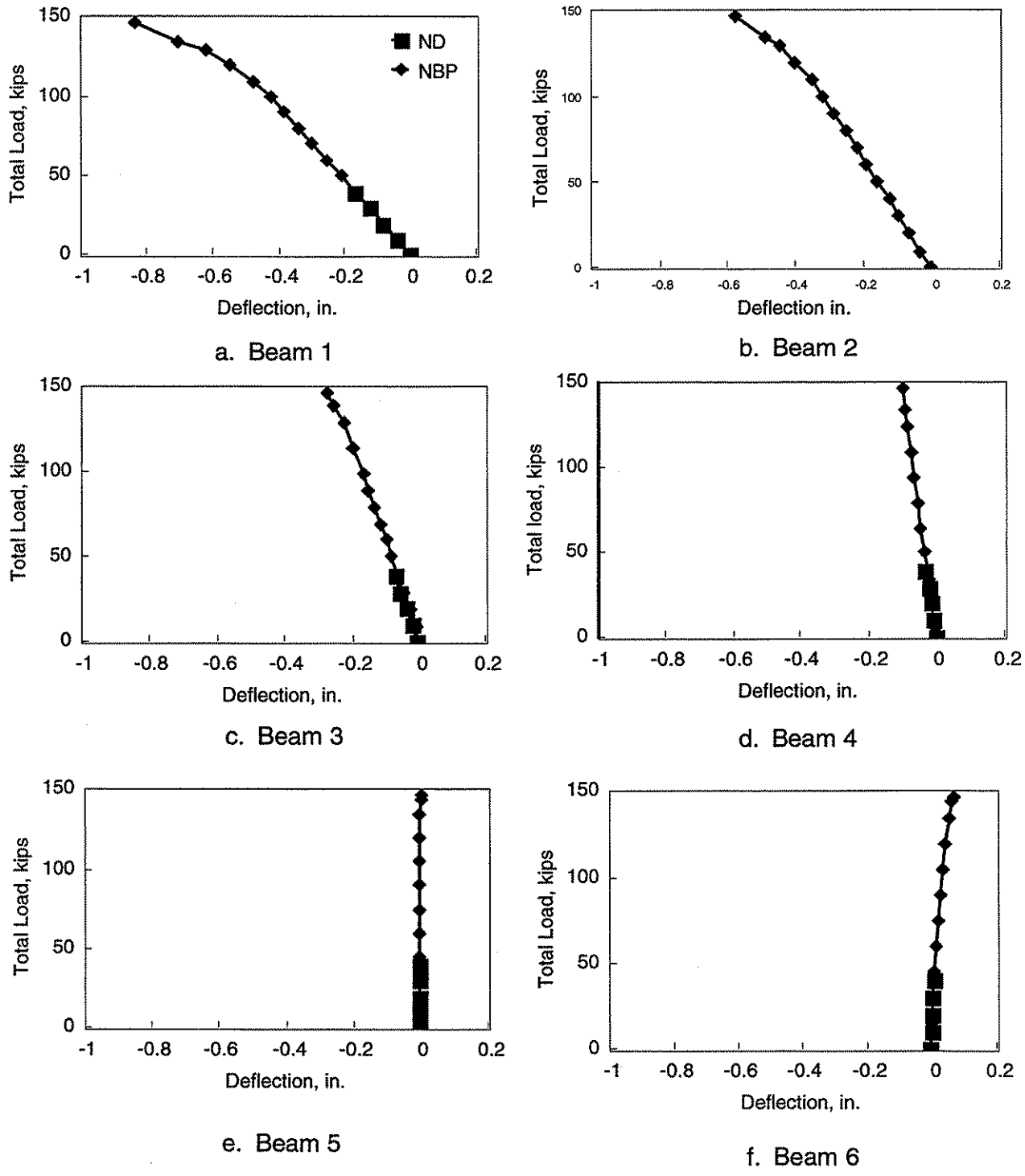

Figure 6.27. Beam centerline deflections for two point overload test.

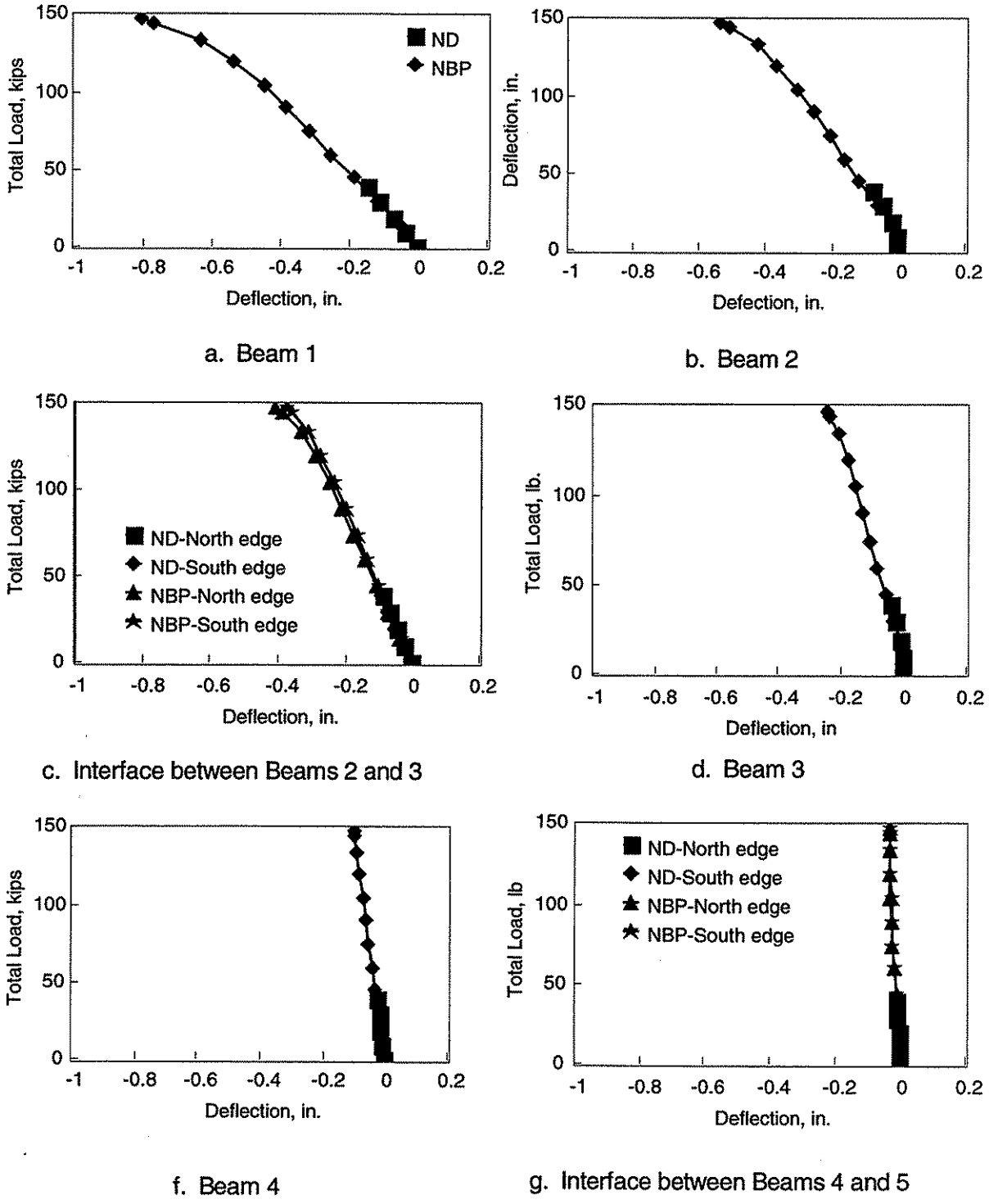

Figure 6.28. Deflections at 3/8 point for two point overload test.

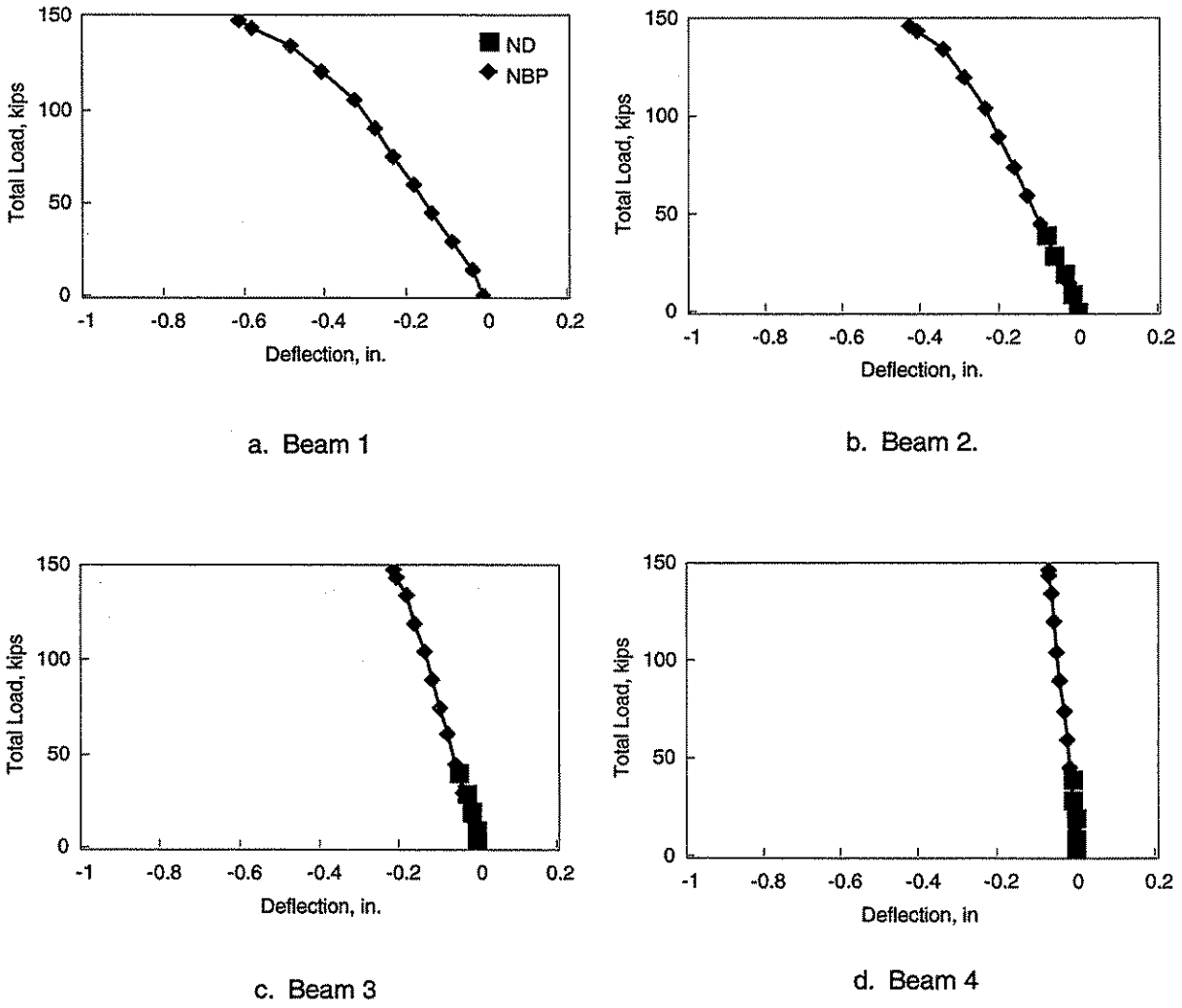

Figure 6.29. Beam quarter point deflection for two point overload test.

was made to load the bridge model to failure by applying load at the two overload points (see Fig. 4.8b). However, the capacity of the load frame was reached without damaging the model bridge (i.e. Overload test 1 - 756,000 N (170,000 lbs), Overload test 2 - 659,150 N (147,000 lbs)) - see Sec. 4.4.2 for more details.

6.3.2.4 Laterally Continuous FEM Bridge Model vs. FEM of Laboratory Bridge

As was noted previously, a FEM was developed that predicted the behavior of a continuous transverse bridge deck with the same geometric properties as the one under investigation (Note; these results are designated "continuous"). The results of these analyses are shown in Figs. 6.30 - 6.32 with the analytical results from the bridge under investigation. Deflections are presented for the load being applied at three points: Load Point D3 (Fig. 6.30), Load Point A2 (Fig. 6.31), and Load Point C1 (Fig. 6.32). The graphs indicate that there is very little difference between the bridge under investigation and a continuous deck bridge. This indicates that with sufficient connectors in place, the bridge system can be designed by conventional bridge design procedures using current AASHTO specifications.

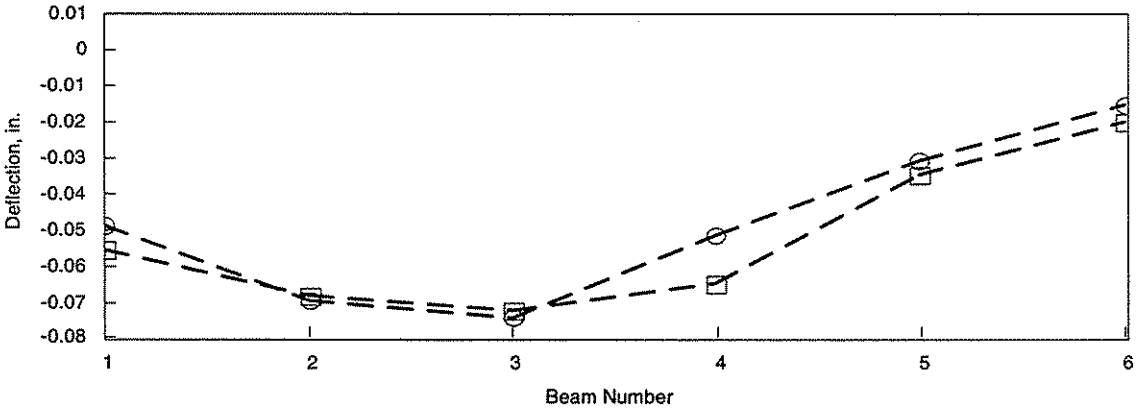

a. Centerline

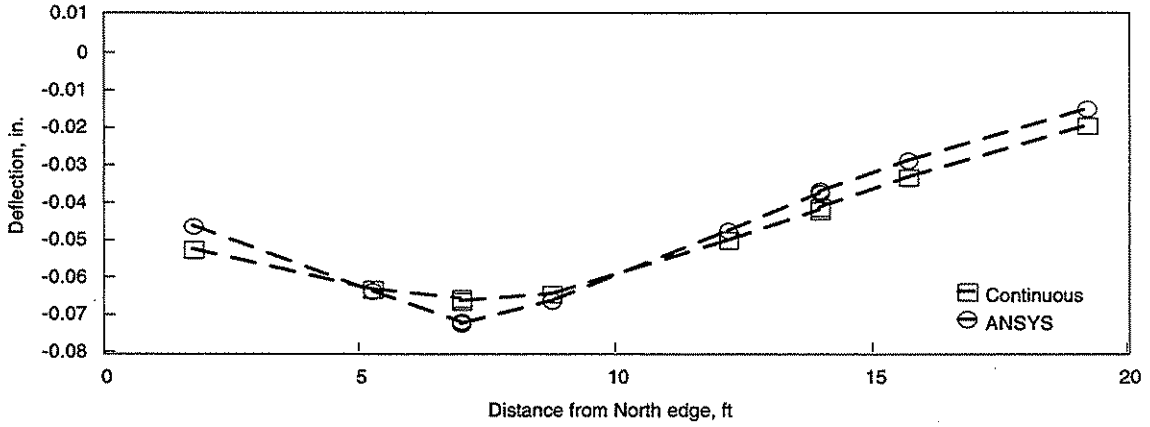

b. 3/8 point

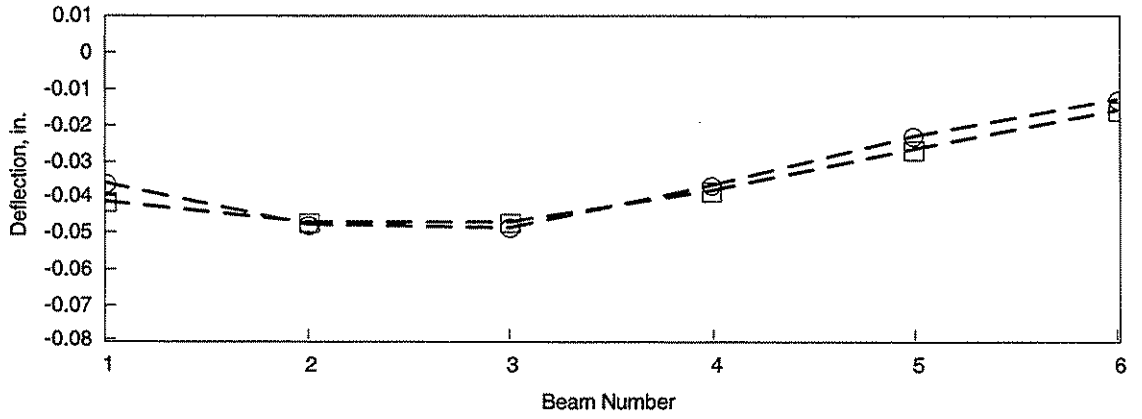

c. Quarter point

Figure 6.30. Deflections for continuous and ANSYS models; load at D3.

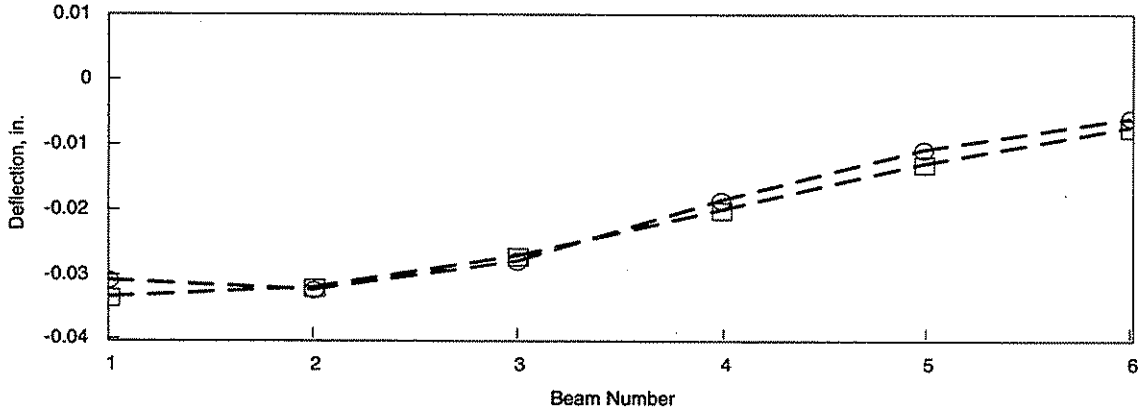

a. Centerline

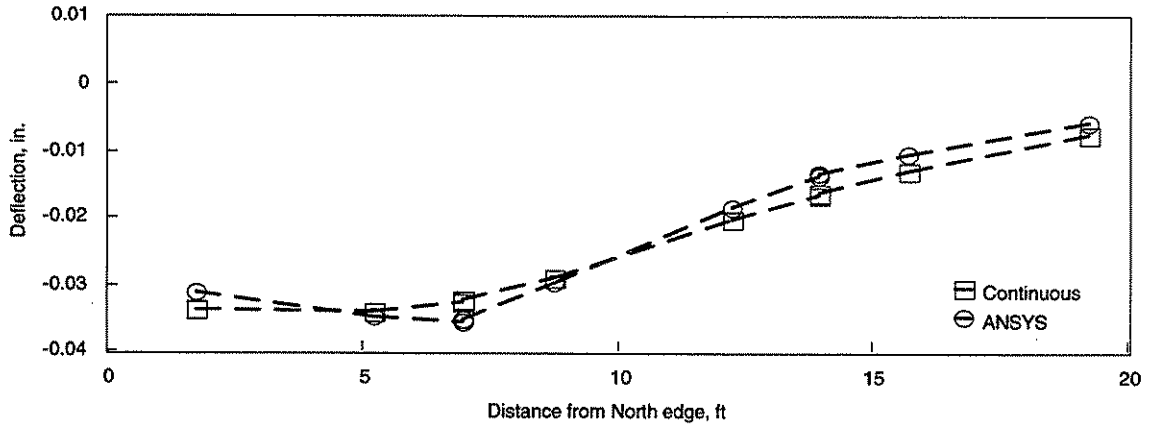

b. 3/8 point

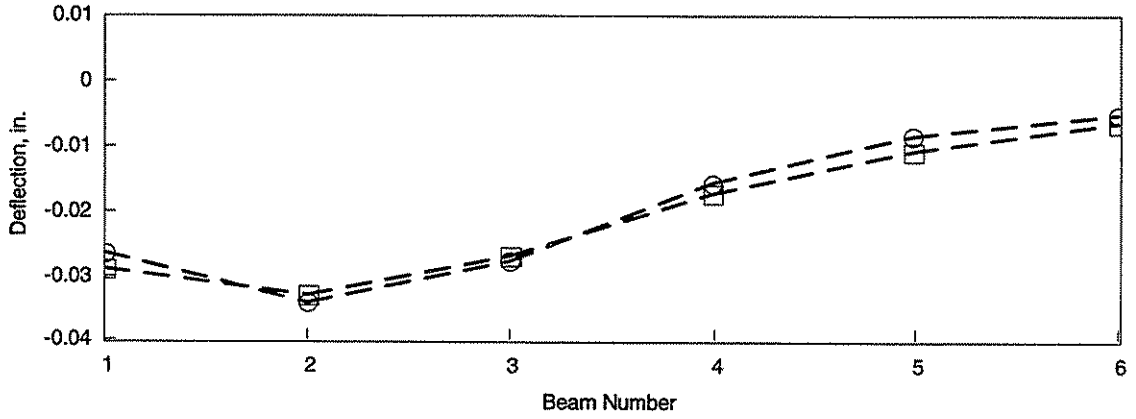

c. Quarter point

Figure 6.31. Deflections for continuous and ANSYS models; load at A2.

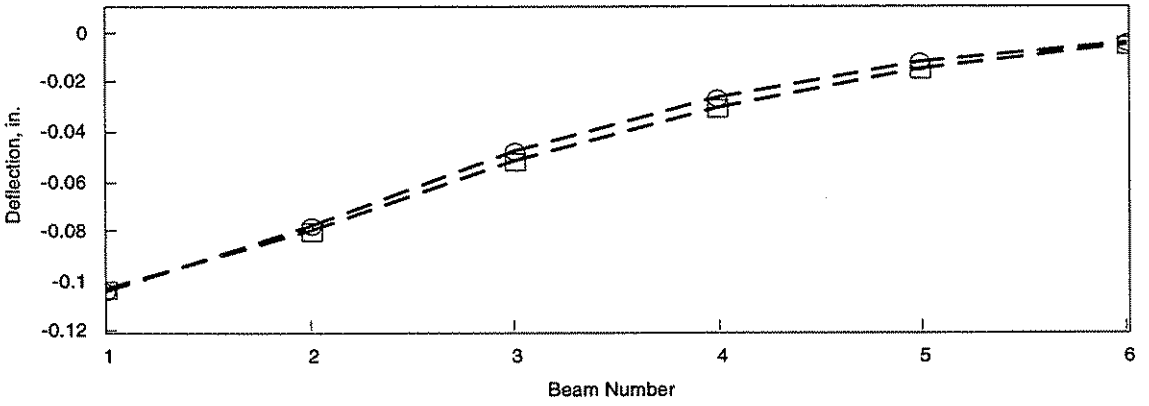

a. Centerline

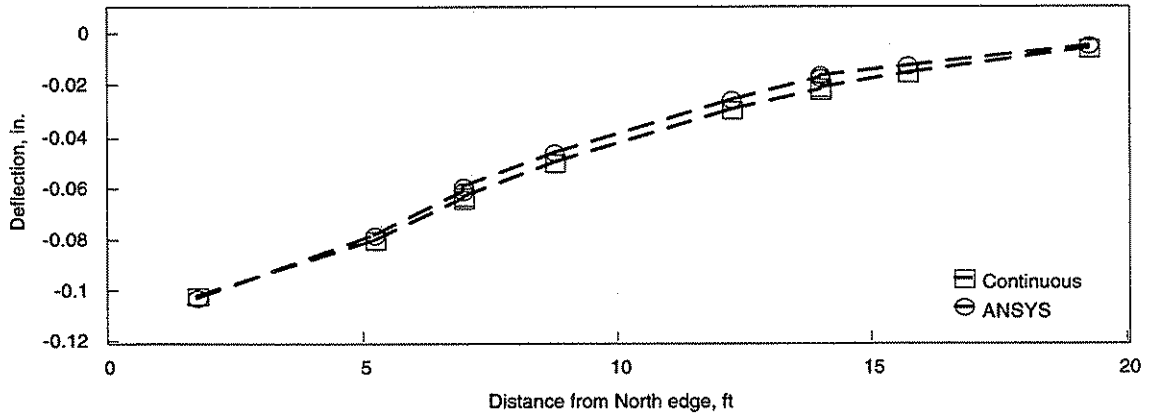

b. 3/8 point

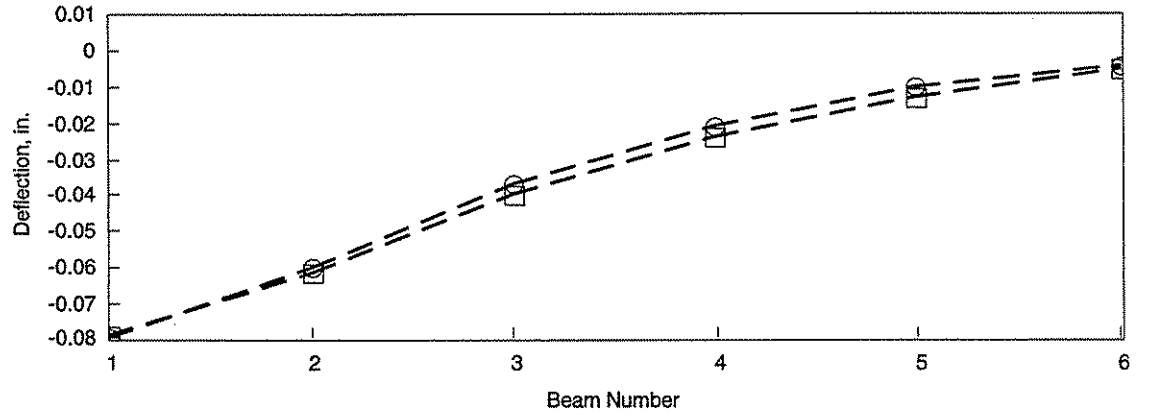

c. Quarter point

Figure 6.32. Deflections for continuous and ANSYS models; for load at C1.

7. SUMMARY AND CONCLUSIONS

In this phase of the investigation, Concept 1 - Precast Steel Beam Units were investigated. The study consisted of several different tasks. In the literature review that was completed, various means of connecting precast units were reviewed as well as procedures for bonding layers of concrete cast at different times. Since Concept 1 is "new", no literature was located on it or similar systems. In the experimental part of the investigation, there were three types of static load tests: small scale connector tests, "handling strength" tests, service and overload tests of a model bridge. In the analytical part of the study, three FEM's were developed which were verified using data from the experimental portion of the investigation. These FEM's were used to predict the behavior of the PCDT units with various connector arrangements, for determining the behavior with the CIP concrete in place, and for determining the behavior of a continuous deck bridge.

The small scale connector tests were completed to determine the best method of connecting the PCDT units. In these tests, specimens were tested with different connector arrangements and with and without the CIP concrete.

"Handling strength" tests were undertaken to determine if the PCDT units had sufficient strength to withstand transportation from a fabrication site to a given bridge site. This testing was obviously completed without the CIP concrete.

In the testing of the model bridge (L = 9,750 mm (32 ft); W = 6,410 mm (21 ft)), a total of 128 service load tests and four overload tests were completed. In the service tests, the following items were investigated: number of connectors required between PCDT units, influence of diaphragms and their vertical positions, load distribution in

model bridge with and without CIP concrete in place, and contribution of bottom connector plates to load distribution when CIP concrete is in place. In the four overload tests, load distribution and behavioral data was obtained.

Based on the laboratory tests (small scale connector tests, "handling strength" tests, and model bridge tests) completed in this part of the investigation the following observations and conclusions can be made. As has been documented in Chp. 6, the majority of these conclusions have also been verified using the FEM's developed.

1. Used in combination, the PCDT units (Concept 1) developed and tested result in a simple-span bridge alternative for low-volume roads that is relatively easy to construct.
2. The connector developed - plates (top and bottom) welded channels embedded in concrete - provides a connection with adequate strength to resist highway loads. This connector is also relatively easy to install.
3. The PCDT units (with their relatively thin concrete PC deck) are strong enough to resist the handling loads imposed on them during construction and transportation. Occasional "rough" handling is expected; if sufficient time is given for the PC concrete to cure, no distress should occur in the PCDT units from lifting, transporting, or placement.
4. No interlayer delamination occurred between the PC and CIP concretes during any of the tests when the recommendations outlined in the literature review were followed.

5. Five PC connectors between adjacent PCDT units gave the desired lateral load distribution. The use of seven or nine connectors did not change the behavior of the bridge system significantly.
6. The addition of the CIP deck significantly improved the load distribution characteristics of the bridge system.
7. The combination of connectors between the PCDT and reinforcement properly placed in the CIP portion of the deck should prevent reflective cracking in the system.
8. During the two overload tests, the bridge was subjected to 756,000 N (170,000 lb) (over 4 times H-20 loading) without any visible signs of distress.
9. The use of diaphragms did not significantly change the behavior of the bridge system. Based on this and the fact that the installation of diaphragms is very costly, and labor intensive, the resulting small improvement in the behavior does not warrant their installation.
10. To investigate the relative contribution of the CIP deck to the lateral load distribution, the model bridge was tested with and without the bottom plate of the connector. In most instances there was no difference in behavior; the only time there was a noticeable difference in behavior was when load was placed on the transverse centerline of the bridge. Thus, it was concluded, under static loading with the CIP concrete in place, in most instances the bottom plates have minimal influence.
11. The FEM's developed in this investigation can accurately predict the behavior of this bridge system with various connector arrangements, with and without

the CIP concrete in place, and with a continuous transverse deck (*i.e., deck* placed in one pour). Thus, these programs can be used to design this type of bridge.

8. RECOMMENDED RESEARCH

On the basis of the work completed in this phase of the investigation, the following two tasks would be logical for bringing this concept to a successful conclusion:

1. Using the analysis developed in this phase of the study, a full scale demonstration bridge should be designed and constructed. This bridge would be instrumented and service load tested upon completion and periodically re-tested during the first two years. All phases of construction would be videotaped and photographed. Using this documentation and the FEM's that have been developed, a combination design/construction manual would be developed so that county engineers could design this type of bridge and train their crews to construct the bridge.
2. The connection developed in this study needs to be subjected to cyclic loading, such as it would experience in the field. Although the connections have performed more than satisfactorily during all the tests in this phase of the investigation, all applied loads were static. Thus, a limited number of small scale connections needs to be subjected to cyclic loading to determine if the connection/CIP concrete combination is adequate to prevent reflective cracking in the CIP deck. If such cracking does develop, appropriate modifications to the connection will be made and tested.

9. ACKNOWLEDGEMENTS

The study presented in this report was conducted by the Bridge Engineering Center under the auspices of the Engineering Research Institute of Iowa State University. The research was sponsored by the Project Development Division of the Iowa Department of Transportation and Iowa Highway Research Board under Research Project 382.

The authors wish to thank the various Iowa DOT and county engineers who helped with this project and provided their input and support. In particular, we would like to thank the project advisory committee:

- Dennis J. Edgar, Ass't County Engineer, Blackhawk County
- Robert L. Gumbert, County Engineer, Tama County
- Mark J. Nahra, County Engineer, Cedar County
- Gerald D. Petermeier, County Engineer, Benton County
- Wallace C. Mook, Director of Public Works , Bettendorf
- Jim Witt, County Engineer, Cerro Gordo County

Appreciation is also extended to Bruce L. Brakke and Vernon Marks of the Iowa DOT for their assitance in obtaining the surplus steel beams used in this investigation.

Special thanks are accorded to the following Civil Engineering graduate and undergraduate students for their assistance in various aspects of the project: Andrea Heller, Trevor Brown, Matthew Fagen, David Oxenford, Brett Conard, Matt Smith, Chris Kruse, Mary Walz, Penny Moore, Dave Kepler, Ryan Paradis, Hillary Isebrands, Ted Willis, and Kevin Lex.

10. REFERENCES

1. "Ninth Annual Report to Congress-Highway Bridge Replacement and Rehabilitation Program", FHWA, Washington, D.C. 1989.

2. "Rural Bridges: an Assesment Based Upon the National Bridge Inventory", Transportation Report, United States Department of Agriculture, Office of Transportation, April 1989.

3. Wipf, T.J., F.W. Klaiber, and A. Pabhakaran, "Evaluation of Bridge Replacement Alternatives for the County Bridge System", Final Report Iowa DOT Proj. HR-365, August, 1994.

4. Seible, F., C. Latham, and K. Krishnan. "Structural Concrete Overlays In Bridge Deck Rehabilitation; Summary of Experimental Results, Analytical Studies and Design Recommendations." Research report submitted to CALTRANS, La Jolla, CA, 1988.

5. American Association of State and Highway Transportation Officials. Standard Specifications for Highway Bridges 15th Edition. Washington D.C.: American Association of State Highway and Transportation Officials, 1992.

6. Bakht, B., L.G. Jaeger, and M.S. Cheung. "Transverse Shear in Multibeam Bridges." ASCE Journal of Structural Engineering, Vol. 109, No.4, April 1983, pp 936-949.

7. Stanton, J.F. and A.H. Mattock. "Load Distribution and Connection Design for Precast Stemmed Multibeam Bridge Superstructures." National Cooperative Highway Research Program Report 287, Transportation Research Board, Washington D.C., Nov. 1986.

8. Biswas, M. "Special Report: Precast Bridge Deck Design Systems." Chicago IL.: Reprint from the Journal of Prestressed Concrete Institute, Vol. 31, No. 2, March-April 1986, pp 2-56.

9. Berger, R.H., "Full Depth Modular Precast, Prestressed Bridge Decks." Transportation Research Record, Washington D.C., National Research Council, 1983, pp 52-59.

10. Huckelbridge, A.A., H. El-Esnawi, and F. Moses. "Shear Key Performance in Multibeam Box Girder Bridges." ASCE Journal of Performance of Constructed Facilities Vol. 9, No. 4, Nov. 1995, pp 271-285.

11. ANSYS User's Manual for Revision 5.1, Swanson Analysis Systems, Inc., Houston, PA. 1992.

12. Dunker, K.F., "Strengthening of Simple Span Composite Bridges by Post-Tensioning", Dissertation, Iowa State Unversity, 1985.

13. Abendroth, R. E., F. W. Klaiber, and M. W. Shafer. "Lateral Load Resistance of Diaphragms in Prestressed Concrete Girder Bridges." Final Report, Iowa DOT Proj. HR-319, ISU-ERI-Ames-92076, Engr. Res. Inst., Iowa State Univ., Ames, Iowa, 1991.